DISSERTATION

FELINE FOAMY VIRUS IN DOMESTIC CATS: USE AS A VACCINE VECTOR, CHARACTERIZATION OF INFECTION, AND ASSOCIATION WITH OTHER DISEASES

Submitted by

Carmen Denise Ledesma-Feliciano

Department of Microbiology, Immunology, and Pathology

In partial fulfillment of the requirements

For the degree of Doctor of Philosophy

Colorado State University

Fort Collins, Colorado

Spring 2019

Doctoral Committee:

Advisor: Susan VandeWoude

Jessica Quimby
Tony Schountz
Randall Basaraba
Melinda Frye

ABSTRACT

FELINE FOAMY VIRUS IN DOMESTIC CATS: USE AS A VACCINE VECTOR, CHARACTERIZATION OF INFECTION, AND ASSOCIATION WITH OTHER DISEASES

Foamy viruses (FVs) are retroviruses from the *Spumaretrovirinae* subfamily. FVs are globally prevalent retroviruses with a unique molecular biology. FVs establish apparently apathogenic lifelong infections. Due to this, FVs are considered attractive vectors for vaccine and gene therapy development. Feline foamy virus (FFV) infects domestic cats and has widespread and high prevalence around the world. However, FFV has also been isolated from cats suffering from concurrent disease, including renal syndromes and other retroviral co-infections such as feline immunodeficiency virus (FIV). Much remains unknown about FFV infection and in vivo experimental infections are rare in the literature.

To test FFV's use as a vaccine vector and understand the interaction between viral proteins and host antiviral restriction factors, we developed an infective chimeric vaccine containing lentiviral FIV *vif* replacing FFV *bet*. FFV Bet and FIV Vif counteract feline innate APOBEC3 (feA3) restriction factors through different mechanisms. FeA3 action on retroviral genomes lead to hypermutation and degradation of viral DNA. In vitro, we show that *vif* can replace *bet* to yield replication-competent chimeric viruses. We experimentally inoculated 12 domestic cats (n=4 per group in naïve, wild-type, and chimera-inoculated groups) with the FFV-Vif chimera and wild-type FFV in order to compare viral replication kinetics through PCR and specific antibody development through ELISA. Inoculation with the chimeric vector resulted in the development of a specific immune response against FFV Gag and Bet and FIV Vif proteins. In addition, we show that the domestic cat can be superinfected with different strains of FFV. The chimeric virus displayed attenuated infection in vivo, as provirus was not detected in PBMC for any chimera-

only inoculated animals. Thus, Bet may have additional functions other than A3 antagonism required for successful in vivo infection. Our studies further exemplify how FV vaccine vectors are an attractive tool to counteract lentiviral infections and poses the possibility to induce immunity against other lentiviral antigens.

In order to further characterize wild-type infection, we also collected blood, saliva, and urine over a 6-month time-period with a necropsy and tissue collection at the end of the study. Animals were monitored daily for clinical signs of disease and temperature and weight data were collected weekly. None of the cats showed clinical signs of infection and complete blood count and chemistry were unremarkable. However, we found significant differences in blood urea nitrogen, one of the markers used to assess renal function, when comparing infected versus control animals. All animals inoculated with wild-type virus showed a persistent proviremia (in PBMCs) and viral tissue tropism was primarily lymphoid with the exception of one cat that had an expanded tissue tropism to other lymphoid tissues and oral mucosa. This animal had altered viral kinetics compared to the rest of infected animals, in addition to a negative correlation between lymphocyte count and viral load. Histopathological analysis showed evidence of microscopic pathology in the kidneys, lung, and brain of infected animals. This same cat had an increase in urine protein at the time of highest PBMC proviremia. Additionally, transmission electron microscopy showed ultrastructural changes indicative of transient renal injury in the kidneys of infected animals. We additionally found electron dense structures in the cytoplasm of tubular epithelial of as of yet unknown origin.

Due to the renal changes we saw in the experimental study and pathology reported in the literature, we conducted a survey of FFV in pet cats in the USA and Australia (AU) suffering from chronic kidney disease (CKD) and compared findings to age- and sex-matched controls without CKD. We found an association between CKD and FFV in males, and males in general are also at a significantly increased risk of FFV infection.

We then assessed through an FFV serosurvey whether FFV was associated with FIV and causing potentiation of FIV disease in two cohorts of naturally FIV-infected cats. One of the groups consisted of cats living in 1-2 cat households that did not experience much FIV-related morbidity and mortality, while the second group of cats housed in a large multicat household suffered from severe clinical symptoms and mortality. We hypothesized the reason for this discrepancy could be an increase in FFV/FIV co-infection rate in the group of cats with higher morbidity and mortality. We found that FFV is associated with FIV in these groups and that males are also at an increased risk for FFV infection. Finally, we conducted an in vitro co-infection study to assess potentiated infection as determined by more rapid development of cytopathic effects (CPE) and higher viral titers in the supernatant. GFox cells were inoculated with FFV and FIV in single, and dual simultaneous and staggered inoculations. A p26 ELISA was used to determine amount of FIV reactivity in the cells, while a chemiluminescent β-galactosidase assay was used to detect amount of β -gal produced in FeFAB FFV reporter cells. The in vitro assays showed increased permissivity of either virus following an initial infection of the other virus, showing these two retroviruses can accelerate and potentiate a secondary infection regardless of which virus infected initially.

Overall, we have demonstrated the suitability of FFV as a vaccine vector candidate. Additionally, we have documented that FFV may cause subclinical alterations that in certain cohorts of domestic cats, may contribute to disease development in chronic cases. Finally, we showed that FFV interacts with another retrovirus and could potentially affect FIV-related disease. More studies should focus on the effects of FFV in chronic infections in addition to the effect of FFV on co-morbidities in a chronic timeline.

TABLE OF CONTENTS

INTRODUCTION

Feline foamy virus structure and replication

Feline foamy virus is a complex retrovirus belonging to the *Spumaretrovirinae* subfamily. Spumaviruses are ancient viruses, with endogenous forms infecting vertebrates over 450 million years ago [1-5]. Foamy viruses (FVs) are unique within the *Retroviridae*, with differences in molecular biology and clinical consequence of infection compared to other feline retroviruses. Despite their ancient nature, much remains unknown about FVs in general in addition to their effect on other disease syndromes in their hosts [2, 6]. A hallmark of in vitro FV infection, and how they were originally incidentally discovered, is that they cause adherent epithelial or fibroblastoid-origin cells in culture to look “foamy” (the derivation of “*spuma*”) [2, 7-12]. FVs are retroviruses, and thus a defining part of their replication cycle is RNA reverse transcription (RT). In contrast to other retroviruses, the infective form of FVs is DNA rather than RNA, and some replication steps are more similar to hepadnaviruses, such as DNA being the infective genome with a late RT step, an intracellular recycling pathway, and temporal regulation of replication [2, 3, 7, 13].

FV particles are spherical, about 100-140 nm in size, and feature prominent 10-15 nm spikes on their surface [2]. Proviral genomes range from 12-13 kilobases and contain the canonical retroviral *gag*, *pol*, and *env* structural genes and FV-specific accessory genes *tas* and *bet* downstream of *env* [3, 7]. Gag is a polyprotein with matrix, capsid, and nucleocapsid subunits [7, 8]. The *pol* gene encodes Pol, which is translated into a protein containing the domains for protease, reverse transcriptase, RNAse H, and integrase [7]. Env proteins includes transmembrane and surface subunits [7]. Tas is a trans-activator of FVs required for replication. Tas proteins bind both the unique spumaviral internal promoter (IP) found in FVs and upstream U3 LTR promoter for upregulated production of viral proteins [3, 5, 7, 8]. Bet is the second accessory protein expressed from terminal *tas* and *bel2* open reading frames (ORF) and is

involved in countering host innate APOBEC3 antiviral restriction factors [5, 7, 14-19]. The genome is under initial regulation by the IP, which is basally active and leads to the production of Tas and Bet [2, 7, 20]. Tas bids both the IP and upstream LTR, leading to a positive feedback loop that produces more Tas, followed by structural Gag, Pol, and Env proteins under the control of the U3 LTR [7, 8]. Temporal regulation of gene expression is not typical in retroviruses [2, 3]. FVs are among the most conserved retroviruses, having one of the slowest rates of mutation for all RNA viruses [1, 4, 21, 22].

The life cycle of FVs begins when the DNA-containing viral particles attach to target cells (for full replication review and diagrams, see [7]). The specific attachment receptor for FV entry into target cells is currently unknown, but it is thought to be widely prevalent due to the wide tissue tropism these viruses display [6, 7, 23]. Heparan sulfate, a glucosaminoglycan present in extracellular matrix, has been shown to be a cellular attachment factor that enhances cellular permissivity for FV entry into target cells [23]. FV replication is characterized by an early phase of proviral integration, followed by a late phase production of progeny virus [7]. Following viral attachment to the (as of yet unknown) cellular receptor, viral entry occurs via pH-dependent Env-mediated endocytosis [6, 7, 24]. The capsids then migrate through the microtubular network to the centrosome and begin to accumulate [2, 6, 7, 25]. FVs require active cellular replication for their own replication cycle, thus if cells are in the G_0 resting phase or arrested during the cell cycle, the capsids remain in the centrosome region [7, 26-28]. Once cells enter mitosis, the nuclear membrane breaks down and disassembled capsids yield DNA provirus that gains access to the chromosome [7, 27, 28]. Viral integrase mediates proviral integration into the host genome with no apparent preference of insertion sites [7]. FVs are less likely to integrate next to actively transcribed genes or into cellular promoters compared to other retroviruses [7, 29-32], a characteristic that makes them attractive candidates as viral vectors. The late phase begins as the integrated provirus usurps host machinery for transcription [5]. While Gag, Pol, Tas, and Bet are translated on free ribosomes in the cytoplasm, Env translation

takes place on endoplasmic reticulum ribosomes [7]. Capsid assembly takes place at the centrosome, and virion budding and release requires Env co-expression [2, 3, 8, 33]. FVs follow either exocytotic budding and/or budding at the plasma membrane, and in the case of FFV, both have been documented [3, 5, 7, 34, 35]. The exact time of reverse transcription into DNA is unknown, but capsids preassembled intracellularly contain reverse-transcribed DNA that is infective; this late RT step is more akin to hepadnavirus replication than other retroviruses [2, 3, 7, 13, 36]. FVs can take one of two routes following infection: remain integrated as a latent provirus or result in productive infection [2, 7]. FV-infected cells contain many viral DNA copies, both integrated and un-integrated into the host genome, suggesting a recycling pathway [3].

APOBEC3 host innate anti-FFV restriction

Various host innate antiviral restriction factors have been described as defenses against FV infection. Classes of restriction factors include tripartite interaction motif (TRIM5α, induces premature disassembly of viral capsids), apolipoprotein B mRNA editing enzyme (APOBEC3, edit complementary DNA – cDNA – during RT), tetherin (block particle release through cytoskeleton interference), and interferon (induces the previous three restriction factors) [5, 7, 37-39]. In the case of APOBEC3 (A3), studies have shown that A3 become incorporated into nascent viral particles and edit viral cDNA intermediates by deaminating C-to-U, which in turn leads to a lethal mutagenesis that renders the viruses non-infectious [5, 7, 19, 40]. Retroviruses have in turn evolved ways to counter these host restriction factors [41]. FFV and feline immunodeficiency virus (FIV) produce accessory proteins that inactivate feline A3 (feA3) proteins, either by binding and inactivation (in the case of FFV) or degradation (as is the case with FIV Vif) [14, 15, 17, 42, 43].

FV infection in the domestic cat (*Felis catus*) and other animal species

FVs are species-specific and have been reported in cows, horses, non-human primates (NHP), domestic and wild felids, and endogenous forms have been found in vertebrates as early as the Paleozoic era [1, 5, 7, 44-46]. Zoonotic transmission to humans is not reported, with the exception of a dead-end simian foamy virus (SFV) infection in humans occupationally exposed to NHP or involved in bush meat trade, where virus establishes latency in the face of a specific anti-SFV immune response [5, 47-54]. FFV (and FVs in general) establishes a persistent and lifelong infection in domestic cats that has historically been considered apathogenic [5, 7, 55-58]. This infection persistence is established even in the presence of a specific immune response, which is usually detectable 2-3 weeks post-infection [7, 56, 57, 59]. It is theorized that FVs are apathogenic due to the long period of co-evolution with their hosts, resulting in attenuated infection [1, 4, 5, 7, 60]. Following initial infection, replicating virus is shed in the saliva while proviral latency is established mainly in circulating white blood cells and lymphoid tissues, but can be detected in most tissues in the body (Chapter 2 and [55, 58, 59, 61]).

Transmission of FVs is primarily horizontal between animals through exposure to infectious saliva, and in the case of FFV, both biting during aggressive encounters as well as amicable grooming have been suggested as routes of transmission [58, 62-65]. The amount of virus shed in the saliva varies greatly between cats (Chapter 2 and [9, 56, 58, 59, 66]). Different species of NHP also shed virus in the saliva at varying levels. In one naturally FV-infected rhesus macaque study conducted in animals bred in a primate center, virus was shed in large quantities but in variable amounts between animals [67]. Another study assessing free-ranging macaque populations throughout Bangladesh found widely variable levels of replicating virus in buccal swabs [68]. Another study examining wild-source and naturally infected African green monkeys detected low levels of replicating virus sporadically in only one animal [69]. Replicating virus has been found in both stroma underlying basal epithelium of oral mucosa in African green monkeys and in surface epithelial cells from pharynx, tongue, and tonsil in rhesus macaques [60, 69].

FFV in utero transmission has been reported but it is not thought to be a main route of transmission [58]. In cows, transmission through milk has also been suggested [70]. FFV is widespread globally, with prevalence rates around the world between 8-80% [62, 71-80]. Variation is related to geography, the specific cat population sampled (feral versus domestic, young vs old, etc), and the specific assay used for detection which have varying rates of specificity and sensitivity. Risk factors for developing infection include aging and sex status (male) (Chapter 2 and [62, 81]).

In contrast to reports in the literature that FFV is apathogenic, there are studies documenting pathology in infected cats. In one report, experimentally FFV-infected cats developed histopathological changes in the kidneys and lungs almost 6 months after infection [59]. We have also found microscopic evidence of injury in the kidneys, lung, and brain of experimentally infected cats (Chapter 2). FFV has been isolated from cats suffering from renal and urinary syndromes [82-84], polyarthritis [85, 86], neoplasia [11, 12, 78, 87], and other viral infections including FIV [62, 63, 71], feline leukemia virus (FeLV) [88, 89], feline coronavirus (FCoV) [78, 90], feline calicivirus (FCV) and feline herspesvirus [9]. While SFV is also considered to be apathogenic in NHP, humans zoonotically infected with SFV show significant alterations in biochemical, hematological and leukocytic parameters [49].

Experimental FFV Infections

Experimental infection studies of specific-pathogen-free (SPF) cats with FFV are rare. Initial studies up to the mid 1980's focused on clinical monitoring and histology. Kasza and others reported non-SPF FFV-inoculated (subcutaneously, intramuscularly, and intraperitoneally) 2-4 week old cats were free of disease 3-5 months post-inoculation (p.i.) and displayed lymphocytosis and an enlarged mesenteric lymph node and thymus but this could not be tied to disease as the cats were also heavily parasite-infested [11]. Pedersen and others intra-articularly inoculated 4 month to 3 year old SPF and conventionally reared cats in order to

reproduce polyarthritic disease but failed to see evidence of disease following clinical and synovial fluid examination [85]. Pedersen has additionally experimentally inoculated cats but only generally described transmission taking place after co-housing cats over 2 years, the appearance of FFV antibodies in the blood 3 weeks p.i., lifelong infection, absence of clinical signs p.i., and a “normal” hemogram for up to 3 years p.i. [58]. Attention to experimental FFV infection again took place in the early 2000’s in the context of FV use as vaccine and gene delivery vectors. Alke and others experimentally inoculated FFV-negative 3-4 month old female cats with 10^6 FFV focus forming units (FFU), given intramuscularly. Cats were monitored for up to 86 days p.i. and blood, peripheral blood leukocytes, and saliva was collected to detect antibodies and re-isolate virus. Humoral kinetics over time, as shown by band intensity on immunoblots, was shown for Gag for only one animal but could not be determined for Bet. After utilizing radioimmunoprecipitation (RIPA) assays, Bet bands could be detected with increasing intensity over time and shown in 2 animals. Virus was re-isolated from saliva and peripheral blood lymphocytes (PBL) through co-cultivation with permissive and reporter cell lines. The authors also determined that FFV established a persistent infection even in the presence of neutralizing antibodies [56]. Schwantes and others developed and tested replication competent FFV-based vectors and compared to wild-type FFV infection in FFV-negative cats. The animals were monitored, and sera collected for 85 days p.i. to detect immunoglobulin G (IgG) by immunoblotting, and the authors found comparable immune response between vector and wild-type inoculated cats, although the detection of the Bet humoral response was again troublesome. Virus derived from the cloned plasmid was similarly re-isolated from saliva and peripheral PBL [91]. Weikel and others experimentally inoculated SPF cats in order to develop an FFV immunohistochemistry (IHC) assay and demonstrated Bet proteins in the cytoplasm of macrophages and fibrocytes of interstitial connective tissue of lymphoid tissues collected after euthanasia on 65 days p.i., and did not see evidence of pathology through histological examination of tissues [55]. In 2008, German and others experimentally inoculated 8 SPF cats

and monitored them for 168 days. Blood and saliva were collected for hematology and biochemistry, anti FFV-IgG response was measured by indirect ELISA, FFV viral load through a qPCR based on the polymerase gene, and euthanasia, necropsy, and tissue collection was performed at the end of the study. The authors reported that the animals remained healthy, showed no alterations in hematological and biochemical parameters, had a bi-phasic rise and decrease of virus in blood, and a bi-phasic trend in IgG response. Virus load was highest in lymphoid tissues, lung and salivary gland, and animals also showed a mild glomerulonephritis and interstitial pneumonia determined through histology. This study however, did not have negative control animals to compare findings to [59].

FFV use as a vaccine and gene therapy vector

Retroviruses have been used in the fields of vaccine and gene therapy vector development in part due to their ability to incorporate as proviruses into the host genome, resulting in transmission of viral genes to cell progeny. Lentiviruses (LV), gammaretroviruses (GV) and FVs have all been used as vectors for gene therapy with varying success [31, 92, 93]. Lentiviral vectors have an advantage over FV vectors in that they do not require active cell division to integrate into the host DNA [28]. However, GV and LV have the potential to cause gene dysregulation and oncogenicity depending on where in the host genome they integrate. For example, human patients undergoing stem cell therapy for SCID-X1, a genetic severe combined immunodeficient disease, developed leukemia following GV vector use [94]. Safety studies have also showed the potential for oncogenicity and enhancer activity in GV and read-through transcription in GV and LV [30, 32]. GVs also show a high frequency of insertions near transcription start sites (TSS) in and near proto-oncogenes [31] and LV have also been found to integrate near TSS and units of active transcription [95]. In comparison, FVs were found to have a safer integration profile compared to GV and LV [29, 31, 32, 96]. Additionally, FVs have been found to have similar stem cell transduction efficiencies as LV [96]. FVs packaging capacity is

ideal, due to relatively small genome size, and self-inactivating properties which can be engineered into the vectors for enhanced safety and less capacity for recombination [97-101].

Taken in combination with the fact that FVs establish apparently apathogenic infections with wide tissue tropism, and in the case of FFV pose no zoonotic risk, it is not surprising FVs are an attractive option for developing vectors. Research into use of FV vectors can yield opportunities for therapeutic technologies in both humans and animals [102]. Some documented examples of FV use in this capacity include anti-HIV therapeutics in humans, canine leukocyte adhesion deficiency, canine SCID, FCV vaccinology, and stem cell technologies [96, 97, 103-107].

FFV and chronic kidney disease in domestic cats

As mentioned earlier, experimentally FFV-infected cats show evidence of renal histopathological changes and FFV has been isolated from cats suffering renal and urinary diseases. Chronic kidney disease (CKD) is the renal disease most commonly affecting pet cats, and its incidence increases as animals age, reaching up to 81% prevalence rates in cats over the age of 15 [108-111]. CKD develops following either acute or chronic insults to the kidneys, leading to functional and structural loss of kidney tissue [112-116]]. The renal lesions most commonly associated with CKD in cats are tubular degeneration and atrophy, interstitial fibrosis, mononuclear cell infiltration, and Bowman's capsule and tubular membrane mineralization [114, 115, 117, 118]. Glomerulopathies are much less common than tubulointerstitial disease and, if present, focal segmental glomerulosclerosis is usually the predominant manifestation [115]. Cats affected by CKD present with varying degrees of azotemia (increased blood urea nitrogen and creatinine), improperly concentrated urine, proteinuria, and increased urine:protein creatinine (UPC) ratio [112, 113]. CKD severity is classified in stages by the International Renal Interest Society (IRIS) based on severity of azotemia, proteinuria, and hypertension [113, 119]. Clinically, cats present with non-specific signs such as lethargy and anorexia, later progressing to polyuria (frequent urination), polydipsia (frequent water drinking), vomiting, uremic syndrome,

retinal detachment, anemia, hypertension, hyperparathyroidism and others as severity of disease progresses [113, 116, 118, 120].

While the specific etiology of CKD is unknown, both congenital or acquired syndromes can lead to the development of CKD [112, 114]. Primary or congenital causes for CKD, such as polycystic kidney disease and renal dysplasia, are considered much less common than acquired causes which include nutritional, toxic, neoplastic, immune-mediated, bacterial, and viral etiologies [112, 114]. Risk factors for development of CKD include aging, breed, gender (some male populations), hypertension, cardiovascular disease, endocrine disease, and urinary tract infections [112, 114]. FIV and FeLV infections have been linked to CKD. FIV infection causes renal amyloidosis, immune complex glomerulopathy, glomerulosclerosis and proteinuria, leading to the development of CKD [121-123]. Immune complex glomerulonephritis has been reported in cats suffering from FeLV and myeloproliferative neoplasms [82].

Domestic cats experimentally infected with FFV developed a glomerulonephritis characterized by increased cellularity in the glomerular tufts and adhesions between Bowman's capsules and glomerular tufts in addition to showing mitoses, sloughed material into tubular medullary tubules, and syncytia formation [59]. In addition, cats suffering from urinary disease have been positive for FFV [9, 59, 78, 83, 84, 124-126].

FIV infection in domestic cats and co-infection with FIV

FIV is a complex retrovirus belonging to the lentivirus subfamily with a global distribution [127]. Like FFV, its genome contains the canonical *gag*, *pol*, and *env* genes, but with different accessory genes *vif*, *rev*, and *orfA* [128, 129]. The gene *vif*, or viral infectivity factor, is involved in countering host innate viral restriction factors (like A3) through proteasomal degradation as described earlier [43]. As opposed to FFV, FIV reverse transcription occurs early, before proviral integration into the host genome (Table 1) [127, 130]. FIV infects T lymphocytes early in infection and macrophages in chronic stages [131-133]. FIV leads to an immunodeficient state

in some cats which predisposes them to secondary infections and neoplasia through a progression of three clinically distinct phases [63, 131, 134-139].

While not as highly prevalent as FFV, FIV can be detected in up to 30% of at-risk cats [63, 136, 138, 140]. Similarly to FFV, the main transmission route for FIV is through saliva via biting during aggressive encounters [63, 127, 139]. In addition to the risk factors seen in FFV of aging and male sex, outdoor access and increased exposure to other cats and fighting is also associated with FIV infection (Table 1) [62, 63, 136, 138, 140].

Co-infection between FFV and FIV is very common, with up to 90% of FIV-infected cats testing positive for FFV [62, 63, 71]. FFV/FIV co-infection experimental studies are rare and have not documented viral kinetics over time during infection or assessed chronic timelines of disease progression [141]. Studies assessing potentiation of infection and disease in NHP co-infected with simian foamy virus (SFV) and simian immunodeficiency virus (SIV) have found increased SIV-related morbidity and mortality, and expanded SFV tissue tropism [67, 142]. In a recent report, FFV was found to be associated with FeLV progression and FCoV infection [88]. Cats co-infected with FFV and either FIV or FeLV might therefore suffer more serious disease consequences than cats with single infection, which could impact the health of cats and could also be factor for at-risk cats for developing CKD.

Table 1. Comparison of FFV and FIV.

	FFV	**FIV**
Subfamily	*Spumaretrovirinae*	*Orthoretrovirinae*
Genus	*Spumavirus*	*Lentivirus*
Infective form	DNA	RNA
RT Step	Late	Early
Anti-A3 gene/Protein	*bet*/Bet	*vif*/Vif
Latency	Lymphocytes, others?	Lymphocytes
Duration of infection	Lifelong	Lifelong
Clinical disease	Contested but considered apathogenic	+/- Immunosuppression, death
Risk factors	Age, male sex	Age, male sex, outdoor access
Transmission (main)	Saliva, friendly grooming?	Saliva, biting
Prevalence	Up to 80%	Around 30% in at-risk cats
Zoonotic	No	No
Viral vector use	Yes	Yes

Dissertation research

My dissertation research is composed of three aims investigating FFV biology, use as a vaccine vector, and interaction with other feline disease syndromes. The first aim (Chapter 1) was to investigate the use of FFV as a vaccine vector as part of an FFV-FIV chimeric vaccine vector that contained the full FIV *vif* gene replacing a truncated FFV *bet* gene. My collaborators generated the infective FFV-Vif chimeras that I tested in SPF cats. I compared viral replication kinetics and specific immune response against FFV Gag and Bet and FIV Vif and found that replication of the FFV-Vif chimera was attenuated in vivo, yet the cats mounted a persistent antibody response towards all FFV and FIV proteins, indicating functional replication of viruses after experimental inoculation. We also noted the capacity of FFV to superinfect the same host after an already established FFV infection, providing an opportunity for vaccine development in pet cat populations that may have already been exposed to FFV.

For the second aim (Chapter 2), I further characterized wild-type FFV infection due to its high prevalence around the world, and to validate reports associating FFV with other diseases in domestic cats. We specifically searched for evidence of pathology and sought to characterize infection to expand what is already reported in the literature. Since FVs are being used to develop vaccines and gene therapy, we felt it necessary to further determine if these viruses are truly apathogenic. I found mildly altered hematological and biochemical parameters potentially associated with renal injury, microscopic changes in the lung and brain, and ultrastructural changes in the kidney. Due to these results, I conducted a survey of FFV in pet cats suffering from CKD and found an association in male cats.

For the third (Chapter 3), we hypothesized that FFV and FIV are associated, and that viral kinetics and/or FIV-associated disease is potentiated during co-infection. I conducted a serosurvey of naturally FIV-infected cats that suffered different outcomes of disease and determined FFV prevalence in these animals. We also found associations between FFV and FIV and in male cats. Based on these results I conducted in vitro assays to determine if the

viruses were potentiating each other as measured by increasing presence of virus and cytopathic effects. My in vitro experiments show that after initial infection with either FFV or FIV, the secondary virus' kinetics are accelerated and enhanced, while kinetics of the initial virus is sometimes slightly dampened by the secondary virus. These results indicate further research regarding interactions of FFV and other viruses is needed.

CHAPTER 1. FFV USE AS A VACCINE VECTOR[1]

Summary

Background: Hosts are able to restrict viral replication to contain virus spread before adaptive immunity is fully initiated. Many viruses have acquired genes directly counteracting intrinsic restriction mechanisms. This phenomenon has led to a co-evolutionary signature for both the virus and host which often provides a barrier against interspecies transmission events. Through different mechanisms of action, but with similar consequences, spumaviral feline foamy virus (FFV) Bet and lentiviral feline immunodeficiency virus (FIV) Vif counteract feline APOBEC3 (feA3) restriction factors that lead to hypermutation and degradation of retroviral DNA genomes. Here we examine the capacity of *vif* to substitute for *bet* function in a chimeric FFV to assess the transferability of anti-feA3 factors to allow viral replication.

Results: We show that *vif* can replace *bet* to yield replication-competent chimeric foamy viruses. An in vitro selection screen revealed that an engineered Bet-Vif fusion protein yields suboptimal protection against feA3. After multiple passages through feA3-expressing cells, however, variants with optimized replication competence emerged. In these variants, Vif was expressed independently from an N-terminal Bet moiety and was stably maintained. Experimental infection of immunocompetent domestic cats with one of the functional chimeras resulted in seroconversion against the FFV backbone and the heterologous FIV Vif protein, but virus could not be detected unambiguously by PCR. Inoculation with chimeric virus followed by wild-type FFV revealed that repeated administration of FVs allowed superinfections with enhanced antiviral antibody production and detection of low level viral genomes, indicating that chimeric virus did not induce protective immunity against wild-type FFV.

[1]Chapter published as: Ledesma-Feliciano C, Hagen S, Troyer R, Zheng X, Musselman E, Slavkovic Lukic D, Franke AM, Maeda D, Zielonka J, Münk C, Wei, G, VandeWoude S, Löchelt, M: **Replacement of feline foamy virus *bet* by feline immunodeficiency virus *vif* yields replicative virus with novel vaccine candidate potential.** *Retrovirology* 2018, **15:**38.

Conclusions: Unrelated viral antagonists of feA3 cellular restriction factors can be exchanged in FFV, resulting in replication competence in vitro that was attenuated in vivo. Bet therefore may have additional functions other than A3 antagonism that are essential for successful in vivo replication. Immune reactivity was mounted against the heterologous Vif protein. We conclude that Vif-expressing FV vaccine vectors may be an attractive tool to prevent or modulate lentivirus infections with the potential option to induce immunity against additional lentivirus antigens.

Background

Foamy viruses (FVs) are ancient retroviruses comprising the only genus of the subfamily *Spumaretrovirinae,* which are different in many aspects from the *Orthoretrovirinae* that comprise all other known retroviruses including lentiviruses (LVs) [2, 3, 7]. Despite having a wide tissue tropism in infected animals, FVs have historically been regarded as apathogenic and are endemic in primates, bovids, felids, and other hosts. Clusters of highly related viruses have been documented in closely related hosts [5, 55, 59, 143]. While humans do not have endemic FVs, they are susceptible to zoonotic infections from non-human primates [51, 144]. FVs and LVs such as feline immunodeficiency virus (FIV) have been used to develop vectors for vaccine antigen delivery and gene therapy in a variety of mammals [96, 97, 102, 105, 145-148]. In domestic cats (*Felis catus*), feline foamy virus (FFV) and FIV establish lifelong infections despite specific host antiviral immune responses [56, 63, 139, 149]. In contrast to FFV infection, FIV infection leads to the development of an immunosuppressive AIDS-like syndrome in some cats [63, 134, 136, 138, 149]. Thus, FVs are an attractive alternative to LV vectors due to their apathogenicity, wide tissue tropism, and establishment of a persistent infection with ongoing virus gene expression and replication [55, 56, 58, 59, 91, 145, 146]. Another advantageous feature of FV-based vectors is a safer integration profile than gammaretroviral and LV vectors [29, 96], a large packaging capacity, and the ability to introduce self-inactivating properties [97-

101]. Investigating FV vector candidates could thus yield potential new therapies to benefit both humans and animals [102].

Both LVs and FVs are complex retroviruses encoding the canonical Gag, Pol, and Env proteins, regulatory proteins essential for replication in all cells, and accessory proteins required only in certain cells. For instance, LV Tat and FV Tas (also designated Bel1) proteins are both transactivators for virus gene expression, however, their mode of action is completely different (for review [20]). Regardless, both regulatory genes induce a positive feedback loop to generate more transactivator protein in addition to transcription of structural genes required for infectivity [20]. FVs additionally encode Bet that is generated via splicing, consisting of N-terminal Tas sequences while the majority of the protein is encoded by another reading frame, the *bel2* gene [20]. Bet is the functional homologue of the LV Vif protein, both of which are involved in countering the host intrinsic antiviral restriction factors of the APOBEC3 (A3) family [14-19].

Like all other viruses, LVs and FVs are restricted by intrinsic cell mechanisms that impair or even suppress the different phases of virus replication, progeny production, and establishment of infection in the new host (for review see [41, 42]). Nonspecific innate immunity and cell-based intrinsic immunity employing antiviral restriction factors are both absolutely required to control pathogen replication before adaptive immunity matures for long-term suppression of viral replication [150, 151]. Therefore, a fine-tuned crosstalk between innate, intrinsic, and adaptive immunity is needed to control and eliminate the pathogen as well as to build up immunological memory [150-152]. Pathogens have evolved a plethora of counteracting strategies in order to evade this control, often by the acquisition of counteracting proteins [41, 42]. The idea and concept of host-encoded restriction factors and the viral counter-defense have been in part established in human immunodeficiency virus (HIV) research. These initial studies analyzed the interplay between host-encoded A3 cytidine deaminases that result mainly in lethal mutagenesis (C to U/T exchanges) of the retroviral HIV genome during reverse transcription, and the counter-

defense by LV Vif (or Bet in FVs) which result in A3 degradation (via Vif) or sequestration (via Bet) [14, 15, 17, 42, 43].

Analogous to human A3 function, feline A3 (feA3) proteins are produced in many cell types and introduce missense and stop mutations into nascent viral genomes, ultimately restricting viral replication through hypermutation and degradation [14, 15, 41]. Several studies on the function of FIV Vif and FFV Bet, which are of very different size and share no obvious sequence or structural homology [17, 19, 153], have revealed that they employ completely different modes of action to achieve the same end goal: preventing the packaging of feA3 proteins into the particle to avoid subsequent viral lethal mutagenesis. The FIV Vif protein (25 kDa) functions as an adapter molecule, binding to cognate or highly-related feA3 proteins and recruiting the ubiquitin proteasome degradation machinery, resulting in the removal of feA3 proteins from the virus-producing cell [43, 154-157]. This is the critical prerequisite to prevent cytidine deamination during or after reverse transcription of the genome. In contrast, FV Bet proteins (of 43 to 56 kDa) tightly bind A3 proteins of their cognate host species without leading to degradation, likely acting via sequestration or blocking of essential binding and multimerization sites [14, 17, 18, 153]. Therefore, *vif* and *bet* are essential viral genes required to allow productive replication in cells with active A3 expression [34, 41, 158].

Domestic cats produce multiple A3 proteins in one and two-domain forms. One-domain feA3 proteins include the A3Z2 (present as A3Z2a, A3Z2b, and A3Z2c) and A3Z3 isoforms, while read-through transcription leads to the production of two-domain feA3Z2-Z3 proteins (in A3Z2b-Z3 and A3Z2c-Z3 isoforms) [159]. These feA3 proteins have differential effects on FFV and FIV: A3Z2s markedly reduce titers of FFV lacking *bet*, while the A3Z3 and A3Z2-Z3 proteins inhibit FIV virions lacking *vif* with intermediate and high efficiency, respectively. Interestingly, both Bet and Vif counteract all feA3 regardless of whether the specific A3 isoforms efficiently restrict FFV or FIV [14, 15, 43, 154, 155, 159], suggesting a more complex relationship between these accessory genes and host restriction factor regulation than has yet been described.

Here we describe the generation and in vitro selection of FFV-Vif chimeras in which FIV *vif* partially or almost fully restored the replication capacity of *bet*-deficient FFV constructs in vitro. An in vitro-selected FFV-Vif variant that drives expression of the heterologous lentivirus Vif independent from any FFV protein and which is highly dependent on Vif expression in A3-producing cells, was used for infection of domestic cats to test the chimera's replication competence and immunogenicity. Replication of the FFV-Vif chimera was attenuated in cats compared to wild-type FFV. Cats infected with the FFV-Vif chimera developed persistent antibody responses towards FFV proteins and FIV Vif but proviral FFV-Vif chimeric genomes were at or below the limit of detection in peripheral blood mononuclear cells (PBMC) of infected cats. In contrast, proviral genomes were consistently detected in wild-type FFV-infected cats. Inoculation of cats in the FFV-Vif chimera cohort with wild-type FFV or re-inoculation with FFV-Vif chimeric virus boosted anti-FFV Gag antibody titer following re-infection. These results suggest that compensatory changes arising in vitro seemingly allowed FIV-Vif to substitute for FFV-Bet function but were incapable of fully supporting FFV-Vif chimeric replication competence in vivo. These findings additionally suggest the capacity of spumaviruses to superinfect cats following prior attenuated FFV replication, indicating the potential suitability of chimeric FFV as a vaccine vector in the face of a pre-existing infection and immunity.

Results

FIV Vif and FFV Bet confer protection from feA3 restriction in vitro

Previous studies have shown that the FIV Vif accessory protein has the capacity to direct proteasomal degradation of all known feA3 cytidine deaminase restriction factors irrespective of whether they strongly or moderately restrict FIV replication [43, 154, 155, 159]. Similarly, FFV Bet binds to all feA3 isoforms and inactivates their restriction potential by a degradation-independent, different mechanism not comparable to FIV Vif [14, 15]. In addition, FIV Vif can

protect the replication capacity of *bet*-deficient FFV while FFV Bet correspondingly counteracts feA3-mediated restriction of *vif*-deficient FIV [41, 43].

To confirm here that the viral defense proteins of FFV and FIV are functionally interchangeable to protect infectivity against feA3 restriction [14, 15, 43, 154, 155, 159], transient transfection studies were conducted, and representative data are shown here. First, we analyzed the susceptibility of FIV**Δ***vif*-luc, a *vif*-deficient FIV luciferase (luc) expression vector ("Methods", [43]) towards one-domain feA3Z3, and two-domain feA3Z2-Z3 isoforms (Appendix File 1A). The efficacy of *luc* marker gene transduction was determined in the presence of co-transfection with FFV *bet*, FIV *vif,* or an empty control vector. Both FIV Vif and FFV Bet restored the FIV vector titer almost fully while different levels of feA3-mediated restriction were detectable only in the absence of any viral defense protein. Similarly, the replication competence of the *bet*-deleted and feA3-sensitive pCF7-BBtr FFV mutant (Table 1, [91]) was rescued by Bet and Vif. In the absence of Vif and Bet proteins, the expression of the feA3Z2b isoform strongly suppressed the titers of *bet*-deficient pCF7-BBtr (Appendix File 1B). This antiviral restriction by feA3Z2b was partially or fully abrogated by co-expression of either FFV Bet or FIV Vif, respectively.

Substitution of FFV Bet by functional Vif confers FFV replication competence in feA3 expressing cells

To initially assess whether FFV Bet could be functionally replaced by FIV Vif, resulting in feA3-resistant FFV variants, *bet* sequences downstream of the essential *tas* transactivator gene (at Bet amino acid 117) in the full-length FFV clone pCF7-BetMCS (Table 1) [34, 91] were replaced by a codon-optimized FIV *vif* gene [43, 159] shown schematically and in detail in Fig. 1A and Appendix File 2.

Table 1. Viral clones and stocks used in this study.

Clones	Viral Stock Name[+]	Major mutation	Effect on Replication (CrFK)
pCF-7 [91]	[‡]wild-type FFV	-	-
pCF7-BBtr	FFV-BBtr	Truncation at Bet amino acid 117	Fully susceptible towards feA3-mediated restriction in vitro
pCF7-BetMCS [34]	FFV-BetMCS	Insertion and replacement of Bet residues at amino acid 117 by insertion of a multiple cloning site	Fully susceptible towards feA3-mediated restriction in vitro
pCF7-Vif-4	FFV-Vif-4	Engineered Bet-Vif fusion protein	Partially susceptible towards feA3-mediated restriction in vitro
pCF7-Vif-39	FFV-Vif-39	Spontaneous frameshift	Fully susceptible towards feA3-mediated restriction in vitro
pCF7-Vif W/*1	[‡]FFV-Vif W/*1	Trp to Stop mutation (TGG to TGA), unlinked *vif* gene	Enhanced, compared to pCF7-Vif-4
pCF7-Vif W/*2	FFV-Vif W/*2	Trp to Stop mutation (TGGG to TAGA), unlinked *vif* gene	Enhanced, compared to pCF7-Vif-4
pCF7-Vif W/*1 M+	-	Optimized upstream Met codon in pCF7-Vif W/*1	Similar to pCF7-Vif W/*1
pCF7-Vif W/*2 M+	-	Optimized upstream Met codon in pCF7-Vif W/*2	Similar to pCF7-Vif W/*2
pCF7-Vif W/*1 M/T	-	Upstream Met codon mutated to Thr in pCF7-Vif W/*1	Similar to pCF7-Vif W/*1
pCF7-Vif W/*2 M/T	-	Upstream Met codon mutated to Thr in pCF7-Vif W/*2	Similar to pCF7-Vif W/*2

[+]FFV-Vif variants collectively referred to as “FFV Vif chimeras”
[‡]Viral stocks used in domestic cat infection experiments

Similar to other Bet fusion proteins engineered in the FFV proviral context [91, 145], an FFV protease (PR) cleavage site was introduced between the truncated N-terminus of Bet and the intact FIV *vif* gene start codon. Gene swapping did not affect FFV *tas*, and we have previously demonstrated that the N-terminal Bet sequence retained in the pCF7-Vif clones does not counteract feA3-mediated restriction of FFV replication [153]. Sequencing of resultant clones was conducted to confirm the genetic identity and correctness of the newly created clone pCF7-

Vif-4 (Table 1). A spontaneous frame shift mutation arose in subclone pCF7-Vif-39 (Table 1), abrogating Bet^{tr}Vif fusion protein expression completely, making this clone suitable for use as a negative control.

Plasmids pCF7-Vif-4, pCF7-Vif-39, and parental wild-type FFV full-length pCF-7 genome (Table 1) were transfected into human embryonic kidney (HEK) 293T cells. Supernatants were passaged twice on Crandell feline kidney (CrFK) cells (known to express feA3 [159]) to assess the ability of the chimeras to replicate in feline-origin cells. The full-length Bet^{tr}Vif fusion protein and the mature Vif processing products were stably expressed by clone pCF7-Vif-4 which was, as expected, not the case for the frame shift mutant pCF7-Vif-39 (Fig. 1B, top panel). FFV Bet was only expressed by the wild-type pCF-7 genome upon transfection and serial passages (Fig. 1B, middle panel). Similar amounts of full-length FFV p52^{Gag} and the processed p48^{Gag} were synthesized by pCF7-Vif-4 and wild-type pCF-7 in transfected HEK 293T and infected CrFK cells while in clone pCF7-Vif-39, Gag expression was almost lost at the second CrFK cell passage (Fig. 1B, bottom panel). The loss of Gag expression of clone pCF7-Vif-39 was paralleled by a very rapid decline of infectivity (Fig. 2A). In contrast, titers of pCF-7 were higher than those of pCF7-Vif-4 and none of them showed a sharp decline of viral infectivity. These data indicate that intact FIV *vif*-chimeric pCF7-Vif-4 is replication-competent in feA3-positive CrFK cells, albeit at lower efficiency than wild-type FFV (Fig. 2A).

Passage through CrFK enhances FFV-Vif chimera replication efficiency

We continued passaging progeny of wild-type pCF-7 and chimeric pCF7-Vif-4 (see above, Fig. 2A) for 20 passages in order to use in vitro selection and evolution to obtain FFV-Vif variants with higher replication capacity in the presence of the feA3 proteins endogenously expressed in CrFK cells [14]. During the first seven passages, wild-type pCF-7 displayed titers between 10^6 and 10^7 focus-forming units per ml (FFU/ml) (Fig. 2A). During this phase, infectivity of the chimeric clone pCF7-Vif-4 was approximately one to two logs lower (10^4-10^6 FFU/ml).

Starting at passage eight, however, titers of pCF7-Vif-4 progeny approached that of wild-type pCF-7, indicating emergence of pCF7-Vif variants with enhanced replicative ability in vitro (Fig. 2A). Selected samples harvested during CrFK passaging were analyzed for FFV Gag and Vif expression (Fig. 2B). FFV Gag expression was consistently detectable in all cell lysates using FFV reference serum from cat 8014 (Fig. 2B, middle panel). Early, during viral passages 2 and 5, the Bet^{tr}Vif fusion protein and its proteolytic cleavage products were the primary Vif-reactive proteins detectable. At passage 10, Bet^{tr}Vif became undetectable and the Vif protein of approximately 25 kDa was detected, along with additional Vif-reactive bands of higher molecular mass. At passage 15, mostly Vif proteins in the 25 kDa size range were identified (Fig 2B, top panel).

To detect potential adaptive genetic changes in the FFV genome, DNA was prepared from FFV-Vif-4-infected CrFK cells at passage 18 and used as template for PCR to amplify and clone the complete *bet^{tr}vif* region. In seven of nine amplicons, a tryptophan codon (TGG, Trp) located in the *bet* sequence 50 codons upstream of the *vif* ORF had mutated to become TAG and TGA stop codons (Fig. 2C and Appendix File 2). These changes were transitions of either the first or second G residue to an A (Fig. 2C, top panel) yielding two different stop codons, indicated by an asterisk (*), as either a TGA (five out of seven sequences, designated W/*1) or a TAG stop codon (two out of seven sequences, designated W/*2). In the five clones that had incorporated the TGA stop codon in the *bet* sequence, a G172R mutation in the overlapping Tas-coding sequence occurred. In the two TGG to TAG mutants, a G residue following the TGG codon was also changed to A (i.e. TGGG was altered to TAGA). This resulted in a G172L exchange in Tas and a D/N change directly downstream of the new *bet* stop codon. All nucleotide exchanges correspond to C/T exchanges of the antisense strand in a sequence context PyPyC (Fig. 2C; Py=pyrimidine residue), corresponding to the canonical A3 mutation context in retroviral genomes [14, 40]. Additional genetic changes were not consistently detected in the *bet^{tr}vif* region.

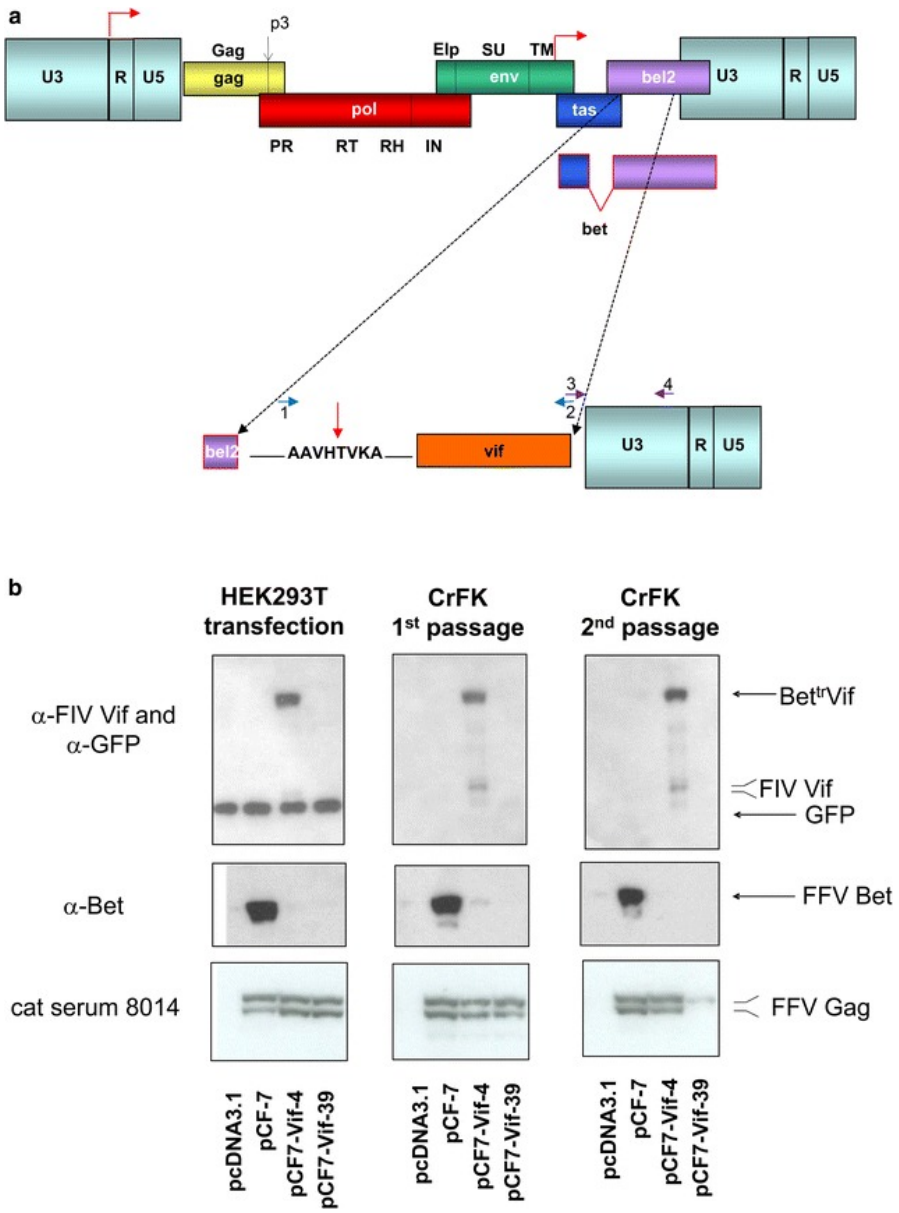

Figure 1. Schematic presentation of the construction of FFV-Vif chimeras and their molecular features. a Schematic presentation of the FFV genome with its genes and protein domains as well as the LTR and internal promoters (red bent arrows, top) and presentation of the engineered Bet^{tr}Vif fusion protein (bottom). The non-functional N-terminus of *bet* (purple) was fused in-frame to the codon-optimized FIV *vif* gene including the *vif* ATG start codon. A short linker encompassing the FFV PR cleavage site (vertical red arrow, bottom) was inserted between the N-terminus of Bet and Vif. Primer pairs used to insert the *vif* gene into the FFV genome are shown in blue and violet and with numbering in the bottom panel. **b** HEK 293T cells were transfected with wild-type pCF-7, functional clone pCF7-Vif-4, non-functional clone pCF7- Vif-39, and pcDNA3.1 control DNA. Two days after transfection, cell culture supernatants and cells were harvested as described in the “Methods” section. Cleared supernatants were used for serial passaging in feA3-expressing CrFK cells and FFV titer determination (Fig. 2A). At 3 days p.i., infected CrFK cells and supernatants were harvested and used as above. Cell lysates from transfected HEK 293T cells and CrFK cells after the first and second passage were subjected to immunoblotting against FIV Vif and co-transfected GFP, FFV Bet, and FFV Gag (cat serum 8014). The positions and names of the detected proteins are given at the right margin.

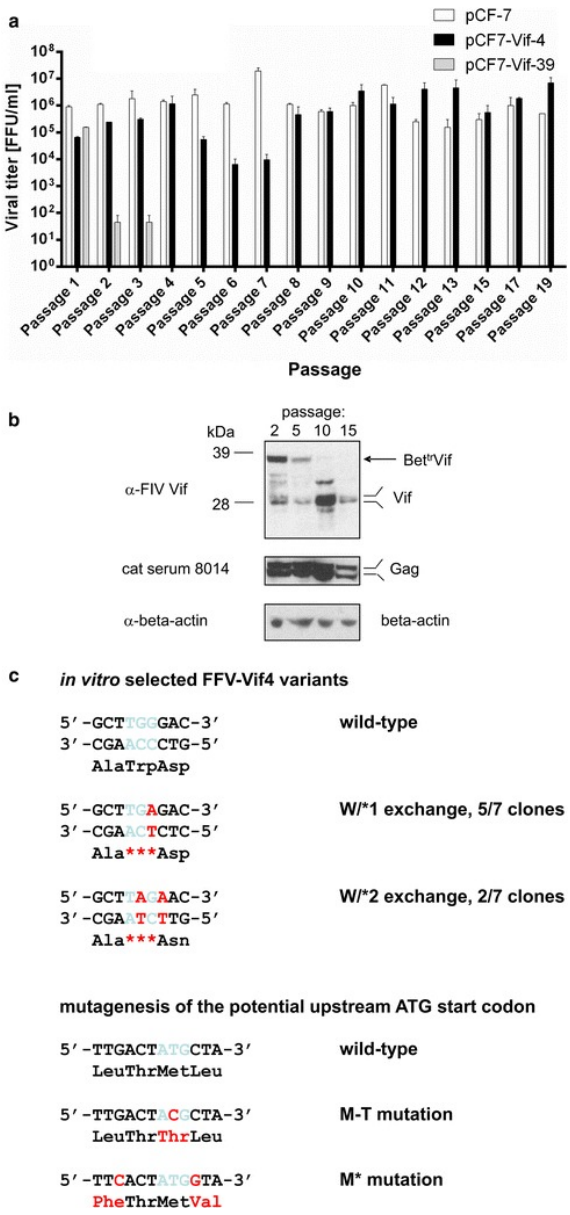

Figure 2. In vitro selection and molecular characterization of pCF7-Vif-4 variants with increased replication competence. Plasmid pCF7-Vif-4, -39, and pCF-7 were transfected into HEK 293T cells. Two days after transfection, cell-free supernatants were inoculated on CrFK cells and serially passaged twice a week on CrFK cells (every 3 or 4 days) as described above for Fig. 1B. **a** FFV titers were determined in duplicate using FeFAB reporter cells and are shown as bar diagram for selected passages over time. Error bars represent the standard deviation. **b** Selected cell extracts from the CrFK passages were subjected to immunoblotting. The immune-detection with a Vif-specific antiserum initially showed mainly the engineered Bet^{tr}Vif and the proteolytically released Vif, then various unidentified Vif variants, and finally (passages 10 and 15) predominantly the authentic Vif protein. FFV Gag proteins were detected in all samples as expected using cat antiserum 8014 while in the bottom panel the β-actin loading control is shown. **c** Sequence context of the in vitro-selected W/* mutations (light blue original Trp to the stop codon in red) suggests feA3 editing of the minus strand of FF7-Vif-4-derived reverse transcription intermediates in the PyPyC sequence context (top panel, Py=pyrimidine residue). Below, mutagenesis of the in-frame ATG 14 codons upstream of the *vif* gene is shown only for the sense strand (bottom panel). The ATG start codon is shown in light blue and the engineered residues and changes amino acids are in red.

Unlinking vif from bet by Trp/stop mutagenesis is essential for increased infectivity

The importance of the identified Trp/stop (W/*) mutations upstream of the *vif* sequence was analyzed using reverse genetics. Both W/* mutations in the *bel2* linker sequence upstream of *vif* were inserted into the original pCF7-Vif-4 to determine whether they represent adaptive mutations increasing the titer of the corresponding FFV-Vif chimera. These clones were named pCF7-Vif W/*1 (TGG/TGA) and pCF7-Vif W/*2 (TGG/TAG, Table 1).

An additional outcome of the W/* mutations was the “emergence” of an in-frame ATG codon between the new W/* stop codon and the authentic *vif* start codon (Appendix File 2). To test whether this ATG codon could serve as an alternative translational initiation codon for the inserted *vif* gene, this Met ATG was replaced in the engineered pCF7-Vif W/*1 and –W/*2 clones and the parental pCF7-Vif-4 clone by a threonine (Thr) codon (suffix M/T, see Fig. 2C lower panel and Table 1). In addition, and as a complementing strategy, the surrounding nucleotide sequence of this ATG codon was converted to an optimal Kozak translational initiation context sequence (GCCA/GCCATGG, start codon underlined, [160]) as shown in Fig. 2C, lower panels. The corresponding clones are labeled by the suffix M+ (Table 1). The M/T mutation resulted in a silent mutation at the *tas* C-terminus while the change to a Kozak sequence resulted in two amino acid exchanges in *tas* at the C-terminus, i.e. D206H and A208G, and, in addition, a leucine to phenylalanine (L/F) exchange upstream, and a leucine to valine (L/V) exchange directly downstream of the potential Met start codon in the linker sequence (see Fig. 2C).

Transient co-transfection studies using a luc FFV LTR reporter construct together with either a CMV-IE promoter-driven Tas expression clone and a CMV-IE-driven β-gal plasmid or the FFV genomes pCF-7, pCF7-Vif-4, pCF7-Vif W/*1, and the different M/T and M+ derivatives thereof were conducted. While the CMV-IE promoter-driven Tas expression clone yielded very high luc activities, the genomic wild-type and chimeric proviral FFV clones described above did not show

significant differences in Tas transactivation, indicating that the mutations introduced do not significantly influence overall transactivation and gene expression (Appendix File 3).

Clones pCF7-Vif W/*1 and -W/*2 and the different M/T and M+ derivatives were transfected into HEK 293T cells and supernatants were tested for the replication competence of the FFV-Vif chimera in feA3-positive CrFK cells by serial CrFK cell passaging as described above. Serial passaging after either 60 h or 84 h (Appendix File 4A and 4B) showed similar outcomes: the pCF-7-encoded wild-type FFV had slightly higher titers (about 5-fold) than mutants pCF7-Vif W/*1 and –W/*2 and their derivatives. For these clones and the corresponding M/T and M+ clones, titers were stable during serial passages. This was not the case for the original pCF7-Vif-4 clone encoding the Bet^{tr}Vif fusion protein, where titers steadily and reproducibly declined upon serial passages in several independent experiments. The data show that both W/* mutations in the FFV *bet* sequence upstream of the *vif* gene cause in feA3-expressing CrFK cells a clear increase of replication competence compared to the pCF-Vif-4 encoding the Bet^{tr}Vif fusion protein. However, the replication competence of the pCF7-Vif W/*1 and –W/*2 clones was slightly lower than that of the wild-type FFV genome pCF-7. In addition, the FFV-encoded, in-frame ATG codon located 14 codons upstream of *vif* is probably not used as a start codon for Vif protein expression since its replacement by a Thr codon, or the optimization of the surrounding residues towards more efficient translational initiation, did not significantly affect viral titers.

*Reduced steady state levels of feA3Z2b by FFV-Vif chimeric clones pCF-Vif-4 and pCF7-Vif W/*1 and –W/*2*

Co-transfection experiments were conducted to study whether the steady state levels of feA3Z2b are decreased by Bet^{tr}Vif fusion protein or the authentic Vif encoded by FFV-Vif chimeric clones pCF-Vif-4 or pCF7-Vif W/*1 and –W/*2, respectively (Table 1). As indicated in Fig. 3 (bottom panel), parental wild-type FFV full-length pCF-7 genome and FFV-Vif chimeric

clones pCF-Vif-4, pCF7-Vif W/*1, and –W/*2 were transfected into HEK 293T cells together with a plasmid encoding HA-tagged feA3Z2b (the major feA3 restriction factor of Bet-deficient FFV) [14, 15]. Cells transfected with the plasmid encoding feA3Z2b and pcDNA as well as pcDNA-only-transfected HEK 293T cells served as controls. Cellular antigens were harvested two d after transfection and subjected to immunoblotting (Fig. 3). The control blots conducted confirm proper loading of samples (anti β-actin, bottom panel) and comparable expression of FFV proteins in wild-type and chimeric FFV provirus-transfected samples and Bet^{tr}Vif fusion proteins and FIV Vif by FFV-Vif chimeric clones pCF-Vif-4 and pCF7-Vif W/*1 and –W/*2, resp. (anti FFV Gag and anti FIV Vif, middle panels). As expected and previously shown [14, 15], the steady-state levels of HA-tagged feA3Z2b were not significantly affected by co-expression of wild-type FFV expressing Bet (anti HA, top panel, compare lanes 2 to 3 and 8 to 9). In stark contrast, levels of HA-tagged feA3Z2b were reproducibly and strongly reduced in cells expressing either Bet^{tr}Vif and/or authentic FIV Vif (compare lane 2 to 4, 5, and 6 and lane 8 to 10, 11, and 12 in Fig. 3, top panel). In another and independent experiment with a highly similar outcome, only co-transfection of CMV-IE promoter-based and codon-optimized FIV Vif expression plasmids reduced feA3Z2b to undetectable levels (data not shown). In summary, the data clearly support the conclusion that the Vif protein in the FFV-Vif chimeric clones leads to decreased steady state levels of feA3Z2b, most probably via proteasomal degradation [15, 43, 154, 155, 159].

*Experimental infection of cats with chimeric virus FFV-Vif W/*1*

To investigate whether the FFV-Vif chimera with the Bet-independent expression of Vif is replication-competent and immunogenic in cats, we performed inoculation experiments with FFV-Vif W/*1 (Table 1). This clone was selected for in vivo infection studies since it is the major variant detected in our in vitro experiments and is caused by only a single nucleotide exchange from the original engineered pCF7-Vif-4 chimera. Cats were separated into naïve (N), wild-type (WT), or chimeric (CH) groups based on inoculum type. The timeline of inoculations, sample

collections, and final necropsy are shown in Fig. 4. None of the cats displayed signs of clinical illness or hematologic changes indicative of disease throughout the duration of the study.

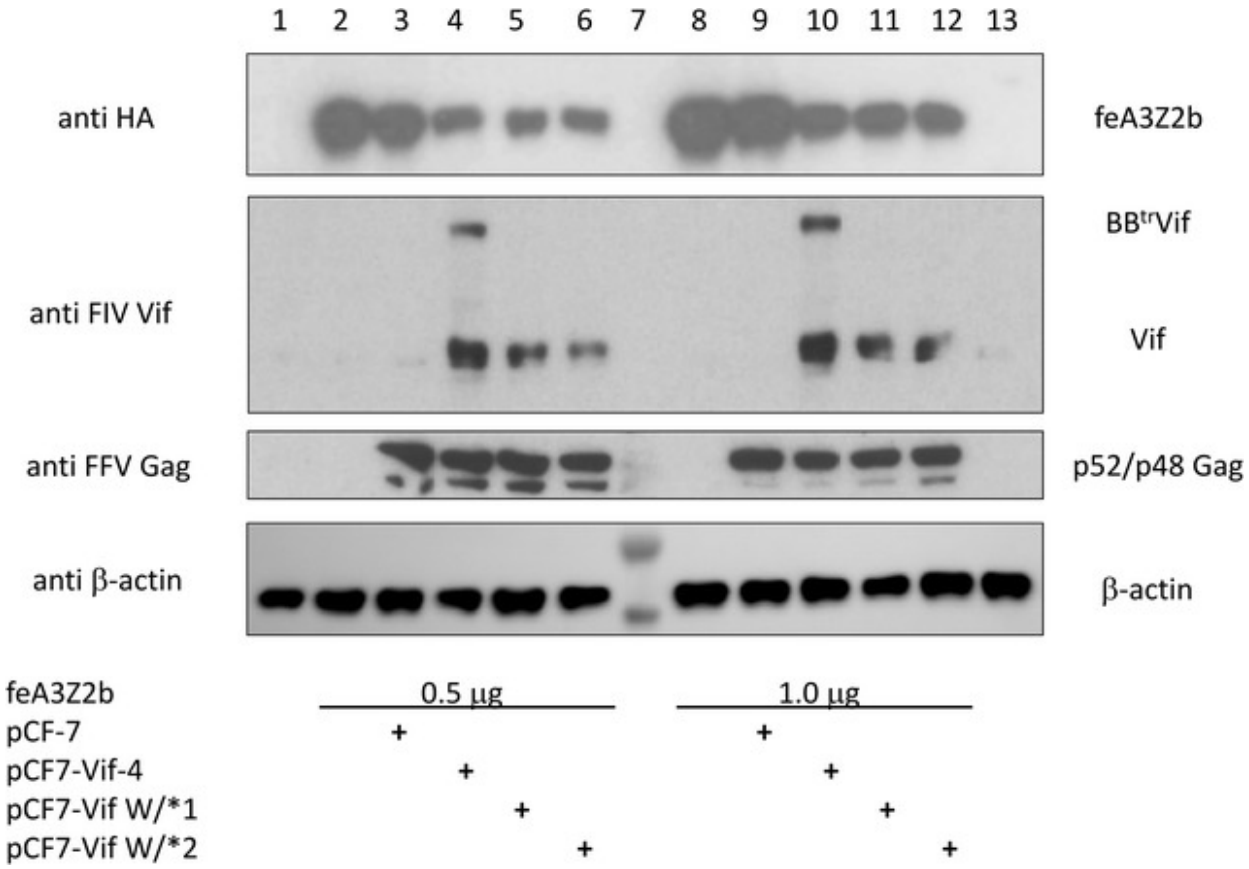

Figure 3. Reduced steady state levels of feA3Z2b in FIV Vif- and Bet Vif-expressing cells. Parental wild-type FFV full-length pCF-7 genome and FFV-Vif chimeric clones pCF-Vif-4, pCF7- Vif W/*1, and –W/*2 were transfected into HEK 293T cells together with 0.5 (Fig. 3, lanes 2 to 6) or 1.0 µg (lanes 8 to 12) of a plasmid encoding HA-tagged feA3Z2b as indicated below the blots. Cells transfected with the plasmid encoding feA3Z2b and pcDNA, as well as pcDNA-transfected cells served as controls (lanes 2 and 8, and 1 and 13, respectively). Cells were lysed 2 d after transfection and 20 µg total of each protein lysate was subjected to immunoblotting against HA (detecting HA-tagged feA3Z2b), FIV Vif, FFV Gag and β-actin (from top to bottom and indicated at the left). Lane 7 was loaded with a pre-stained protein marker. The bands corresponding to apparent molecular masses of 40 and about 55 kDa are seen below and above the B-actin of 42 kDa (bottom panel developed in an Intas ECL Chemocam Imaging device). All other blots were exposed to autoradiography films and thus, pre-stained protein markers are not visible in lane 7. The names of proteins specifically detected by immunoblotting are given at the right-hand side.

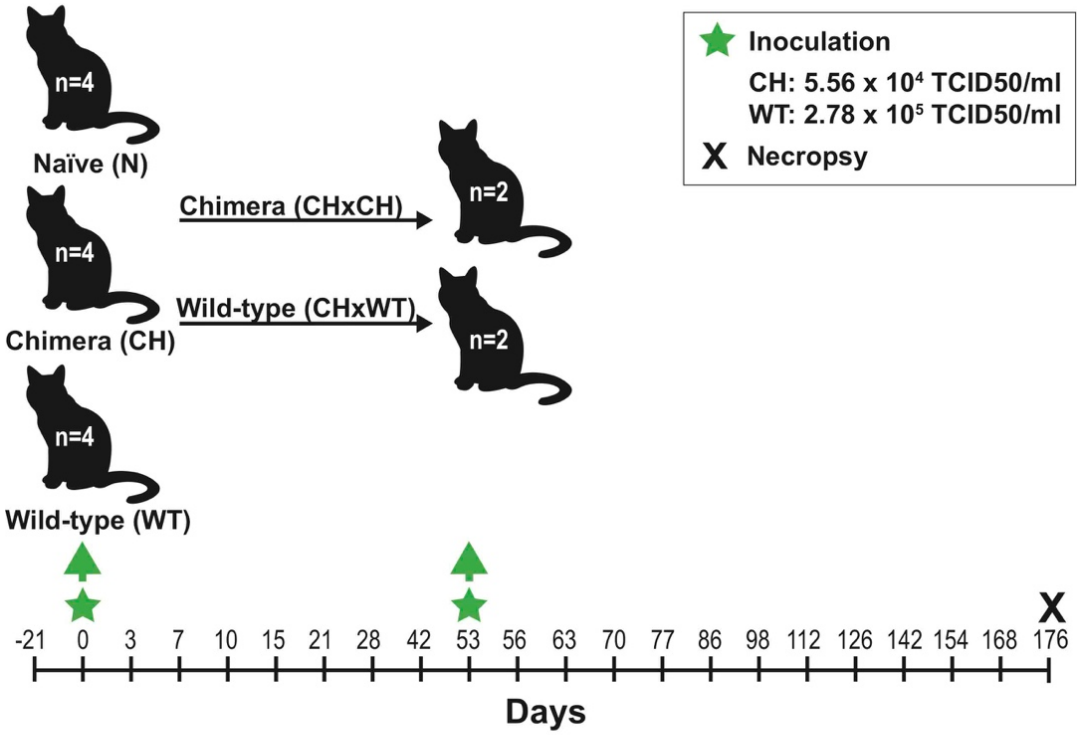

Figure 4. Experimental infection of cats with wild-type FFV and the FFV-Vif W/*1 chimera. Twelve SPF cats were separated into groups (n = 4 each) based on the inoculum type administered at day 0: naïve (N), wild-type FFV (WT), and chimeric FFV-Vif W/*1 (CH). Cats received 10^5 $TCID_{50}$ of either wild-type or chimera. Animals were monitored daily for clinical signs of infection and blood samples were collected on days specified on the timeline above to characterize infection and immune responses. Samples were collected for baseline data on day -21. On day 53, cats in the CH group were re-inoculated with either undiluted wild-type FFV of 2.78×10^5 $TCID_{50}$/ml (n = 2, referred to as CH1WT and CH2WT) or undiluted FFV-Vif W/*1 of 5.56×10^4 $TCID_{50}$/ml (n = 2, referred to as CH3CH and CH4CH). Inoculation time points are marked by green stars. Animals were humanely euthanized and necropsied on day 176 p.i. (black X).

Wild-type inoculated cats exhibited persistent FFV DNA proviral loads in PBMC in contrast to chimera-inoculated cats

To compare viral load and kinetics between inoculation groups, we evaluated the presence of FFV proviral DNA in PBMC over time (Fig. 4 and 5). Naïve control cats remained absolutely PCR-negative at all time points tested (Appendix File 5). Cats in the WT group developed a persistent PBMC proviral load as early as 21 days post-infection (p.i.) (Fig. 5A and 6), while indeterminate PCR reactions were detected earlier (Fig. 5A and Appendix File 5). By day 42 p.i., all WT cats were PCR positive and positivity was consistently detected throughout the rest of

the study (Fig. 5A). Cat WT3 (subsequently also referred to as “outlier”) had a PBMC FFV DNA pattern that differed from the rest of the WT cohort (Fig. 6). This animal was not PCR-positive until day 42 (versus day 21 as in its cohort-mates). Throughout the rest of the study, the outlier cat’s overall viral load was however much higher (highest at 5,920 viral copies/10^6 cells on day 142 p.i.) than the other WT cats (WT2 had the highest viral load at 1,230 viral copies/10^6 cells on day 28 p.i.) (Fig. 6).

Three out of four cats inoculated with only FFV-Vif chimeric virus (CH group) showed indeterminate results for FFV PBMC provirus DNA by qPCR analysis at some of the time points tested prior to re-inoculation on day 53 p.i. (Fig. 5B and Appendix File 5). One of the chimera-inoculated cats re-inoculated on day 53 with wild-type virus (cat CH2WT) demonstrated FFV proviral DNA in PBMC 24 d post re-inoculation, while the other cat in this cohort remained indeterminate or negative throughout the study (Fig. 5C). The highest viral load recorded for cat CH2WT was 656 viral copies/10^6 cells 24 days post re-inoculation (Fig. 6). Both cats re-exposed to the FFV-Vif chimera displayed repeated indeterminate PCR results in blood before and after superinfection (Fig. 5B and D).

Gag-specific immune reactivity in infected animals confirms replication competence of wild-type FFV and FFV-Vif chimera

All FFV-infected cats strongly seroconverted against Gag while all naïve control animals were negative (Appendix File 6, reactivity at 1:50 dilution). In order to determine the kinetics and strength of anti-Gag reactivity, selected serum samples from wild-type FFV and FFV-Vif-infected animals were analyzed before and after superinfection (only cats in the CH group received a second inoculation, Fig. 7A and B). Wild-type FFV-infected cats had detectable specific anti-Gag antibody responses as early as 21 or 28 days p.i. (Fig. 5A and Appendix File 5).

Antibody levels for these cats continued to increase to final titers between 500 and 2,500 (Fig. 7A). FFV Gag antibodies of FFV-Vif-infected animals were first detected by day 15 p.i.

(Fig. 5B and Appendix File 5) and increased gradually until superinfection, after which Gag-specific titers were attained that were equivalent to wild-type-infected cats (Fig. 7A and B). Anti-Gag reactivity was detected in all four CH group cats at approximately the same seroconversion rate as wild-type FFV-infected cats, though titers tended to be lower prior to re-exposure in the CH group (Fig. 7B and Appendix File 5).

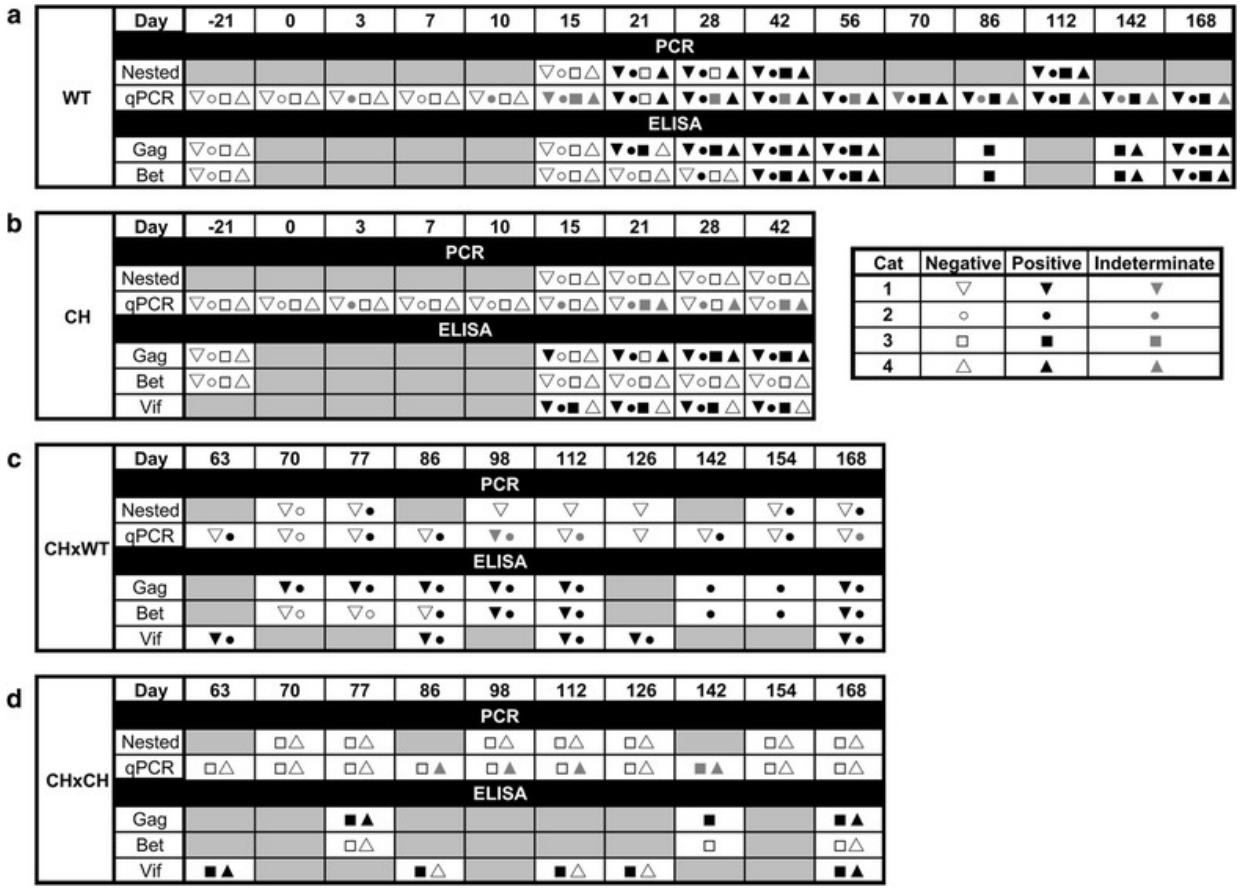

Figure 5. Results of PCR and ELISA assays over the entire study period. Summary of real time quantitative and nested PCR (qPCR and nPCR, respectively) on PBMCs and ELISAs for FFV Gag and Bet and FIV Vif performed before and following inoculation as given in the panels. The same symbols were used for cats 1–4 in WT and CH groups. Only the cats for which symbols are present (see inserted legend) were tested at the corresponding time point. Gray boxes represent time points where animals were not tested. CH-group cats were re-inoculated on day 53 (not shown) as described in "Methods". **a** WT group results (days -21 to 168 p.i.). **b** CH group results (days -21 to 42 p.i.). **c** CH×WT group results (days 63 to 168 p.i.). **d** CH×CH group results (days 63 to 168 p.i.)

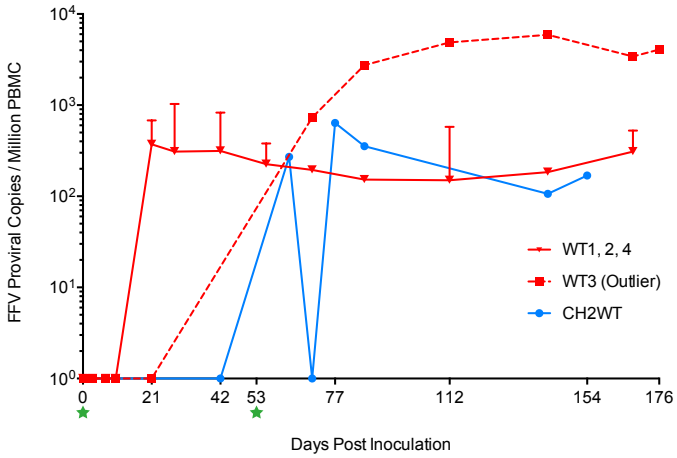

Figure 6. Wild-type FFV inoculated cats developed persistent infection of PBMCs. Real time quantitative PCRs (qPCR) were performed on PBMCs following inoculation on day 0 (left green star). The solid red line illustrates the proviral load mean of three WT-inoculated cats with similar viral kinetics. These cats had detectable PBMC FFV DNA on day 21 p.i. by both qPCR and nested PCR and developed persistent proviral loads between 100 and nearly 1500 copies per million PBMC. The dotted red line displays a different PBMC FFV DNA pattern observed in cat WT3 ("outlier") which was not PCR-positive until 42 days p.i. (nPCR, see Fig. 5a). This individual had a mean proviral load 1–2 logs higher than the other WT cats and almost 6000 viral copies per million PMBC at peak viremia. The blue line represents cat CH2WT, which was re-inoculated with wild-type virus on day 53 p.i. (right green star). This was the only re-inoculated cat to test unambiguously positive on day 63 p.i. (qPCR). The other cat in this cohort (CH1WT) and the two cats in the CH×CH group are not represented in the graph due to indeterminate qPCR and negative nPCR results (see "Methods" and Fig. 5c and d). Naïve cats were completely PCR-negative throughout the study and are also absent on this graph. Error bars represent standard deviation.

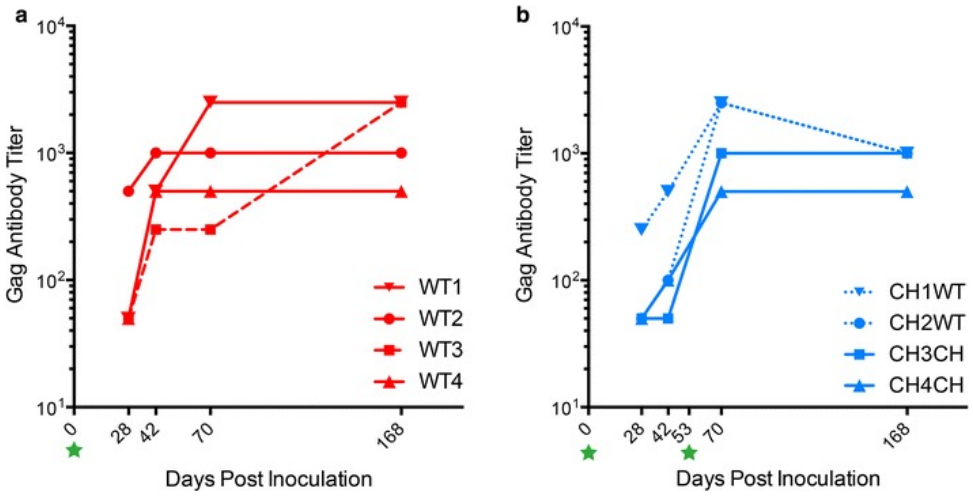

Figure 7. Cats infected with wild-type FFV and FFV-Vif W/*1 developed FFV Gag-specific immunoreactivity. A GST-capture ELISA was performed to evaluate antibody response to FFV infection. **a** Anti-Gag antibody titers in WT cats on days 28, 42, 70, and 168 p.i. The dotted red line represents WT3, the outlier cat. Animals displayed rising levels of antibody by day 42 which either continued to increase over time or plateau. **b** Anti-Gag antibody titers in CH cats that were re-inoculated with wild-type (CH×WT, dotted lines) or FFV-Vif W/*1 chimera (CH×CH, solid lines). These cats similarly had increasing anti-Gag antibodies around day 42 that continued to increase or plateau following re-inoculation. In order to detect low-level reactivity, sera were assayed at a 1:50 dilution leading to some reactivities which were out of the linear range of the assay.

Infected cats seroconverted against accessory FFV Bet and FIV Vif proteins

All cats infected with wild-type FFV only (WT 1-4) or FFV-Vif plus wild-type FFV (CH1WT and CH2WT) demonstrated substantial FFV Bet sero-reactivity by day 168 p.i. (Fig. 5A and C, Fig. 8A, and Appendix File 5). As observed in previous studies [56, 145], Bet-specific antibodies appeared slightly later than Gag sero-reactivity (Fig. 5 and Appendix File 5). Naïve controls and cats CH3CH and CH4CH were Bet-antibody negative as expected. Most importantly, Vif reactivity in three out of four FFV-Vif-infected animals was clearly positive at day 42 p.i., prior to superinfection on day 53 p.i. (Fig. 8B). Surprisingly, Vif-specific reactivity in these animals was detectable by day 15 p.i. despite the fact that qPCR did not detect provirus (Fig. 5B and Appendix File 5). Re-inoculation of these cats with either wild-type FFV (animals CH1WT, CH2WT) or FFV-Vif chimera (CH3CH) resulted in a boost in Vif sero-reactivity at day 63 p.i. Animal CH4CH, which showed no Vif reactivity prior to superinfection, exhibited only transient FIV Vif reactivity after re-exposure (Fig. 8B).

Discussion

This study describes the generation of replication-competent variants of FFV that express FIV Vif in lieu of FFV Bet. An engineered FFV genome expressing a fusion protein of a non-functional N-terminal Bet domain fused to the full-length Vif was clearly attenuated in vitro. Second-generation FFV-Vif chimeras expressing the authentic codon-optimized *vif* gene showed much higher *vif*-dependent replication competence in feA3-expressing cells, only slightly decreased in vitro compared to wild-type FFV. In experimentally infected cats, replication of the chimeric FFV-Vif variant was attenuated but led to the induction of FFV Gag-specific antibodies together with those directed against the engineered heterologous FIV Vif protein. Importantly, cats infected with the FFV-Vif chimera could be superinfected with wild-type FFV or the chimera, in both cases resulting in a strong immunological boost of sero-reactivity against FFV and FIV Vif.

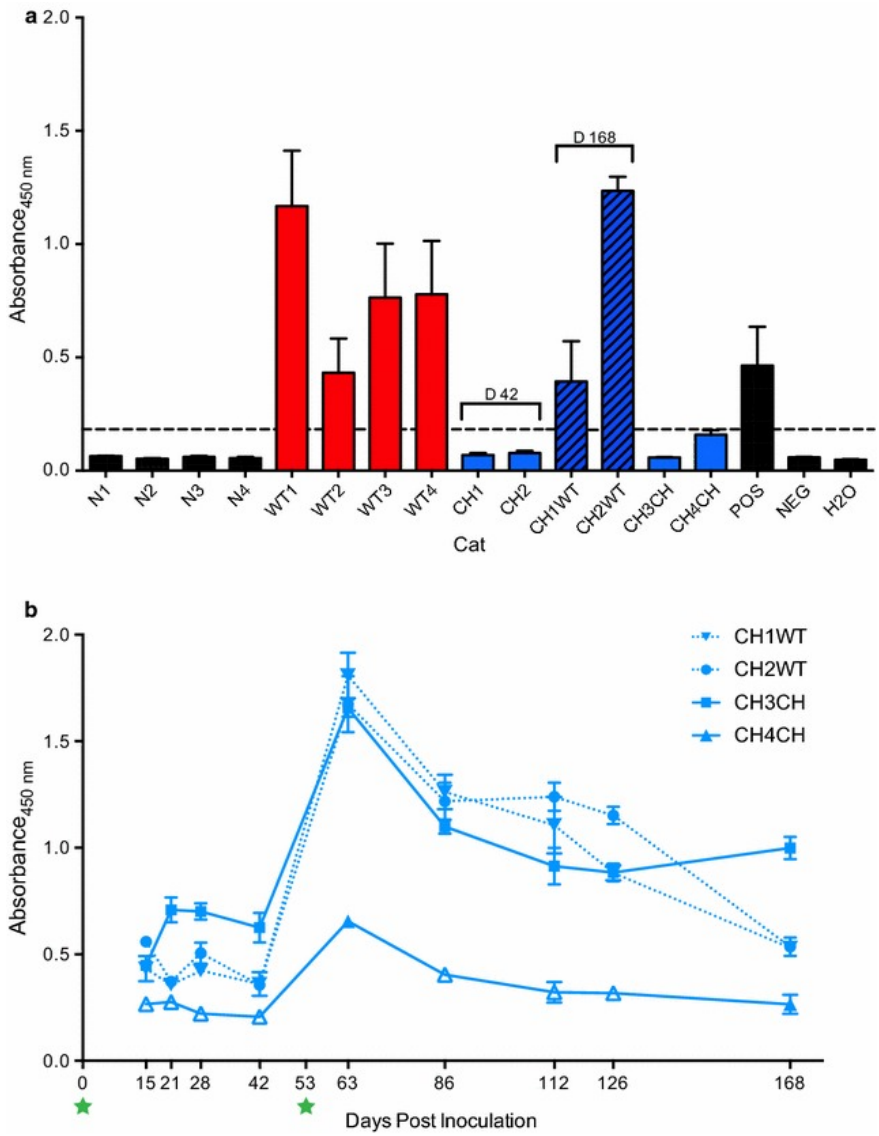

Figure 8. Animals inoculated with wild-type FFV or FFV-Vif chimera seroconverted to FFV Bet or FIV Vif. Antibody response against FFV Bet and FIV Vif antigens were measured by antibody capture ELISAs as described in the “Methods” section. **a** Anti-Bet antigen reactivity for each animal at final time points unless specified. WT cats (red bars), and cats that received chimera and then wild-type FFV (CH×WT, black and blue striped bars) seroconverted against Bet. Animals exposed to only FFV-Vif W/*1 (cats CH1 and CH2 prior to day 53, and CH3CH and CH4CH, solid blue bars) were negative for anti-Bet antibodies as expected. Black bars show naïve cats, and positive and negative control samples. **b** Three out of 4 animals inoculated with chimeric virus developed a detectable anti-Vif immune response as early as 15 days p.i. Antibody response increased following re-inoculation for all animals, causing a detectable response in the fourth animal (CH4CH), though sero-reactivity was low compared to other animals for this individual, and only rose above positive cutoff absorbance on days 63 and 168. Filled shapes indicate positive ELISA absorbance values compared to negative controls (> 2 standard deviation above the mean of duplicate negative samples), whereas open triangles for CH4CH indicate ELISA absorbance values below positive cutoff. Values reported represent mean of duplicate samples and bars indicate standard deviation.

The successful replacement of FFV *bet* by FIV *vif* in the context of the FFV genome may have been aided by two mechanisms. First, a codon-optimized and thus Rev-independent FIV *vif* gene was inserted, allowing for efficient translation of the Vif protein [20]. Second, LV Vif proteins function as catalytic regulators of proteasomal feA3 degradation; therefore, much lower amounts of fully functional Vif may be required to inactivate A3 activity compared to FV Bet, which acts stoichiometrically via direct binding to the feA3 protein [15]. Thus, the attenuated replication of the initially constructed pCF7-Vif-4 chimera was likely due to high expression levels of the functionally impaired Bet^{tr}Vif fusion protein.

In support of the hypothesis that Bet and Vif are differentially expressed in vivo, Bet sero-reactivity is high and has diagnostic value in infected cats and bovines [70, 80]. In contrast, while anti-Vif antibodies have been described in HIV patients [161, 162], Vif has not been shown to be a major humoral immune target of FIV infection, and seroconversion against Vif has not been well studied in FIV infection (personal communication, Dr. Chris Grant).

Apparently, inhibitory effects of either the complete N-terminal part of Bet plus the linker sequence, or the N-terminal residues of the linker residues present downstream of the engineered FFV PR cleavage site (see Fig. 1A) favored the emergence of Trp/stop (W/*) variants. This is strongly suggested by the fact that two independent, yet highly related mutational events led to the W/* mutation in the linker sequence upstream of *vif.* The reverse genetic experiments conducted do not support translational initiation at the upstream Met residue located in the linker sequence as important for Vif protein expression. We thus assume that in the in vitro-selected clones, fully functional Vif is expressed from its authentic start codon, though the exact mechanism by which FIV Vif protein is expressed from pCF7-Vif W/*1 and pCF7-Vif W/*2 is unknown. We assume that internal re-initiation of protein biosynthesis may be involved, but other mechanisms cannot be excluded. While the mechanism of Vif expression of clones pCF7-Vif W/*1 and pCF7-Vif W/*2 is unknown, all FIV Vif proteins engineered into the FFV genome including the first-generation clone pCF7-Vif-4 encoding the Bet^{tr}Vif fusion protein

lead to dramatically reduced steady state levels of feA3 proteins as shown for the major restriction factor of FFV, feA3Z2b (see Fig. 3).

In line with the assumption that the original Bet^{tr}Vif fusion protein conferred suboptimal protection against feA3 restriction, both mutations leading to the adaptive W/* mutations occurred in a sequence context of the negative strand that is indicative of feA3 editing, suggesting the chimeric viruses did not confer robust protection against feA3. Both mutated C residues of the negative strand are preceded by C residues in the sequence 5'-TC**CC**-3' (deaminated C residues in bold face letters, see also Fig. 2C), and therefore should function as optimal feA3 substrates, however, alternative mutational pathways might have also played a role. The fact that suboptimal feA3 inhibition leads to adaptive changes induced by feA3 DNA deamination supports our proposed concept that the heterologous and functionally relevant transgene FIV *vif* is essential for efficient propagation of the replicating virus, and thus confers a strong selective advantage by protecting against feA3 restriction. Consequently, the transgene *vif* has to be stably maintained in the absence of *bet* during serial passages, as demonstrated in Fig. 2B. The importance of the *vif* transgene for FFV-Vif replication is further underscored by the fact that additional adaptive changes, such as unlinking from N-terminal Bet sequences, were required to restore full biological activity as an inhibitor of feA3 restriction.

The advantage of adapting this replication-competent FV vector system as a vaccine delivery vehicle is that the immunogen Vif is essential for replication and should be thus stably maintained by the engineered vector. Further, LV Vif has been shown to elicit T and B cell reactivity in HIV-infected individuals [163-167]. A corresponding PFV-based replicating vector system carrying the HIV *vif* gene may therefore be an interesting vector for the development of anti-HIV immunotherapies.

The *in vivo* wild-type FFV inoculations confirm that experimental infection of outbred, immunocompetent cats with clone pCF-7-derived wild-type FFV leads to a persistent infection with consistent detection of FFV proviral DNA in PBMC and a strong sero-reactivity against Gag

and Bet proteins, similar to other reports [56, 145]. In contrast, animals inoculated with FFV-Vif W/*1 remained either proviral DNA negative or indeterminate throughout the study based on nested and qPCR analysis of PBMC DNA (Fig. 5B and D). Surprisingly, despite the inability to unambiguously detect FFV provirus in cats exposed to FFV-Vif W/*1, clear sero-reactivity against FFV Gag and heterologous Vif protein were detected after primary inoculation (Fig. 5 and 7). This observation is consistent with previous studies in different FVs that serology is much more sensitive for the identification of exposed animals than PCR-based studies using PBMC [56, 62, 80, 168].

FFV in vivo infection experiments were conducted with wild-type FFV or chimeric FFV-Vif W/*1. This resulted in detectable, but low, proviral load in wild-type-infected animals and either undetectable or indeterminate proviral loads in cats infected with the FFV-Vif chimera. It is feasible that the exchange of Bet for Vif altered tissue tropism and site of viral replication in FFV-Vif W/*1 exposed cats, and this contributed to the inability of tracking viral infection via peripheral blood PCR. While initially either negative or indeterminate based on PCR results, cat CH2WT was superinfected with wild-type FFV on day 53 p.i. and showed a productive PBMC FFV infection on a similar timeline after inoculation as the wild-type-infected animals.

The animals in the chimeric cohort did not seroconvert against Bet as anticipated but they displayed clear anti-Vif antibody responses starting at day 15 p.i., demonstrating that substituting Bet by Vif elicited specific immune responses. Given that anti-Vif antibodies have not been widely reported during FIV infection, our findings may indicate replication is occurring in cells or cell compartments where it is more easily recognized as a foreign antigen. Antibody production against Vif was initially not robust but following re-inoculation with both wild-type and FFV-Vif chimeric virus, anti-Vif antibody response markedly increased (Fig. 8B). Following re-inoculation of the FFV-Vif-infected animals with wild-type FFV virus, both cats initially infected with FFV-Vif W/*1 also produced anti-Bet antibodies, demonstrating that infection with the chimera did not protect against subsequent infection with wild-type FFV (Fig. 5C and 8A).

The data document that, despite a lack of consistent detection of FFV provirus DNA, FFV-Vif W/*1 is able to induce persistent antibody responses in domestic cats that were boosted by re-inoculation. As noted above, we were able to document superinfection with two highly related FFV variants. Clinical evaluations following exposure to wild-type FFV or chimera suggests that FFV produces an apathogenic infection during the study period. Further studies should be conducted to understand chronic FFV infection and potential associated pathologic changes as well as the possibility of worsened pathology following superinfection with other FFV serotypes or other viral infections [74]. It would also be important to challenge wild-type FFV-infected cats with chimeric virus to determine whether infection with wild-type FFV may induce neutralizing immunity thus preventing superinfection with an attenuated FFV vaccine construct.

It cannot be ruled out that the antibody response detected in FFV chimera-infected animals was related to exposure to viral inoculum versus actively replicating virus, since PCR results were indeterminate. However, anti-Vif antibody production in three out of four FFV-Vif chimera-inoculated cats detected throughout the monitoring period, and an anti-Gag response equivalent to wild-type antibody titers is supportive of the conclusion that low-level viral replication occurred [56, 62, 80, 168]. Whether or not FFV-Vif W/*1 replicated poorly or not at all, the fact that pCF7-Vif W/*1 was highly replication-competent in CrFK cells but strongly attenuated in vivo suggests that Bet may play a currently unknown critical role in viral replication competence in vivo in addition to antagonizing A3-mediated restriction. Here, inactivation of other components of the host's innate or intrinsic immunity as well as an essential co-factorial role for the replication in specific cell types in vivo are plausible reasons for the attenuated phenotype. Alternatively, other aspects of the manipulated pCF7-Vif W/*1 genome may impede replication in the native host. Further studies may elucidate additional complex host-virus restriction pathways that are relevant in vivo but are functionally masked or not relevant during in vitro infections.

Findings presented here illustrate a role for pCF7-Vif W/*1 to be used as a novel anti-LV vaccine delivery scaffold. This system would exploit a non-pathogenic vector that has to stably

retain the Vif vaccine antigen and may be a therapeutic option to boost immunity towards an existing HIV infection in order to eliminate infected cells. The option to insert additional B and T cell epitopes at the terminus of the truncated Bet may be a means to extend and direct the host immune response towards additional epitopes (Slavkovic Lukic and Löchelt, unpublished observations). The ability to administer repeatedly or simultaneously the FV-based vaccine vector, directing expression of additional or newly acquired antigens, is an additional strength of our system as low level or absence of replication would hinder use of pCF7-Vif W/*1 as a vector delivery system that requires greater viral replication. Our results suggest that prior infection with wild-type FFV might not impair response to FFV-Vif, though superinfection studies will need to be conducted before this vector could be commercially developed. Experiments determining the viability of FV-LV Vif chimeric variants would also have to include assays to determine stability and functionality of inserted heterologous epitopes. Since we have documented that seroconversion occurs against Vif and Gag during FFV-Vif W/*1 exposure in the absence of intentional adjuvation, the attenuated replication does not impair its use as an antigen expression platform for eliciting antibodies against foreign antigens and could even improve its biological safety.

Conclusions

Our in vitro and in vivo studies show the feasibility of constructing a replicative FFV-Vif vector that incorporates FIV Vif and replaces FFV Bet protein expression to counteract intrinsic feline A3 restriction factors. The FFV-Vif chimera inoculation of domestic cats induced a specific immune response against the heterologous Vif protein which under superinfection boosted antibody production against both FFV Gag and FIV Vif. Superinfection was also possible using wild-type FFV as evidenced by seroconversion against FFV Bet in animals initially inoculated with the chimeric construct, which provides plausibility of using this vector in domestic cat populations which may already be infected with wild-type virus. These findings demonstrate that

this and additional FV vector systems may be further studied to develop potential therapeutic or preventive avenues against lentiviral infections including HIV.

Methods

Cells, culture conditions, and DNA transfection

Crandell feline kidney (CrFK) cells were used for FFV infection and propagation [14, 74, 79]. Human embryonic kidney (HEK) 293T cells used for plasmid transfection were propagated as described [169]. FeFAB cells (CrFK-derived cells that carry a β-galactosidase gene under the control of the FFV LTR promoter that is activated via FFV infection and subsequent Tas expression) were used to determine viral titer as described previously [169]. PBMC were purified from feline blood using Histopaque gradients (Sigma Aldrich, St. Louis, MO). HEK 293T cells were transfected or co-transfected by using a modified calcium phosphate method described previously [169]. In serial passage experiments, wild-type pCF-7 and Vif-chimera pCF-Vif-4 were transfected into HEK 293T cells [146]. Supernatants were harvested 2 days post transfection and used to infect feA3-positive CrFK cells. Supernatants from these infections were serially passaged twice a week (every third or fourth day p.i.) to new, uninfected CrFK cells. A total of 20 serial passages were conducted.

FFV propagation and titration

For viral propagation of wild-type FFV and chimera (generated by transfection of HEK 293T cells), 10^6 CrFK cells/ml were seeded and infected at a multiplicity of infection (MOI) of 0.1. Supernatants were harvested and used for viral titer estimation and further viral propagation. FFV titers were determined using 5 x 10^4 FeFAB cells/well grown in 24-well plates and infected with serial 1:5 dilutions as described [146]. Titers were calculated by determining the highest dilution that contained blue-colored infected cells through light microscopy.

Wild-type and FFV-Vif chimera viral propagation and titration for cat infections

2 µg of FFV pCF-7 [91] or pCF7-Vif W/*1 plasmid were transfected into CrFK cells using Lipofectamine and supernatants were harvested for amplification in CrFK cells. Microscopic observation of cells was conducted daily and considered to be infected if they displayed cytopathic effects (CPE) of vacuolization, cytomegaly, and multinucleation [10-12]. Supernatants of infected cells were harvested and frozen on 2, 6, 9, and 13 days p.i. CPE end-point dilution titration was conducted on CrFK cells to determine $TCID_{50}$/ml. CrFK (3×10^4 cells/well) were incubated with 25 µl of virus-containing supernatants in five-fold dilutions from the aforementioned days and observed for CPE up to 17 days p.i. The number of CPE-positive wells was used to determine $TCID_{50}$/ml using the method of Reed and Muench [170]. Supernatants that yielded the highest titers were selected for animal inoculations.

FIV titration system and FFV LTR luc reporter assay

Production of FIV luc reporter viruses, normalization according to reverse transcriptase activity, and target cell infection and reporter readout were done as previously described [43]. FFV reporter assays using co-transfection of HEK 293T cells with the full-length FFV LTR luc reporter plasmid pFeFV-LTR-luc and the different FFV chimeras generated in this study or the FFV Tas expression construct pFeFV-Bel1 were conducted as described previously [171].

Molecular cloning

Replacement of FFV *bet* coding sequences by a codon-optimized FIV *vif* gene in the FFV provirus vector pCF7-BetMCS, which carries a multiple cloning site directly downstream of *bet* without affecting *tas* [34], was done via fusion PCR cloning using the proof-reading *Pfu* polymerase as specified by the supplier (New England Biolabs, Frankfurt Germany) [146]. For PCR primer sequences, see Table 2. In brief, the codon-optimized *vif* gene was first amplified using a sense primer with upstream sequences encompassing a terminal *Nhe*I site, followed by

a *Sac*II site and the sequence encoding the FFV protease (PR) cleavage sequence AAVHTVKA (see Fig. 1A, and Appendix File 2) directly fused in-frame to the start codon of *vif* while the antisense primer was complementary to the terminal *vif* sequence followed by an *Age*I restriction site (Fig. 1A, bottom panel, pair of blue primers, # 1 and 2). The other amplicon was generated with a sense primer also containing an *Age*I site and annealed to FFV sequences about 120 nt upstream of the essential FFV poly-purine tract while the antisense primer was downstream of a unique *Sph*I site in the U3 region of the FFV LTR (Fig. 1A, bottom panel, pair of violet primers, # 3 and 4). The amplicons generated were fused in a third PCR using only the sense primer of the first and the antisense primer of the second reaction (primers # 1 and 4). The amplicon was digested with *Nhe*I and *Sph*I and inserted into pCF7-BetMCS [34] digested with *Nhe*I and *Sph*I. The resulting clone pCF7-Vif was analyzed by DNA restriction analysis and DNA sequencing. Similarly, site-directed W/* mutagenesis in pCF7-Vif-4 and mutagenesis of the methionine codon and its flanking sequences in pCF7-Vif W/*1 and –W/*2, were done using PCR primers shown in Table 2. The resulting fragments were inserted into the clones pCF7-Vif W/*1 and pCF7-Vif W/*2 via three component ligations using unique *Bsp*EI, *Nhe*I and *Xho*I restriction sites.

Cloning and sequencing of in vitro selected FFV-Vif variants

DNA from CrFK cells infected with in vitro selected variants of pCF7-Vif-4 was harvested at passage 18 using the DNeasy extraction kit as specified by the supplier (Qiagen, Hilden, Germany). Sense primer FFV 9366 and antisense primer 10288 (Table 2) were used to amplify a 923 nt fragment of the *bel1*–*vif* region. Amplicons were cloned into pCR-TOPO TA vectors (Invitrogen, Karlsruhe, Germany) and subjected to in-house Sanger DNA sequencing of both strands.

Table 2. Primers used for cloning and PCR detection.

Primer Name	Sequence (5' – 3')
pCF7-Vif cloning	
FFV-Vif #1	GCGGGCTAGCGCCGCGGTACACACCGTCAAAGCCATGAGCGAGGGGACTGGCAG
FFV-Vif #2	GTGCTCTCCAAAGACCGGTTATCACAGCTCGCCGCTCCACAGCAGATTCC
FFV-Vif #3	GGCGAGCTGTGATAACCGGTCTTTGGAGAGCACAAGCTGATG
FFV-Vif #4	CGCTCTGTTGCATGCCG
Mutagenesis of the upstream start codon	
FFV 9233-F	GCGGTCCGGAACACCCAAGACGGATCCTACTCG
M/T-R	CGGC**GCTAGC**TCTAGTTAG**CGT**AGTCAAATCCCTCTCCCCAC
M+-R	CGGC**GCTAGC**TCTAGTTAC**CAT**AGTGAAATCCCTCTCCCCAC
PCR amplification of in vitro-selected FFV-Vif variants	
FFV 9366-F	CCACTTCTGTTTGGACCTTACC
FFV-10288-R	CAGCTTGTGCTCTCCAAAGC
Nested FFV PCR	
FFVgag-F1	CTACAGCCGCTATTGAAGGAG
FFVgag-R1	CCCTGCTGTTGAGGATTACC
FFVgag-F2	TTACAGATGGAAACTGGTCCTTAGT
FFVgag-R2	CATCAGAGTGTTGCTGTTGTTG
Real-time quantitative PCR	
FFVgag -F	GGACGATCTCAACAAGGTCAACTAAA
FFVgag-R	TCCACGAGGAGGTTGCGA
FFVgag-TM	AGACCCCCTAGACAACAACAGCAACACT

Animals and experimental design

Twelve specific-pathogen-free (SPF) cats, aged 6-8 months and negative for common feline pathogens including FFV and FIV, were obtained from the Colorado State University (CSU) SPF Colony and housed in an Association for Assessment and Accreditation of Laboratory Animal Care International-accredited animal facility at CSU. All procedures were approved by the CSU Institutional Animal Care and Use Committee prior to initiation of the study. Cats were separated into three groups (n=4 per group) based on inoculation type: FFV-negative CrFK culture media (naïve, N), wild-type FFV (WT), or chimeric FFV-Vif W/*1 (CH) (Fig. 4). Virus-inoculated animals received 10^5 $TCID_{50}$ in 2 ml under ketamine anesthesia, split into 1 ml intramuscularly (i.m.) and 1 ml intravenously (i.v.). Cats were monitored daily for clinical signs of disease, and body temperature and weight were measured weekly. Peripheral blood was collected via cephalic or

jugular venipuncture and processed to obtain serum and PBMC. On day 53 p.i., all cats in the CH cohort were re-inoculated each with 5 ml of undiluted virus (wild-type virus 2.78 x 10^5 $TCID_{50}$/ml or chimeric virus 5.56 x 10^4 TCID50/ml, split into 1 ml i.m., 2 ml i.v., and 2 ml subcutaneously). Two of these cats were re-inoculated with wild-type FFV virus (henceforth referred to as CH1WT and CH2WT) and the other two cats with FFV-Vif W/*1 (now referred to as CH3CH and CH4CH). Animals were humanely euthanized for necropsy on day 176 p.i. (Fig. 4).

Nested and real-time quantitative PCR assays

Nested FFV PCR (nPCR) was performed on PBMC DNA to screen for initial infection status. Proviral DNA was purified and amplified using 0.5 μM *gag*-specific forward and reverse primers listed in Table 2 under the following cycling conditions for the first round of nPCR: 94ºC for 2 min, 35 cycles of 94ºC for 30 s, 57ºC for 30 s, 72ºC for 1 min, and a final elongation step at 72ºC for 5 min. For the second round, 2 μl of first-round product was added to the reaction and amplified in these conditions: 94ºC for 2 min, 35 cycles of 94ºC for 30 s, 57ºC for 30 s, 72ºC for 30 s, and 72ºC for 5 min. Products were electrophoresed in 1.5% agarose gel in Tris-acetate buffer and stained with GelRed™ Nucleic Acid Gel Stain (Biotium, Hayward, CA) then visualized to look for the 333 base-pair PCR product. Real-time quantitative PCR (qPCR) was performed in triplicate on viral DNA as previously described [168] using 0.5 μM forward and reverse *Gag*-based primers and 0.1 μM probe (Table 2) with the following modified conditions: 95°C for 3 min, 45 cycles of 95°C for 10 s, and 60°C for 40 s. Viral copy number quantification was based on a plasmid standard curve prepared from plasmid pCF-7. FFV-Gag real time PCR assay sensitivity is 1-10 viral copies per reaction [168]. Infection status was divided into 3 categories: positive, negative, and indeterminate. Animals considered unequivocally “positive” had qPCR results with Cq values less than or equal to 37 in 2-3 out of the three reactions, consistent with viral load greater than 10 copies/reaction. Animals considered “negative” were negative for all

triplicate tests (this included all naïve cats and “no template” controls at all defined times). Animals classified as “indeterminate” had qPCR replicates with Cq values > 37, equivalent to 0-10 copies per well. Indeterminate copy number calculations were not used in Fig. 6 since values obtained were below the assay’s lower limit of quantitation.

Gag, Bet and Vif immunoblotting

Cell lysate from FFV-infected CrFK cells or transfected HEK 293T cells were subjected to immunoblot analyses as described [56, 146]. Identical amounts of proteins were separated by SDS-PAGE, blotted, and reacted against different anti-FFV sera. FFV Gag and Bet proteins were detected by rabbit anti-Gag polyclonal serum (1:3,000 dilution) and rabbit anti-Bet polyclonal serum (1:2,500 dilution) [146]. FIV Vif was detected by a mouse anti-FIV-Vif antibody (NIH AIDS repository, Maryland, USA) at a 1:500 dilution. Membranes were incubated with secondary anti-rabbit polyclonal antibodies or anti-mouse IgG (Sigma, Munich, Germany) conjugated to horseradish peroxidase (1:5,000 to 1:2,000 dilution) and visualized by chemiluminescence (ECL Western Blot Kit, Amersham Buchler, Braunschweig, Germany). Blots were then probed against actin using mouse anti-actin antibody (1:8,000 dilution, Sigma).

GST-capture ELISA for detection of Gag and Bet seroconversion

GST-capture ELISA was performed to detect anti-FFV Gag and anti-FFV Bet antibodies as previously described [80, 172]. Glutathione casein was used to coat 96-well plates (Thermo Fisher Scientific, Waltham, MA) overnight at 4°C then plates were blocked with casein blocking buffer (0.2 % (w/v) casein in PBS and Tween20, Thermo Fisher Scientific). Plates were incubated with BL21 *E. coli*-produced lysates containing GST-tag, GST-Gag-tag, or GST-Bet-tag recombinant proteins (0.25 µg/µl in casein blocking buffer). Cat sera were pre-adsorbed with GST-tag lysate (2 µg/µl) in a 1:50 dilution and then incubated in duplicate (Fig. 7A and B) or triplicate (Appendix File 6) with each GST conjugate. The plates were incubated with anti-cat-

IgG Protein A peroxidase (1:50,000 dilution, Sigma Aldrich). For the substrate reaction, plates were incubated with TMB substrate before stopping the reaction with sulfuric acid. Absorption (optical density, OD) at 450 nm was measured and the mean reactivity for each was used. Detection cutoff values were determined from negative sera as 2 x (mean + 3 standard deviations). A significant number of reactions at the serum dilution used were out of the linear range of the assay. For anti-Gag antibody titrations, sera from days 28, 42, 70, and 168 p.i. were diluted at 1:100, 1:250, 1:500, 1:1,000, 1:2,500, and 1:5,000. Titer was determined as the highest dilution the cat tested positive for anti-Gag antibodies, using the cutoff formula mentioned above.

FIV Vif antibody capture ELISA

Sera were subjected to an FIV Vif antibody capture ELISA to detect corresponding antibodies in chimeric FFV-Vif-inoculated cats. 96-well plates were coated with 2 ng/µl Vif antigen and incubated overnight at 4°C. Mouse Vif monoclonal antibody (obtained from Dr. Chris Grant, Custom Monoclonals International, Sacramento, CA) was used as a positive control. After blocking, cat sera (1:100 dilution) or Vif monoclonal antibody (10 ng/µL) were applied in duplicates, then goat anti-cat (or anti-mouse) IgG-HRP (MP Biomedicals, Santa Ana, CA) was used as secondary antibody (1:1,000 dilution). TMB reagent was used for the substrate reaction then stopped with sulfuric acid before measuring absorption (450 nm). For detection cutoff, the mean negative sera absorbance readout was used in the following formula: mean + (2 x SD). A number of reactions at the serum dilution used were out of the linear range of the assay.

CHAPTER 2. FFV INFECTION AND ASSOCIATION WITH CHRONIC KIDNEY DISEASE[2]

Summary

Foamy viruses (FVs) are globally prevalent retroviruses with a unique molecular biology that establish apparently apathogenic lifelong infections. Feline foamy virus (FFV) has been isolated from domestic cats with concurrent diseases, including renal syndromes. We experimentally infected five cats with a well-characterized FFV strain to further describe viral kinetics and tropism, immune phenotype, renal parameters, and presence of pathology. A persistent infection of primarily lymphoid tropism was detected. One cat with a significant negative correlation between lymphocytes and PBMC proviral load displayed an expanded tissue tropism. Significantly increased blood urea nitrogen, increased urine protein-to-creatinine ratio, and ultrastructural kidney changes were noted in infected cats. Histopathological changes were observed in the brain, large intestine, and other tissues with increased severity in infected animals. We performed an FFV prevalence survey of pet cats with chronic kidney disease (CKD) and age- and sex- matched controls in the United States of America (USA) and Australia. We identified an association between CKD and FFV infection in male USA cats. While FFV did not cause clinical signs during acute experimental infection, findings in experimentally infected cats and pet cats with CKD support subclinical impacts of FFV infection potentially contributing to renal dysfunction, a common syndrome of unknown etiology in domestic cats.

Introduction

Feline foamy virus (FFV) is a retrovirus belonging to the ancient *Spumaretrovirinae* subfamily that infects domestic cats (*Felis catus*) and was originally incidentally discovered

[2]Chapter being prepared for publication as: Ledesma-Feliciano, C.; Troyer, R.; Zheng, X.; Miller, C.; Cianciolo, R.; Bordicchia, M.; Dannemiller, N.; Gagne, R.; Lappin, L., et al. **Feline foamy virus infection: characterization of experimental infection and association with chronic kidney disease in domestic cat populations**. Viruses 2019, (Manuscript in preparation)

following development of cytopathic effects (CPE) in feline cell lines. Foamy viruses (FVs) cause multiple CPE in vitro including multinucleation, giant cell formation, and vacuolization, leading to cells looking “foamy” (and where the “*spuma*” originates) [1, 9, 11, 12, 173]. In naturally-occurring infections of the domestic cat, however, FFV infection does not cause obvious disease, and has not been definitively associated with pathology despite establishing a persistent, life-long infection with a wide tissue tropism [11, 55-59, 61]. It is believed the apathogenicity of FVs in general is due to long periods of co-evolution within their hosts that has led to a disease-free or highly attenuated infection [1, 9, 56]. FV transmission is thought to primarily occur via salivary shedding and ongoing contact between animals, though alternate routes such as vertical transmission through lactating dams have been reported [58, 70]. In cats, biting and amicable prolonged contact, such as grooming, have been suggested as possible routes of transmission [58, 62, 139]. Global FFV prevalence in pet and feral domestic cats can be high and varies from 8 to 80% based on geographic location, population sampled, and assay type [62, 71-80]. FFV prevalence studies of cats in the USA have documented infection rates of 10 to 75%, with age and male sex identified as risk factors in some cohorts [58, 62, 81].

FVs are generally host-specific with the exception of non-human primates (NHP) where simian foamy virus (SFV) virus may be transmitted to related species and zoonotically to humans [48, 49, 52-54, 66, 174, 175]. Zoonotic transmission of FFV to humans has not been detected thus far [5, 47, 73]. Because of the apparent apathogenicity, wide tissue tropism, and large genome size, FVs have been used to develop vaccine and gene therapy vectors in multiple species including cats and as a model for future human therapies [29, 57, 91, 97, 102, 104-106, 146]. Many aspects about FV biology, including target cells, latency reservoirs, the specific receptor used for cell entry, viral kinetics over time following infection, and peripheral blood mononuclear cell (PBMC) phenotype changes during infection have been poorly documented [5, 6, 23, 59]. Experimental FFV infection studies in disease-free SPF domestic

cats with age- and sex-matched negative controls using modern and specific assays are rare [11, 55, 56, 58, 59, 85, 91, 106].

While FFV has been detected in apparently disease-free and healthy animals and has historically been considered apathogenic, it has been detected in animals suffering from renal and urinary tract disease [9, 59, 78, 83, 84, 124-126], polyarthritis [85, 86], neoplasia [11, 12, 78, 87], upper respiratory illness [59, 78], and myeloproliferative diseases [58]. FFV has also been associated with other pathogens, such as during co-infections with feline immunodeficiency virus (FIV) [62, 63, 71, 86], feline leukemia virus (FeLV) [85, 88, 89], feline coronavirus [78, 90], and *Bartonella henselae* [72]. German et al. have reported kidney and lung histopathological changes following experimental FFV inoculation [59]. A recent study of zoonotic infections of SFV to African hunters found significantly decreased amounts of hemoglobin and basophils and alterations of renal parameters including blood urea nitrogen (BUN) and serum creatinine, among other hematological changes [49]. The findings in both cats and humans thus may call into question whether chronic infections with FVs are truly apathogenic.

Chronic kidney disease (CKD) is the most commonly diagnosed renal disease syndrome in cats. CKD prevalence rates can reach up to 50% in cat populations and up to 85% as cats become geriatric [108-110]. CKD is characterized by functional and structural loss of kidney tissue likely resulting from prolonged or repeated insults to kidneys [112-115]. Cats affected by CKD can present with increased BUN and serum creatinine, improperly concentrated urine, and increased urine protein:creatinine (UPC) ratio. While the etiologies of CKD are often unknown, a list of comorbidities have been associated with the development of CKD, including retroviral infections [82, 121-123].

Due to the widespread and prevalent presence of FFV in domestic cat populations and the knowledge gaps that remain about FFV pathogenicity, especially considering its use in vaccine and gene therapy development, the data of a previous in vivo FFV experimental infection in

healthy SPF domestic cats [57] were further analyzed in detail to specifically assess clinical, immunological, and pathological characteristics and changes during early infection, and compared findings to age- and sex-matched negative controls. We identified altered hematological and biochemical parameters potentially associated with renal damage, histopathological changes in the lung, brain, and other tissues, and ultrastructural changes in the kidney. Based on these findings, and reports in the literature mentioned above regarding FFV's potential effect on renal tissue, we conducted an FFV survey of pet cats suffering from CKD in the USA and Australia (AU) and compared to age- and sex-matched cats without CKD to more fully elucidate potential links between the two conditions. We found that in males, there is an association between FFV and CKD, in addition to an association between male sex and FFV infection overall.

Materials and Methods

Cells and virus generation

Plasmid pCF-7 encoding an FFV genome that is replication-competent in vitro and in vivo was used as virus source [91]. Virus production has been described in more detail previously [57]. Crandell feline kidney (CrFK) cells [14, 74, 79] were used for transfection, viral propagation, and titer determination as described [57]. A CPE end-point dilution assay was used to determine viral titer (50% tissue culture infectious dose, $TCID_{50}$/mL) for cat inoculations [57, 170]. CPE consistent with FFV infection include cytomegaly, vacuolization, and syncytia formation [10-12].

Animals and study design for experimental FFV inoculation

Cats were infected with pCF-7-derived FFV as a control group for a previous study testing an experimental molecularly modified FFV vector [57]. This present report provides further detailed analyses about FFV-associated hematologic and microscopic pathologies to identify

any FFV-induced changes during experimental infection. Briefly, nine cats (male castrated and intact females, aged 6-8 months) from the Colorado State University (CSU, Fort Collins, CO) specific-pathogen-free (SPF) colony, which is free of FFV, were housed in an animal facility at CSU accredited by the Association for Assessment and Accreditation of Laboratory Animal Care International. All animal procedures were approved by the CSU Institutional Animal Care and Use Committee (IACUC, Protocol #: 13-4104A, approved December 05, 2013). Cats were separated into naïve (N) and FFV groups based on inoculum (Fig. 1, modified with permission from [57]): cats N1-4 received FFV-negative CrFK culture media and FFV1-4 cats were inoculated with 10^5 FFV particles (based on a 2.78 x 10^5 $TCID_{50}$/ml determined by end-point dilution titration in CrFK cells) in CrFK culture supernatant [57]. Each cat was inoculated with 2 ml, divided into 1 ml intravenously (i.v.) through the cephalic vein and 1 ml intramuscularly (i.m.) into hindlimb musculature. A fifth cat was inoculated at the start of the study with 10^5 viral particles (5.56 x 10^5 $TCID_{50}$/ml, also determined through end-point dilution titration in CrFK cells) of the afore-mentioned chimeric FFV but remained PCR negative. This cat was subsequently inoculated with 1.4 x 10^6 $TCID_{50}$/ml of the pCF-7-derived FFV on day 53 of the study and became FFV PCR positive [57]. This animal, referred to as FFV5, was included in our analyses to increase the statistical power of this study. The study timeline and sample collection schedule (blood, saliva, urine, and tissues) are shown in Fig 1.

Cats were monitored daily for clinical signs of infectious disease, and body temperature and weight measurements were taken on a weekly basis. Peripheral blood obtained through venipuncture (cephalic or jugular veins) was used for flow cytometric PBMC phenotype analysis or processed to collect serum and plasma shortly after collection. Whole blood and sera were submitted to the CSU Veterinary Diagnostic Laboratory (VDL) for complete blood count (CBC) and chemistry analyses. Saliva was collected by swabbing oral mucosa with a sterile cotton-tip applicator and freezing in -80°C.

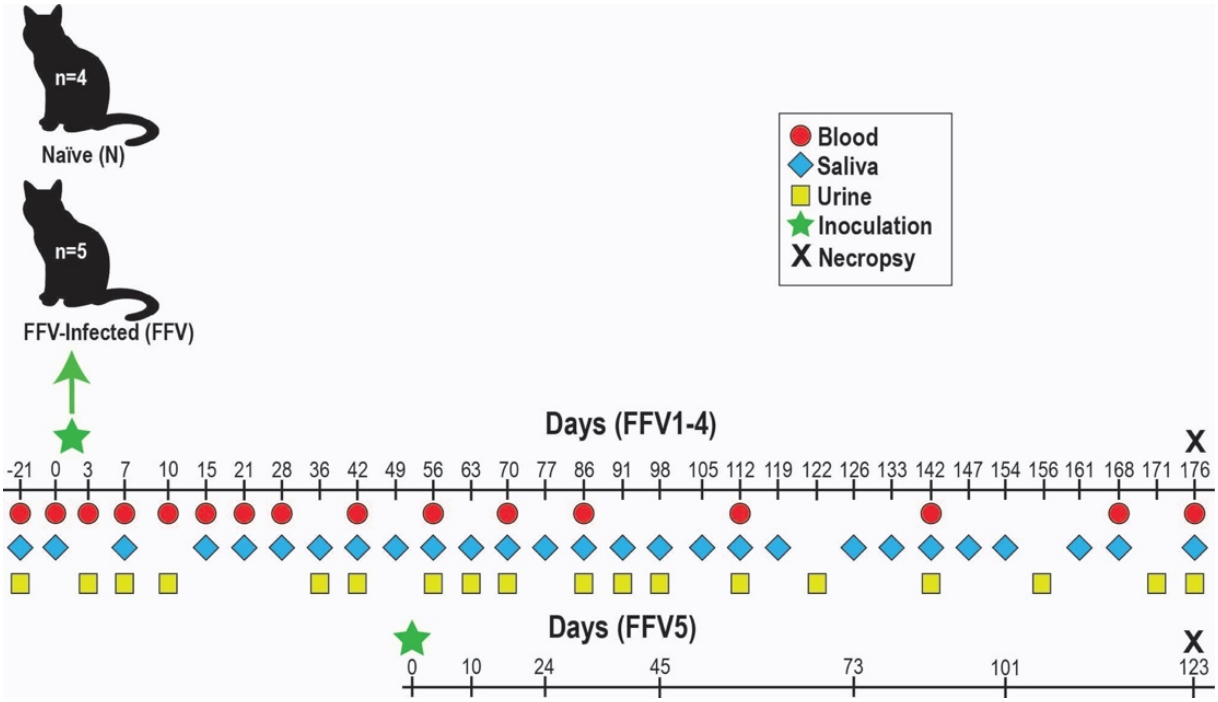

Figure 1. Experimental timeline of FFV (strain pCF-7) inoculation and sample collection in domestic cats. Cats were separated into groups based on inoculum type: negative CrFK culture media (naïve control cats N1-4) or 10^5 $TCID_{50}$ FFV in CrFK cell culture supernatant (cats FFV1-5). Blood, saliva, urine, and tissues were collected on dates specified. Sample collection for cat FFV5 was on a different schedule than the rest of the cohort. Samples for baseline data were collected on day -21. On day 176 post-inoculation, cats were euthanized to perform necropsy and tissue collection (black X). Figure modified with permission from [57].

Urine was collected through cystocentesis and submitted to the CSU VDL for urinalysis, urine sediment, and urine protein:creatinine (UPC) ratio determination. Urine was considered properly concentrated if it had a urine specific gravity (USG) over (>) 1.035. UPC ratio was considered normal if below 0.2 and borderline proteinuric if between 0.2 and 0.4 [119]. On day 176 post-inoculation (p.i.), cats were euthanized and necropsied to assess gross pathology and harvest tissues for virus detection, histopathology, and renal-specific assays at the International Veterinary Renal Pathology Service (IVRPS) in The Ohio State University (OSU, Columbus, OH).

Sample selection for client-owned cats with CKD and age-matched controls without CKD is described below (section 2.7).

Nested and real-time quantitative PCR for virus detection and quantification

Nested PCR (nPCR) and real-time quantitative PCR (qPCR) for FFV provirus DNA detection and quantification were performed as described [57, 168]. DNA was purified from whole blood, saliva, and plasma using the DNeasy Blood and Tissue Kit (QIAGEN, Hilden, Germany) and amplified using 0.5 μM forward and reverse primers under conditions described [57, 168]. nPCR products were electrophoresed in agarose gel and stained to identify the desired PCR product. qPCR was performed in up to triplicate on purified FFV DNA as described [57, 168]. Tissue DNA was purified with the DNeasy Blood and Tissue Kit after homogenizing in Buffer ATL and Proteinase K using the FastPrep-24 Instrument (MP Biomedicals, Santa Ana, CA). Saliva and plasma RNA was purified using the QIAamp Viral RNA Mini Kit (QIAGEN). RNA was reverse transcribed to cDNA using Superscript II and random hexamer primers (Invitrogen, Carlsbad, CA) and resulting cDNA was used for qPCR as described above.

Hematological and flow cytometric analyses for PBMC phenotyping

White blood cell (WBC) populations (lymphocytes, neutrophils, and monocytes), red blood cells, and hematocrit (HCT) were measured over the study period. For flow cytometric PBMC phenotype analysis, EDTA-anticoagulated blood was incubated with fluorescent-labelled antibodies (Appendix File 7) diluted in cold flow buffer (PBS with 5% bovine fetal serum and 0.1% sodium azide) and processed by the IMMUNOPREP whole blood lysis method on a Q-Prep EPICS Immunology Workstation (Beckman Coulter, Fort Collins, CO) to lyse red blood cells. Samples were analyzed with a Gallios Flow Cytometer (Beckman Coulter). Output data were analyzed using FlowJo software (FlowJo, Ashland, OR). Data from the CBC were used to determine absolute neutrophil, lymphocyte, and monocyte cell numbers by multiplying the number of nucleated cells by percentages of each cell population. These absolute population numbers were then multiplied by percentages of each cell subpopulation obtained through flow cytometry for each cat per timepoint. PMBC phenotype analyses were divided into two panels.

Panel A assayed T lymphocyte populations while Panel B determined number of B cells, natural killer (NK) cells, and monocytes. Markers for activation (CD134+, CD125+, MHCII+) and apoptosis (Fas+) were also assayed. In total, 24 populations were measured for each cat per timepoint (Table 1). General WBC activation and apoptosis were determined by multiplying WBC counts by MHCII+ and Fas+ percentages.

Table 1. White blood cell populations assayed for PBMC phenotype analysis.

Assay	Population	Cluster of Differentiation
CBC	WBC	-
	Monocytes	-
	Lymphocytes	-
	Neutrophils	-
Flow Cytometry (Panel A)	Th[1] lymphocytes	CD4+
	Activation	CD4+CD25+
	Activation	CD4+CD134+
	Apoptosis	CD4+Fas+
	Tc[2] lymphocytes	CD8+
	Activation	CD8+CD25+
	Activation	CD8+CD134+
	Apoptosis	CD8+Fas+
	Double positive T cells	CD4+CD8+
Flow Cytometry (Panel B)	B cells	CD21+
	Activation	CD21+MHCII+
	Apoptosis	CD21+Fas+
	NK cells	CD56+
	Activation	CD56+MHCII+
	Apoptosis	CD56+Fas+
	Monocytes	CD14+
	Activation	CD14+MHCII+
	Apoptosis	CD14+Fas+
	WBC activation	MHCII+
	WBC apoptosis	Fas+

[1]T helper, [2]T cytotoxic

Renal pathology assays on FFV-inoculated and naïve control cats

Renal tissues collected from cats FFV1-5 and N4 during necropsy were submitted to the IVRPS for comprehensive analysis with light microscopy (LM), transmission electron

microscopy (TEM) and immunofluorescence (IF). Samples were submitted in 10% buffered formalin for LM, 3% glutaraldehyde for TEM, and Michel's transport media for IF, and were processed as previously described [176]. Briefly, formalin-fixed paraffin embedded samples were sectioned at 3 μm thickness and stained with HE, Periodic Acid Schiff (PAS), Masson's Trichrome (MT), and Jones Methenamine silver method (JMS). Samples for TEM were processed routinely and examined with a JEOL JEM-1400 TEM microscope (JEOL USA, Inc., Peabody, MA) and representative electron micrographs were taken with an Olympus SIS Veleta 2K camera (Olympus Soft Imaging Solutions GmbH, Münster, Germany). For IF, samples were washed to remove residual plasma constituents, embedded in Optimal Cutting Temperature (OCT, Sakura Finetek USA INC, Torrance, CA), and frozen until sectioning. The OCT blocks were sectioned at 5 μm thickness and direct IF performed with FITC-labeled goat anti-feline Immunoglobulin (Ig)G, IgM, and IgA antibodies (Bethyl Laboratories, Montgomery, TX) as well as FITC-labeled rabbit anti-human lambda light chain (LLC), kappa light chain (KLC), and C1q antibodies (Dako-Agilent, Santa Clara, CA). Stained sections were examined using an Olympus BX51 epifluorescence microscope and representative images were taken with a Nikon Digital Sight DS-U2 camera (Nikon, Tokyo, Japan). TEM assessment was not performed on control cat N4.

Gross necropsy and histologic characterization of tissues

To evaluate pathologic changes associated with FFV infection, necropsy was performed on cats FFV1-5 and control cat N4 on day 176 p.i. The following tissues were collected and stored either frozen in -80°C for viral tropism determination (qPCR) or in 10% buffered formalin for histopathological evaluation by light microscopy: lymph nodes (submandibular, mesenteric, pre-scapular, retropharyngeal, and ileocecocolic), thyroid, tongue, tonsil, oral mucosa, salivary glands, thymus, heart, lung, spleen, liver, kidney, ovary, testis, mammary tissue, brain (cerebrum, cerebellum, brainstem), small intestine (jejunum, ileum), colon, bone marrow, and

hindlimb skeletal muscle. For histopathological assessment, formalin-fixed tissue samples were embedded into paraffin and 5 μm sections were collected onto charged slides (Superfrost; CSU CDL, Fort Collins, CO). One slide of each tissue was stained with hematoxylin and eosin (HE) for microscopic examination. Tissues were scored using the following scale: 0 = no apparent pathology/change, 1 = minimal change (minimally increased numbers of small lymphocytes, plasma cells, macrophages, and/or mast cells), 2 = mild change (mild inflammation, edema, and/or parafollicular expansion, secondary follicle formation, and presence of tingible body macrophages within lymph nodes), 3 = moderate change (as previously described, but more moderately extensive), 4 = marked changes (as previously described, but with severe inflammation, edema, and/or lymphoid reactivity).

CKD sample collection and classification criteria

In order to determine associations between FFV infection and chronic renal lesions, we opportunistically collected blood samples from pet domestic cats following routine clinical care in the USA and AU. Samples in the USA group were obtained from the CSU Veterinary Teaching Hospital (VTH) and AU samples were obtained from the University of Sydney VTH (Sydney, Australia). Pet cats were considered to be CKD-positive (+) based on presence of clinical signs on presentation, history, serum creatinine > 1.6 mg/dl, and improperly concentrated urine when normally hydrated, signified by USG less than (<) 1.035 [119]. Severity of CKD was staged from I to IV based on International Renal Interest Society algorithms [119]. For comparison of FFV infection and CKD incidence, we selected samples from age- and sex-matched CKD-negative cats (-) that did not display clinical and biological changes indicative of CKD. Urine specific gravity for CKD-negative cats was not validated.

An overall total of 223 samples were analyzed for FFV infection by either nPCR (whole blood) or an FFV Gag ELISA (sera/plasma) as described previously [57]. There were 53 sera/plasma samples in the CKD+ USA group, 45 sera/plasma samples in the CKD- USA

group, 59 whole blood and 28 sera/plasma samples in the CKD+ AU group, and 38 whole blood samples in the CKD- AU group. Normal reference values varied for BUN and creatinine based on equipment used at each location. In the USA group, the normal range for BUN was 18 – 35 mg/dl and serum creatinine 0.8 – 2.4 mg/dl. Four different laboratories were used for testing cats from AU and serum creatinine and BUN were classified as abnormal based upon the references established for each laboratory (BUN: 7.2 – 10.7 mmol/L, 5.7 – 12.9 mmol/L, 5 – 15 mmol/L, or 3 – 10 mmol/L; serum creatinine: 91 – 180 µmol/L, 71 – 212 µmol/L, 40 – 190 µmol/L, or 0.08 – 0.2 mmol/L). CBC, blood chemistry, USG, UPC ratio, and sex were recorded when available. Cats for which sex data were not known (n=7) were omitted in sex-specific data analyses. USG data was not available for the CKD- US cohort.

Statistical analyses

Data are presented as mean of duplicate or triplicate values and standard deviations displayed as error bars in corresponding graphs. For the experimentally FFV-inoculated cats, two-tailed Student's t test were performed on hematology, flow cytometry, BUN, serum creatinine, and USG data sets. A P-value less than (<) 0.05 was considered statistically significant. For cat FFV5, the timeline following re-inoculation on day 53 with FFV was adjusted so that day 53 equaled day 0 p.i. Timepoints from there on were grouped with either the equivalent day or the nearest date post-inoculation to adjust FFV5's timeline to be consistent with FFV 1-4. A Pearson's correlation coefficient was calculated to determine presence of a correlation and its significance between lymphocyte population numbers and FFV proviral load over time. To assess distributions of viral load to lymphocyte counts, we ran a generalized linear mixed model (GLMM) with the individual cat as a random factor and lymphocyte count as a fixed factor. Data was only run through the GLMM if viral load was at detectable levels and the data fit a negative binomial distribution.

For the CKD analyses, Student's t tests were performed on BUN, serum creatinine, and USG data as described above. Risk ratios (RR) and chi-square tests were performed to assess the independence of three pairs of categorical variables: 1) sex and FFV infection, 2) sex and CKD, and 3) FFV infection and CKD. For each pair of variables, cats were stratified by location (USA or AU), sex (M or F), FFV status (+ or -), and CKD status (+ or -). If a chi-square test produced a P-value < 0.05, RRs and 95% confidence intervals (95% CI) were calculated as an additional post-hoc test. RRs describe the probability of a health outcome occurring in an exposed group to the probability of the event occurring in a comparison, non-exposed group. A RR > 1 suggests an increased risk of that outcome in the exposed group, and a RR < 1 suggests a reduced risk in the exposed group.

Excel (Microsoft Corporation, Redmond, WA) and Prism (GraphPad, La Jolla, CA) were used to conduct the Student's t tests, calculate the lymphocyte and proviral load Pearson's correlation coefficient, and produce graphs. GLMM and CKD analyses were run using the statistical program R version 3.4.2 [177]. The "fitdistrplus" package [178] was used to determine error distributions of the viral load data and the "glmmTMB" package [179] was used to run the GLMM. Chi-square tests and RRs for CKD were calculated using the 'epitools' package [180].

Results

FFV-infected cats did not show clinical signs of infection despite a persistent FFV proviral load and specific humoral response

As previously reported, all FFV group cats became PBMC FFV DNA positive (PCR), starting at 21 d p.i. (Fig. 2) [57]. One cat (FFV3) was not PCR positive until day 42 but maintained a much higher proviral load than the rest of the cohort from that point on (Fig. 6 in [57]). Cat FFV5 was FFV PCR positive by 10 days p.i. with FFV pCF-7 (Fig. 2 and 3). FFV DNA was consistently detected in PBMC once the animals showed positivity [57]. Out of 80 FFV saliva samples tested, FFV RNA was detected only once (cat FFV4 on day 133 p.i.). All plasma

samples tested were FFV-negative (Table 2). Cats in the naïve group remained negative at all times. Additional proviral kinetics and anti-FFV antibody responses have been reported previously [57].

Despite evidence of productive infection and specific immune response [57], none of the cats developed a fever, had changes in body weight, or displayed signs of clinical illness related to infection (such as anorexia or lethargy). CBC and chemistry values did not change significantly from baseline or indicate disease (data not shown).

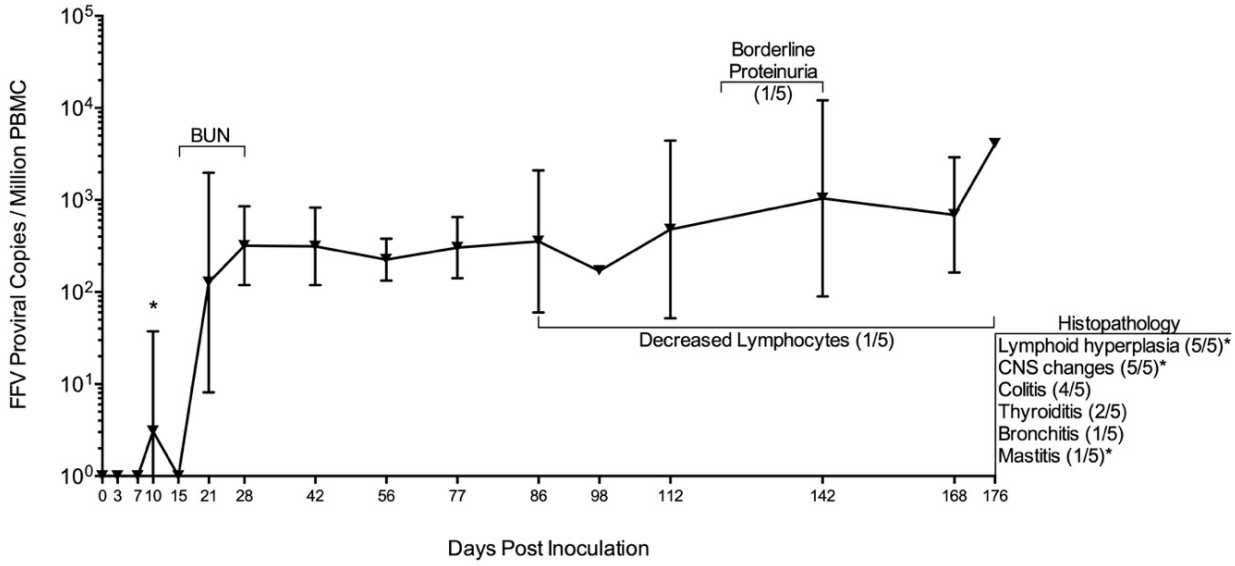

Figure 2. FFV proviral load in PBMC of cats FFV1-5 with summary of significant findings. FFV-infected cats began showing PBMC provirus 21 days p.i. Cat FFV5 was re-inoculated and its timeline adjusted to match the rest of the cohort; this cat showed FFV positivity on day 10 post-reinoculation (*) [57]. BUN was significantly increased in infected cats compared to naïve on days 15, 21, and 28. Cat FFV3 had decreased lymphocytes compared to the rest of its cohort, which was negatively correlated to proviral PBMC load (see "Results"). FFV3 also had borderline proteinuria on days 122 and 142 p.i. Histopathological changes found after necropsy on day 176 are shown at the right-hand margin. Graph shows mean of FFV group cats' FFV proviral load with bars denoting standard deviation. Numbers in parenthesis indicate number of cats out of the FFV cohort showing findings, with an asterisk (*) indicating findings also observed in the control cat to a lesser severity.

FFV provirus tissue tropism is primarily lymphoid in nature

FFV DNA was detected in the tissues of four out of the five FFV-inoculated cats primarily in lymphoid tissue including lymph nodes (submandibular, retropharyngeal, and prescapular,

which are involved in draining lymph from head, neck, and forelimbs), tonsil, and spleen (Table 3).

Table 2. Summary of findings for diagnostic assays used in this study. Bold font indicates that at least one cat was positive for the measured value, or differences in values between naïve and FFV-infected animals were significant. Cat FFV5 was on a different inoculation and sample collection schedule following re-inoculation on day 53 p.i. (see Fig. 1).

Assay	Days Tested	Summary of Findings
Saliva qPCR (RNA)	36, 42, 49, 56, 63, 86, 112, 119, 126, **133**[1], 142, 147, 154, 161, 168, 176	Only cat FFV4 was RNA-positive at 133 d p.i.
Plasma qPCR (DNA)	42, 86, 142, 176	FFV not detected and/or too little DNA extracted.
Plasma qPCR (RNA)	15, 56, 112	FFV not detected.
Tissue qPCR (DNA)	176	Virus shows primarily lymphoid tissue tropism. Cat FFV3 had expanded tropism to other lymphoid and non-lymphoid tissues compared to cohort (see Table 3). FFV not detected in cat FFV4's tissues.
CBC, Chemistry	-21, 0, 3, 7, 10, 15, 21, 28, 42, 56, 63, 70, 77, 86, 98, 112, 126, 142, 154, 168, 176	Not indicative of disease for infected cats.
PBMC Phenotype	-21, 0, 3, 7, **10**, **15**, 21, 28, **42**, 56, 70, **86**, **112**, 142, 168	Significantly increased populations in FFV cats included monocytes and CD21+MHCII+, while CD8+CD25+, CD8+CD134+, CD8+FAS+, CD56+, and CD56+MHCII+ cells were decreased.
BUN, Creatinine	-21, 0, 7, **15**, **21**, **28**, 42, 56, 63, 70, 77, 86, 98, 112, 126, 142, 154, 168, 176	While BUN remained within normal limits for all cats, values were significantly increased in FFV group cats compared to naïve on bolded days. Creatinine values were within normal ranges and did not rise above 1.8 mg/dl.
Urinalysis	-21, 3, 7, 10, 42, 56, 63, 70, 86, 91, 98, 112, 122, 142, 156, 171, 176	USG was >1.035 for all cats throughout study. Urinalysis and urine sediment were unremarkable.
UPC Ratio	36, 70, 86, 91, 98, **122**, **142**, 156, 171, 176	UPC ratio was 0.1 (normal) for all cats, except for cat FFV3 where it increased to 0.2 (borderline proteinuric) on 122 and 142 d p.i., coincidentally the time of highest PBMC viral load [57].

[1] DNA PCR also performed

Table 3. FFV provirus has a primarily lymphoid tissue tropism. Viral load was determined through DNA qPCR and is presented as viral copies per million cells. Cat FFV3 had altered PBMC FFV DNA kinetics and expanded tissue tropism compared to the other FFV cats. Cat FFV5 was on a different inoculation schedule than the rest of the FFV cats (see Fig. 1, "Materials and Methods"). Bold text indicates difference in either proviral load or presence compared to other cats in the group.

Tissue	N4	FFV1	FFV2	FFV3	FFV4	FFV5	Total
Salivary gland	-	-	-	-	-	-	0
Tongue	-	-	-	-	-	-	0
Oral Mucosa	-	-	-	2.10×10^2	-	-	1
Tonsil	-	2.41×10^2	4.03×10^2	-	-	5.10×10^2	3
Prescapular LN	-	5.89×10^3	-	-	-	4.96×10^2	2
Submandibular LN	-	3.35×10^2	2.26×10^2	-	-	5.78×10^2	3
Retropharyngeal LN	-	1.86×10^2	1.19×10^2	1.49×10^2	-	2.35×10^2	4
Mesenteric LN	-	-	-	-	-	-	0
Thymus	-	-	-	3.48×10^2	-	-	1
Spleen	-	5.93×10^2	3.11×10^2	2.10×10^2	-	3.35×10^2	4
Ileum	-	-	-	-	-	-	0
Bone marrow	-	-	-	6.10×10^2	-	-	1
Kidney	-	-	-	-	-	-	0
Muscle	-	-	-	-	-	-	0

Cat FFV3 showed an expanded tissue tropism to central lymphoid tissues (thymus and bone marrow) in addition to non-lymphoid tissue (oral mucosa). The prescapular lymph node was the tissue with highest viral load (cat FFV1). Cat FFV5 showed an FFV tissue tropism similar to the rest of the FFV group, with the submandibular lymph node having the highest viral load (Table 3). Control cat N4 and cat FFV4 did not have detectable provirus in any of the tissues examined.

Significant PBMC phenotypic changes were rare though a negative correlation was found between lymphocytes and FFV proviral load in cat FFV3

Out of the 24 cell populations and activation or apoptosis markers assayed for each cat per timepoint (Table 1), there were only 9 instances where significant differences ($P < 0.05$) were found between infected and control animals (Table 2). Significantly increased populations were found between FFV (1-5) and N (1-4) groups in the following instances: (1) absolute monocyte

numbers on days 15 (P = 0.036) and 42 (P = 0.025) p.i. and (2) CD21+MHCII+ cells on d 86 p.i. (P = 0.0076). FFV-group cats had decreased populations in the following instances: (1) CD8+CD25+ cells on d 112 p.i. (P = 0.044), (2) CD8+CD134+ cells on d 10 p.i. (P = 0.031), (3) CD8+FAS+ on d 10 p.i. (P = 0.015), (4) CD56+ cells on d 112 p.i. (P = 0.00038), and (5) CD56+MHCII+ cells on days 15 (P = 0.049) and 112 p.i. (P = 0.00070).

We further evaluated WBC populations in cat FFV3 due to the altered PBMC FFV provirus pattern observed [57]. This cat appeared to have lower lymphocytes and a trend for decreasing lymphocyte count over time compared to the rest of the infected and naïve cats (Fig. 3A, blue line) as PBMC proviral load increased over time (Fig. 3B, black line). A Pearson's correlation coefficient test for this cat showed a significant negative correlation between lymphocyte cell number and viral load over time (r = -0.653, P = 0.006). There was no correlation found in the rest of the infected cats (data not shown) and there was no significant relationship between viral load and lymphocyte count when we analyzed all cats as a group (GLMM Estimate -0.530, P= 0.596).

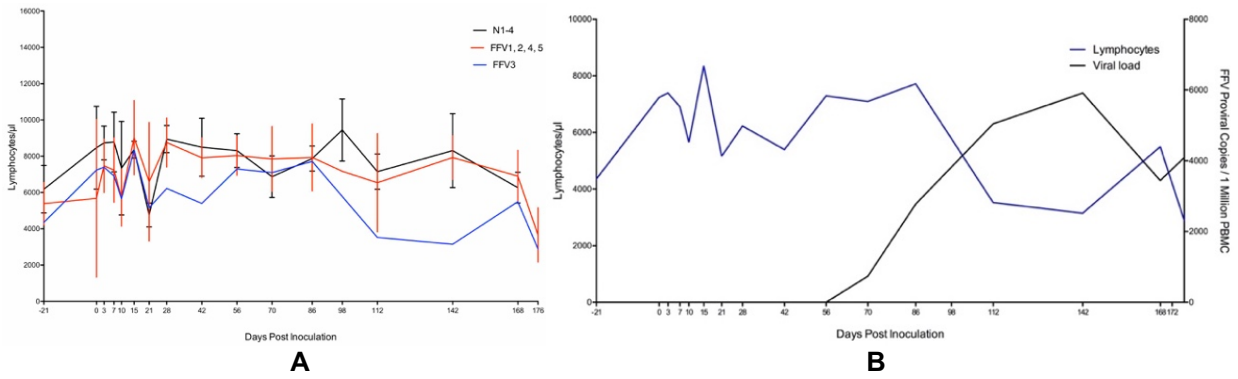

Figure 3. High viral load correlates with decline in circulating lymphocytes in cat FFV3. A Absolute lymphocyte population numbers determined through complete blood count for cat FFV3 (blue line) appeared to decrease over time compared to all other cats in the study. Naïve cats are grouped on the black line and the rest of the FFV-group cats are displayed in the red line. **B** A significant negative correlation (r = -0.653, P = 0.006) was found between lymphocytes and FFV proviral load [57] in cat FFV3 as lymphocyte population numbers (blue line) decreased and proviral load (determined by qPCR, black line) increased over time. Bars denote standard deviation.

Significant differences in renal parameters were detected in experimentally infected compared to control cats

UPC ratios were 0.1 (normal) for all cats throughout the study, with the exception of two timepoints in cat FFV3 (d 122 and 142 p.i.) where its UPC ratio increased from 0.1 to 0.2 (borderline proteinuric), before decreasing back to normal (0.1) on day 176 p.i. (Fig. 2) [181]. This mild transient increase in UPC coincided with the timepoint when this cat's PBMC FFV proviral load was highest (d 142 p.i.) (Fig. 3B, black line) [57]. BUN concentration remained within normal ranges (18-35 mg/dl) for all cats throughout the study, however values tended to be higher in infected cats compared to naïve controls (Fig. 4). BUN was also significantly increased in FFV cats compared to naïve controls on three consecutive timepoints: days 15 (P = 0.012), 21 (P = 0.039), and 28 (P = 0.025) (Fig. 2 and 4). All cats had properly concentrated urine (USG > 1.035) and urinalyses and urine sediment were unremarkable throughout the study. Serum creatinine concentrations were below 1.8 mg/dl at all timepoints, and there were no significant differences in serum creatinine between infected and control cats.

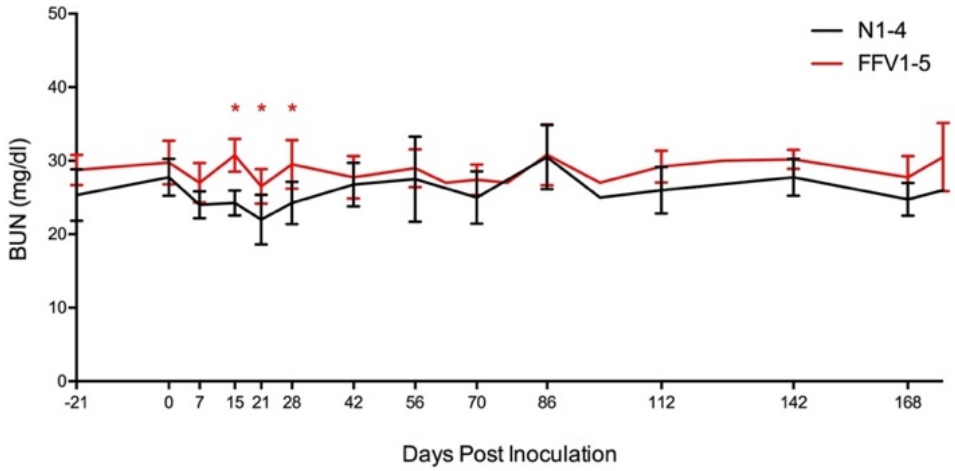

Figure 4. Blood urea nitrogen (BUN) levels are higher in FFV infected cats compared with naïve control cats. While BUN, one of the biomarkers used to assess renal health, remained within normal range (18-35 mg/dl) for all cats, concentrations tended to be higher in infected cats (red line) compared to naïve cats (black line) on days 15, 21, and 28 p.i. (red asterisks, $P < 0.05$). Lines represent mean of BUN measurements for the cats in each group. Vertical lines denote the standard deviation for each grouped measurement.

Ultrastructural changes were noted in kidneys of FFV infected cats

Histopathology of the kidneys from cats FFV1-5 and N4 (Table 4) demonstrated a few small foci of tubular degeneration encompassing fewer than 15 tubular cross-sections per focus in cats FFV1 and FFV2; cat FFV1 also had associated atrophy of the tubules. Glomeruli from the remaining cats in this cohort and the control cat were within normal limits.

Table 4. Summary of pathological findings in glomeruli of FFV-infected cats. Kidney tissue was collected during necropsy on day 176 and submitted to the International Veterinary Renal Pathology Service for analysis.

Analysis	Finding	FFV1	FFV2	FFV3	FFV4	FFV5	Cats Affected
Histology	Tubular degeneration (+/- atrophy)	+	+	-	-	-	2
TEM	Podocyte effacement	+/+	++	++	+	+++	5
	Cytoplasmic electron dense figures	-	+	+	+	+	4
	Cytoplasmic myelin figures	+	+	-	+	-	3
	Cytoplasmic vacuolization	-	+	+	-	-	2
	Wrinkled glomerular capillary walls	-	-	-	-	+	1

+ = minimal, +/+ = minimal to mild, ++ = mild, +++ = moderate

TEM evaluation of glomeruli from cats FFV1-5 (Fig. 5) demonstrated minimal to moderate segmental effacement of podocyte foot processes in all infected cats (Fig. 5 top left panel, and Table 4). There were a few small segments of wrinkled glomerular capillary walls in cat FFV5 (Table 4). Electron-dense whorls resembling myelin figures appeared free in the cytoplasm or within cytoplasmic vacuoles in tubular epithelial cells of three of the infected cats (Table 4). Cytoplasmic vacuolization of parietal or tubular epithelial cells was present in two cats (Table 4).

Within the cytoplasm of the proximal tubular epithelial cells of four of these cats, there were small electron-dense spirals and linear structures of 10-15 nm in length arranged in pairs, stacks, polygonal shapes, or spirals, and of variable length (Fig. 5, top right and bottom panels). Sometimes the linearly shaped ones had a beaded appearance or formed structures resembling a zipper. Mitochondria occasionally wrapped around the structures. In cat FFV5, the structures

were similar to the ones found in the other FFV cats but appeared significantly more organized.

TEM evaluation was not conducted on cat N4.

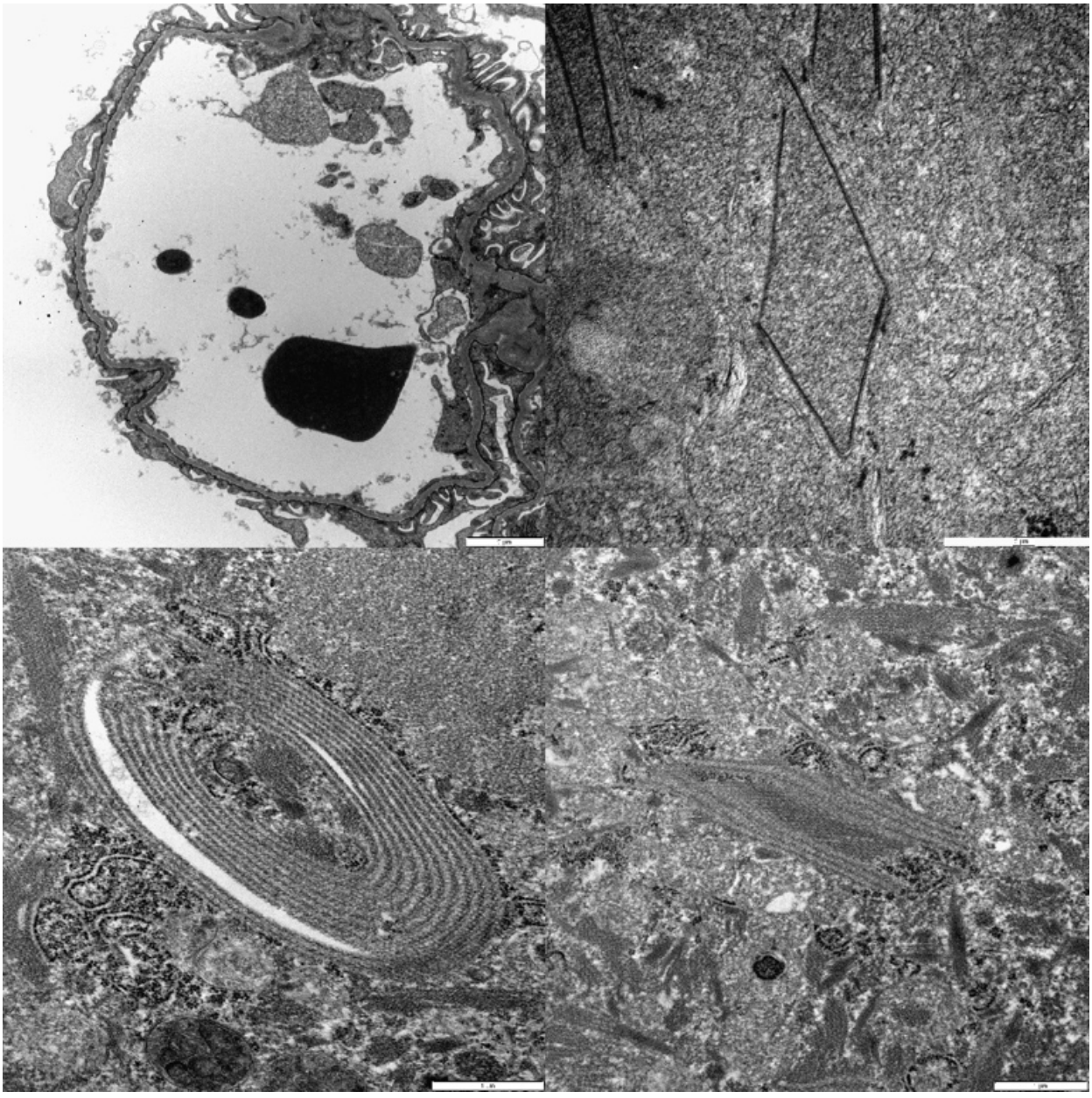

Figure 5. Transmission electron microscopy (TEM) documents podocyte foot process effacement and structures in the cytoplasm of epithelial cells. Podocyte foot process effacement (top left panel). Examples of organized linear structures in tubular epithelial cell cytoplasm are depicted in top right and bottom panels. These structures ranged from polygonal (top and bottom right panels) to ovoid (bottom left panel). Some structures were composed of a single electron dense line (top right panel), whereas others were composed of numerous parallel electron dense lines separated by regularly spaced electron lucent lines (bottom panels).

Immunofluorescence did not demonstrate definitively positive (granular) labeling for any of the antibodies (IgG, IgM, IgA, LLC, KLC, and C1q). Cat FFV3 had weak blush to linear staining with IgM of the glomerular mesangium and some capillary walls but based on the pattern of staining, it was considered non-specific. Naive control cat N4's immunofluorescence was negative.

Mild lymphoplasmacytic infiltrates and lymphoid hyperplasia of multiple tissues were associated with FFV exposure

No significant clinical or pathological findings were grossly observed in control (N4) or FFV-infected cats (FFV1-5) during necropsy. Microscopic evaluation of tissues from FFV-infected cats revealed mild (n=3) to moderate (n=2) lymphoid hyperplasia in retropharyngeal, submandibular, mesenteric, and prescapular lymph nodes, characterized by numerous secondary follicles that contain abundant tingible-body macrophages. The tonsils of infected animals exhibited minimal (n=1), mild (n=3), and moderate (n=1) lymphoid hyperplasia with multifocal infiltration of small numbers of lymphocytes beyond the capsule in one mildly affected animal. Two infected cats exhibited mild thyroiditis characterized by multifocal infiltrates of small lymphocytes, plasma cells, and macrophages within the interstitium and surrounding colloid-filled follicles of varying size. Within the ileum, Peyer's patches were minimally (n=1) to mildly (n=4) hyperplastic, and one animal exhibited multifocal lymphoplasmacytic infiltrates extending deep into the submucosa. Additionally, minimal (n=3) to mild (n=1) lymphoplasmacytic colitis was observed in FFV-infected cats, with lymphoplasmacytic infiltration into the submucosa that caused disruption of the submucosal architecture (n=3), as well as small numbers of degenerate neutrophils scattered within the submucosa (n=1). In the cerebrum of FFV-infected cats, there were minimally (n=2) to mildly (n=3) increased numbers of glial cells (gliosis) and paired astrocytes (astrocytosis) surrounding scattered neurons within the gray matter (satellitosis), a feature that was most prominently noted within the frontal lobe and thalamus

(Fig. 6B). Cat FFV5 also had small numbers of small lymphocytes within the meninges (lymphocytic meningitis) (Fig. 6C). Scattered neurons within these regions were multifocally swollen, rounded, and demonstrated mild central dispersion of Nissl substance (chromatolysis), as well as rare, scattered neurons that exhibited hypereosinophilic and/or fragmented cytoplasm (potentially indicative of neuronal necrosis) (n=2) (Fig. 6D). One cat had mild multifocal lymphohistiocytic mastitis.

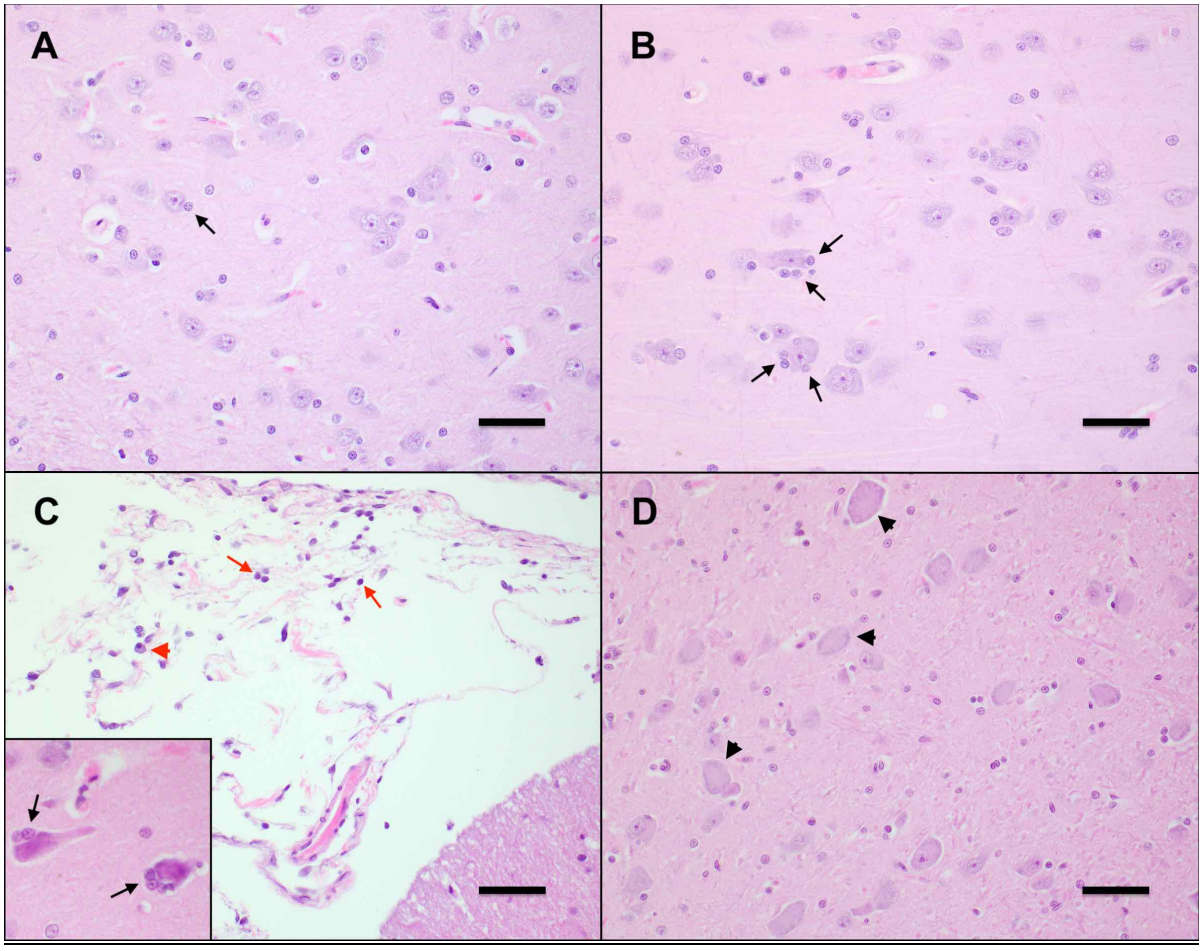

Figure 6. FFV-infected cats exhibit early neurodegenerative changes in the central nervous system. A Neurons in the CNS of naïve, uninfected cats contain uniform, round nuclei, abundant basophilic Nissl substance, and flanked by few glial cells (black arrow). Frontal lobe, Hematoxylin-eosin (HE) 400x. Scale bar = 100μm. **B** Neurons in the CNS of an FFV-infected cat (FFV3) exhibit moderate satellitosis, characterized by increased numbers of glial cells (black arrows). Thalamus, HE 400x. Scale bar = 100μm. **C** The meninges of an FFV-infected cat (FFV5) are expanded by minimal numbers of mature small lymphocytes (red arrows) and plasma cells (red arrowheads). Cerebellum, HE 400x. Scale bar = 100μm. Neurons in the frontal lobe of this animal (inset) are shrunken, with hypereosinophilic cytoplasm, and exhibit moderate satellitosis (black arrows). Frontal lobe, HE 400x. **D** Neurons in the CNS of an FFV-infected cat are swollen and rounded, with an indistinct nucleus and a dispersed Nissl substance (chromatolysis). Thalamus, HE 400x. Scale bar = 100μm.

Histologic changes in cat FFV5 were more pronounced when compared to the other infected animals and included moderate lymphoid hyperplasia in the tonsil with moderate numbers of lymphocytes and macrophages within the tonsil medullary sinus, and enlarged germinal centers in the Peyer's patches. Within the lung of this cat, the parabronchial interstitium and alveolar septa were multifocally expanded by small numbers of small lymphocytes, intact neutrophils, and macrophages (interpreted as mild interstitial pneumonia). Alveoli were occasionally filled with small numbers of alveolar macrophages and frequently lined by plump, cuboidal epithelial cells, indicating type 2 pneumocyte hyperplasia, with occasional clubbing of alveolar walls due to mild smooth muscle hypertrophy.

Non-specific histologic findings in control cat N4 included mild lymphoid hyperplasia in the mesenteric lymph node, tonsil, and thymus, minimal to mild inflammatory infiltrate in the tongue, and mammary tissue, and minimal chromatolysis in the cerebrum. Findings in this control cat ranged from very subtle to mild and were less severe than in infected animals.

FFV is prevalent in domestic pet cats and there is an association between FFV and CKD in males

Overall FFV prevalence was 57%, with AU prevalence (67%) being higher than in the USA (44%) (Appendix File 8). Prevalence rates were slightly higher in CKD+ compared to CKD- cohorts for the AU, USA, and Overall (Fig. 7). Males tended to have higher FFV prevalence in CKD+ versus CKD- groups (Fig. 7). Cats in all groups had an average IRIS stage between II and III with the majority of cats in stage II (data not shown). Results show there is no significant association between CKD and FFV infection when all cats from all locations are included.

To measure the strength of association between sex, FFV infection, and CKD, we additionally calculated relative risk ratios among groups. Amongst all CKD+ cats, there was a significant association between sex (male) and FFV infection status ($P = 0.037$). Male CKD+ cats across all sites had a RR of 1.37 with a 95% CI of (1.04, 1.81) and female CKD+ cats

across all sites had a RR of 0.73 with a 95% CI of (0.55, 0.96). Amongst the USA cats there was a significant association between sex and FFV infection status (P = 0.023), and male USA cats had a RR of 1.77 with a 95% CI of (1.13, 2.78). Female USA cats had a RR of 0.57 with a 95% CI of (0.36, 0.89). Finally, amongst USA CKD+ cats there was a significant association between sex and FFV infection status (P = 0.010). Male USA CKD+ cats had a RR of 2.42 with a 95% CI of (1.26, 4.65) and female USA CKD+ cats had a RR of 0.41 with a 95% CI of (0.22, 0.80). No significant differences were found in the BUN and blood creatinine concentrations between FFV infected and non-infected CKD+ cats sampled.

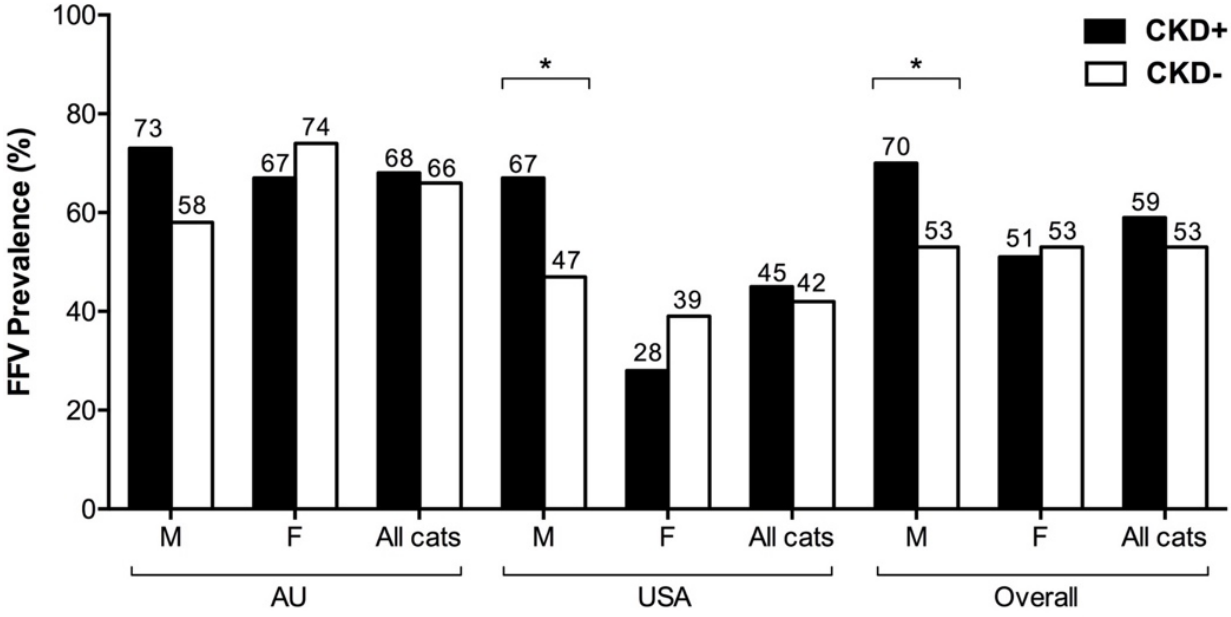

Figure 7. Male cats with CKD are more likely to have FFV infection. We found a significant association between CKD and FFV infection in male cats. Males with CKD have higher FFV prevalence rates than females in Australia (AU) and United States (USA). Australia had increased FFV prevalence rates compared to the USA. M=male; F=female. Asterisks denote significant associations between sex, CKD, and FFV status (P-value < 0.05) as analyzed by Chi-square test. Additional statistical details in "Results" section *Statistical analyses*. Chi-square test statistics and P-values are reported in Appendix File 8.

Discussion

One of the aims of this study was to further characterize FFV infection and host immune response in healthy SPF domestic cats through experimental FFV inoculation over the acute phase of infection. In addition to clinical monitoring, assessing viral kinetics and tropism, determining specific antibody response, and a histopathological assessment of different tissues, we conducted assays to expand infection characterization. This included flow cytometric assessment of specific white blood cell subsets suggested to be involved in FFV infection and renal-specific assays to determine the extent of FFV involvement in renal health or disease. Experimentally infected cat samples used in this study were obtained from cats reported in a previous study in which an FFV-based vaccine candidate was tested and PBMC FFV proviral load and antibody response compared to wild-type FFV infection [57]. Based on microscopic findings from the wild-type FFV-infected cohort indicating that renal displayed evidence of injury during early FFV infection, we next investigated the potential association of FFV with CKD in client-owned cats following natural FFV infection.

FFV established a detectable, persistent, and clinically apathogenic infection during the relatively acute 6-month time period of our study [56, 57, 59, 91]. Provirus was primarily isolated from lymphoid tissues, mainly PBMC, the retropharyngeal lymph node, and spleen, demonstrating lymphoid tropism as previously reported [55, 59, 81]. The expanded tissue tropism found in cat FFV3 with 10-fold higher proviral load than other cats also included the oral mucosa. Surprisingly, we were unable to detect virus in the tissues of one cat (FFV4) which also tended to have lower PBMC proviral loads [57]. Viral RNA was detected once in the saliva (also in cat FFV4), indicating that in our acute time period, limited amounts of virus were being shed, and salivary excretion may not correlate with widespread tissue distribution. A recently published report on FFV-infected cats in Brazil detected FFV DNA in buccal swabs via nested and quantitative PCR and found over 46% FFV positivity in buccal swabs through both methods [66]. Animals in this study were more likely to be FFV positive in PBMC than in buccal swabs,

as can be seen in primates due to a delay in salivary positivity of virus compared to blood [182]. A wide variability of FV positivity has been reported in different nonhuman primate species and even within the same species [68, 69, 183]. Samples from cats in the Brazilian study were also sourced from pet and feral cats with unknown time periods of FFV infection. It is possible that due to the acute time period in our study, infection had not yet reached high enough levels in the oral cavity in order to show positivity in the saliva. Nevertheless, the Brazilian study and this one suggest individual variability in salivary FFV shedding.

A significant negative correlation between lymphocytes and proviral load was notable in cat FFV3, despite the fact that PBMC phenotype analysis did not indicate increased cell death or lymphocyte subset contraction in any of the FFV-infected cats, thus PBMC phenotyping appears to not be useful as an indicator of FFV infection. These findings may indicate that a subset of FFV-infected cats experience higher viral loads that correlate with expanded tissue distributions and potential for lymphocyte decline. Further work analyzing correlates of FFV infected cats with hematologic indices are warranted to investigate this limited observation in one animal.

Necropsy and histologic analysis of experimentally infected cats yielded minimal to moderate changes in the lymphoid compartment, CNS, large intestine, lung, and thyroid. FFV-associated lung lesions have previously been noted in another experimental FFV infection study, including mixed cellular infiltrates and eosinophilic fluid within alveolar walls [59], similar to findings reported here. The consistent changes in tissue histology and in renal indices particularly warrant further investigation. Alterations in CNS histopathology of FFV-infected cats suggest viral replication or associated inflammation as is seen in other retroviral infections [184-186]. FFV has previously been isolated from the CNS of cats, and may therefore indicate that FFV is capable of productive CNS infection and subtle neurologic alterations [187]. Future studies should be conducted to identify potential target cells of infection in the CNS and assess for development of neuropathogenic effects. These findings suggest a potential role for FFV in the development of mild acute inflammation in a variety of parenchymal organs and brain. The

pathogenic mechanisms and overall consequence of these lesions are undetermined, especially considering the low number of cats studied and that some of the histopathological changes were found in the negative control cat to a lesser extent, but suggest some microscopic alterations can occur during acute FFV infection.

FFV has previously been detected in animals suffering from renal and urinary syndromes [9, 59, 78, 83, 84, 124]. BUN concentrations remained normal during FFV-infection but were statistically elevated in FFV-infected compared to naïve groups on days 15, 21, and 28 p.i., which coincided with the days when animals were first FFV PCR and ELISA positive [57]. Borderline proteinuria (increased UPC ratio to 0.2 [119]) was also seen in cat FFV3 on days 122 and 142 p.i., which coincided with the timing of the highest viral load measured in the study period. These mild increases in renal parameters could be considered a transient systemic alteration due to infection. Mildly increased UPC could also develop due to non-infectious reasons including fever, hypertension, exercise, and others [188-190]. The cats in our study, however, remained clinically normal and no changes were made in their management that could account for increased periods of activity during that time. Interestingly, a recent report on chronically zoonotically SFV-infected people also noted increased BUN compared to un-infected controls, in addition to other hematological alterations [49].

Ultrastructural kidney changes (glomerular podocyte foot process effacement, myelin figures, vacuolization, and wrinkled glomerular capillary walls) are non-specific and reversible changes. If enough podocytes are irreversibly injured, then the patient can develop segmental to global glomerulosclerosis, a disease process in humans and small animals that can cause proteinuria, usually with UPC > 2. Although a cut off for the number of irreversibly injured podocytes has not been established in cats, a model of glomerulosclerosis in rats estimated that >40% of the podocytes have to die and detach in order for glomerulosclerosis to develop [191]. Notably, glomerulosclerosis was not identified in any of the cats in the present study. Tubular atrophy noted on histopathology is an irreversible lesion and often seen in cats with clinical

evidence of CKD [114, 115]. Electron-dense structures identified in proximal tubular epithelial cells in the kidney could represent viral structures at immature stages of assembly before forming the spherical shapes of FFV virions reported in the literature [12, 34, 192]. Similar structures have been found in the central nervous system in both cats and humans. Cook and others described similar tubular structures as “paramyxovirus nucleocapsid-like” in the cytoplasm of oligodendrocytes taken from a demyelinating lesions in the optic nerve of three clinically healthy adult cats [193]. These inclusion-body like structures were of 16-17 nm in diameter and fused into penta- to septa-laminar shapes and 900 nm in length. The authors suggested a possible viral etiology. Wilcox and others (1984) reported similar structures in optic nerves and brains of 24 clinically healthy cats from which FFV was isolated [187]. While also finding 10-18 nm wide and 500 nm long structures they also reported structures in much smaller shapes, appearing as “short, disorganized fragments,” located next to where budding virions were observed, in addition to intranuclearly. These structures were, however, found in the cytoplasm of cells that did not display CPE and thus these lesions were not attributed to FFV but perhaps a morbillivirus [187].

A higher FFV prevalence in Australia versus the USA may be attributable to the lifestyle of cats in Australia, which are commonly allowed outside [194, 195], where contact with other infected cats would lead to greater chance of exposure and transmission of virus compared to cats in the US which are more typically housed indoors. All of the USA samples were evaluated by ELISA, while Australian samples consisted of serological samples assayed by ELISA but also whole blood samples analyzed by PCR. PCR is not as sensitive as ELISA for detection and can yield false negatives [56, 57, 62, 80, 168] therefore, it is possible that the FFV prevalence is even higher in Australia.

We found that in male cats with CKD, there was a significantly higher risk of FFV infection compared to CKD-negative males, especially in the USA. This further supports some role of FFV infection in development of CKD, but additional studies should be conducted to verify this

observation. Male sex has not been found to be an overall risk factor for CKD, however males can be overrepresented in certain age groups affected by CKD [196].

The association of FFV with male sex, particularly in the USA, is also notable. One reason for this could be the increased testosterone-associated territorial aggression in males that leads to a higher incidence of infection of male cats as is seen with FIV, another retroviral infection of cats [62, 197, 198]. A recent study of feral cats in the US found an association between FFV infection and male sex [81]. However, our epidemiological results were obtained from desexed animals. An epidemiological study of FFV in Australia did not find an association between sex and FFV infection in desexed domestic cats, but did see higher incidences of FFV in female feral cats [62]. Thus it appears that the association between male sex and FFV is not due to desexing and ensuing behavioral patterns due to hormonal influence. Estradiol has been shown to be associated with decreased apoptosis of female cat lymphocytes [199]. Studies evaluating the effect of sex and hormones in cat response to infection are rare. Sex differences in innate and adaptive immune system response, genetic and hormonal mediators are differentially expressed in male and female mammals in general and could account for sex-based differences in response to infection with males being more susceptible to infection [200, 201]. Why this association was significant in the USA and not Australia is currently unknown. It is possible that there were false negatives in this cohort, as some of the samples tested in the AU cohort were whole blood and assayed by qPCR which is not as sensitive as the GST capture ELISA [56, 62, 80, 168]. Also since specific gravity was not calculated in US cats, it is possible that the CKD negative cohort was actually positive. Experiments to elucidate the reason for increased FFV susceptibility in males and due to geographical location are warranted.

Conclusions

Collectively, our findings reinforce and expand on the current established notion that FFV is widely prevalent and apathogenic over an acute time period, corroborating decades long

assumptions that FFV is well adapted to the domestic cat host. However, our detailed analysis of hematological and histopathological changes indicates sub-clinical alterations that could contribute to metabolic or degenerative diseases over time, supporting work conducted by earlier researchers [9, 11, 12, 58, 59, 78, 83-87, 124-126]. The negative correlation between lymphocytes and viral load in one cat with higher viral load suggests that a differential susceptibility and potential pathogenicity may exist in some individuals. Further, multiple lines of evidence outlined above hint that FFV may play a role in renal disease that has yet to be fully elucidated.

Since FFV is widely prevalent in both domestic and feral cat populations, practitioners and researchers should be aware of the potential for FFV to be associated with lymphoid depletion and worsening of CKD symptoms, especially in males. Until more information is determined about correlates of disease that are dependent upon FFV infection, it might be prudent for clinicians to screen cats acting as blood donors for FFV prior to using potentially infectious blood for transfusions to immunocompromised individuals as one relatively easily attained precaution.

CHAPTER 3. FFV ASSOCIATION WITH FIV

Background

The viral family *Retroviridae* consists of clinically significant viruses that cause specific disease syndromes in domestic cats (*Felis catus*). *Retroviridae* is composed of two subfamilies: the *Orthoretrovirinae* and *Spumaretrovirinae*. Feline immunodeficiency virus (FIV), a lentivirus from the *Orthoretrovirinae,* and feline foamy virus (FFV), a spumavirus, both establish lifelong infections with differing clinical outcomes in the feline host and are frequently found co-infecting the same animal [62, 63, 71]. While FFV is generally considered apathogenic [58, 141], it has been linked to other retroviral infections and potentiation of those infections has been documented [88, 142].

FIV infects and replicates in CD4+ T lymphocytes and in some cats, leads to an immunodeficient state predisposing the host to secondary bacterial infections and neoplasia (typically lymphoma or leukemia) [63, 131, 134-139]. Prevalence of FIV in healthy cats is 2% and in sick or at-risk cats up to 30% [63, 136, 138, 140]. Many FIV-infected cats live an asymptomatic life following infection [138], however, about 18% of cats infected with FIV will develop disease and require euthanasia or die within 2 years post-infection (p.i.) [136]. Virus is typically transmitted in the saliva via biting during antagonistic encounters [63, 127, 139]. Risk factors for FIV infection include sex (male), aging, and outdoor access [62, 63, 136, 138, 140].

FIV clinical disease typically progresses through three distinct phases: an initial acute phase, a longer asymptomatic phase, and in some cats, a final terminal clinical stage that may warrant euthanasia in client-owned cats [135, 136]. The initial acute phase can last from days to months and is characterized by a detectable plasma viremia that peaks around 2 weeks p.i., transient lymphadenomegaly, fever, enteritis, stomatitis, respiratory tract disease, ocular problems, and dermatitis, while appetite, body weight, and social behaviors tend to remain normal [63, 131, 135-137, 139, 202]. The following asymptomatic phase is marked by

alterations in various leukocyte subset populations including peripheral white blood cells (WBC), CD4+, CD8+, and CD21+ lymphocytes, and lasts on average about 8 years [131, 135, 140, 202, 203]. During this latent phase, FIV plasma RNA can become undetectable and remain at low levels for the remainder of the animal's life [131, 135]. The terminal stage of FIV clinical disease, when it occurs, is characterized by fever, anorexia and weight loss, marked panleukocytopenia leading to feline acquired immunodeficiency disease syndrome (FAIDS), non-regenerative anemia, secondary infections, neurologic disorders, and immune-mediated disease due to hypergammaglobulinemia (such as glomerulopathy and polyarthritis) [63, 136, 138, 140]. A hallmark of FIV infection is an inversion of the CD4+:CD8+ ratio due to decreasing CD4+ cells [131, 136, 137, 202, 203]. Cats in terminal FAIDS become non-responsive to symptomatic therapy and require humane euthanasia [63, 135]. In natural FIV infection, not all of these phases are apparent, and some cats that have progressed to FAIDS can still return to an asymptomatic stage following proper treatment [136].

In contrast to FIV infection and the associated immunosuppressive disease seen in some cats, FFV has not been linked to a specific disease process. Transmission of FFV is thought to occur through salivary shedding and ongoing intimate contact between cats such as grooming [58, 62, 139]. Prevalence of FFV varies by geographical location, population sampled, and assay used but can range between 8-80% [62, 71-80]. FFV experimental infections in domestic cats have been infrequent, and while some have not documented pathology [55, 56], one report found evidence of microscopic renal and pulmonary pathology [59]. In our laboratory, we have also found mild pathology and alterations in hematological parameters that could potentially lead to disease in chronic infection (Chapter 2). Additionally, others have isolated FFV from sick cats suffering from polyarthritis [85, 86], urinary syndromes [82-84], other retroviral infections including FeLV [88, 89], feline infectious peritonitis [78, 90], feline herpesvirus and feline calicivirus [9], and neoplasia [11, 12, 78, 87]. Recently, a group studying humans zoonotically infected with simian foamy virus (SFV) found hematological alterations indicative of anemia,

azotemia, and others [49]. Thus, infection is not obviously associated with clinical disease, however clinical implications of FFV are as of yet indistinct.

Epidemiological studies have documented significantly higher rates of FFV/FIV co-infection versus single FIV infection, with up to 90% of FIV-infected cats showing FFV positivity [71]. A potentiating role of FFV in FIV disease, either by directly affecting host immune response or through direct interactions between viruses, has been suggested [62, 63, 71]. Only one study, conducted over two decades ago, has reported outcomes of experimental FIV/FFV co-infection [141]. While the study found no association between co-infection and worsened FIV disease, the authors evaluated a very limited number of hematologic indices and did not assess relevant parameters such as viral kinetics and immune activation during single versus co-infection. The authors suggested that FFV could potentially affect later stages of FIV infection that were not monitored in this study [141].

Increased pathology in macaques co-infected with simian foamy virus (SFV) and simian immunodeficiency virus (SIV) has been reported [142]. In that study, naturally SFV-infected macaques were experimentally infected with SIV. Co-infected animals showed a higher SIV viremia, more pronounced decreases in CD4+ T lymphocyte population numbers, and higher morbidity and mortality rates than singly SIV-infected macaques [142]. A second study identified active replication of SFV concurrently with CD4+ T lymphocyte depletion in the jejunum of SIV-infected macaques, suggesting that co-infection might accelerate immune depletion [67]. An in vitro study also found that SFV-infected cells displayed increased permissiveness to HIV [204]. SFV has also been found to infect CD4+ cells [61].

Based on evidence showing that FFV and FIV are frequently co-isolated, and reports of worsened pathology in co-infected macaques, we hypothesized that FFV infection potentiates FIV infection and disease progression. In order to determine if there is an association between these viruses, we conducted a serosurvey of naturally FIV-infected cats to measure FFV prevalence. The cats were part of a previous study comparing clinical outcomes in two groups

of FIV-infected cats housed differently: one group consisted of 1-2 cat households in Chicago, IL and the second of a large multi-cat household in Memphis, TN [205]. Cats in the multi-cat household had increased FIV-related pathology and mortality compared to the singly-housed group. We theorized that a reason for the increased pathology and disease was due to higher rates of FFV/FIV co-infection in the multicat group. We additionally conducted an in vitro FFV/FIV co-infection study to assess potentiated infection as determined by more rapid development of cytopathic effects (CPE) and/or higher viral titers in the supernatant. Findings described below show that FFV and FIV natural infections are associated and that these viruses enhance each other's in vitro replication based on order of infection.

Methods

Naturally FIV-infected domestic cat samples used in the FFV serosurvey

Plasma samples from naturally FIV-infected, desexed cats used in our FFV serosurvey were obtained opportunistically from Dr. Carolyn Guptill (Purdue University, West Lafayette, IN); blood collection and FIV testing methods are described [205]. Plasma samples from FIV-infected cats were separated into two groups based on geographical origin and housing method (Table 1). Group 1 consisted of 39 plasma samples from cats that were adopted from a shelter in Chicago, IL and lived in 1-2 cat households. Group 2 consisted of 23 plasma samples from cats that were housed together in a large multi-cat household in Memphis, TN with unrestricted access to each other. Plasma samples were obtained from FIV-negative control cats that were age-, sex-, and location-matched, and lived in households of 3 cats or less (32 cats in Group 1 and 47 cats in Group 2) [205]. A total of 141 samples were assayed. The authors found that animals in Group 1 did not develop significant morbidity or mortality during the study period, while 63% of cats in Group 2 suffered from weight loss, neoplasia, and death. Sex, FIV plasma viral load, FIV strain, white blood cell (WBC) count, lymphocyte numbers, and CD4+:CD8+ ratio

data was obtained for each cat if available. The authors did not find significant differences in FIV plasma load, CD4+:CD8+ ratio, or FIV strains between the two groups [205].

Table 1. Comparison of the two naturally FIV-infected groups used in our serosurvey. Expanded group descriptions and results are published [205].

	Chicago (Group 1)	Memphis (Group 2)
Source	Large metro area shelter	FIV+ cat rescue
Living condition	1-2 cat households	Large multicat household
Morbidity	Relatively healthy	Anorexia, weight loss, and lymphoma
Mortality rate	5.9%	63%

FFV GST-capture ELISA for specific antibody detection

A GST-capture enzyme-linked immunosorbent assay (ELISA) was performed on plasma samples from naturally FIV-infected cats to detect anti FFV Gag antibodies as described previously [57, 80, 172]. 96-well plates were coated with a glutathione-casein carbonate buffer overnight at 4°C then blocked with casein-blocking buffer (CBB, 0.2% w/v casein in PBS and Tween20, Sigma Aldrich, St Louis, MO) for 1 hr at 37°C. Plates were then incubated with 0.25 µg/µl recombinant GST-Gag antigen or GST control for 1 hr. Cat sera (diluted 1:50 in CBB) was incubated for 1 hr, followed by a 1 hr incubation with anti-cat-IgG Protein A horseradish peroxidase conjugate (1:50,000 diluted in CBB). TMB substrate was incubated on the plates for 5-8 min, then the reaction was stopped with sulfuric acid. Absorbance (measured as optical density, OD, at 450 nm) was immediately read. Samples were tested in duplicate, and the mean of ODs used as read-out. A cut-off value was determined from FFV-negative cat sera OD with the formula of 2 x (mean OD + 3 standard deviations). Samples that resulted in ODs closely above the cut-off were re-assayed with an additional pre-adsorption step of sera with 2 µg/µl GST-tag lysate in CBB for 1 h before incubating the sera on the plates.

Viruses and cells used for in vitro FFV/FIV co-infection assays

FFV plasmid pcf-7 [57, 91] was used for in vitro infections. 3 µg of FFV plasmid was transfected into human embryonic kidney (HEK) 293T cells (seeded at 1.5 x 10^6 cells/well in a 6-well plate) using Lipofectamine 2000 (Thermo Fisher, Waltham, MA). Virus-containing supernatant was cleared of cells by low-speed centrifugation, and this cell-free viral stock was used to infect Crandell feline kidney (CrFK) cells for virus production [9, 74, 79]. Cell-free supernatant of FIV strain C36, a well-characterized immunopathogenic strain, was used for infection studies [128, 132, 206]. GFox cells were used for the FFV/FIV co-infection and FIV titration assays; these cells are genetically modified CrFK cells, which are inherently permissive for FFV infection [34, 74, 79], that express the CD134+ receptor, thus rendering them susceptible to FIV infection as well [128, 133]. FeFAB cells were used for FFV titration; these are genetically modified CrFK reporter cells that express the *β-galactosidase* (*β-gal*) gene in the presence of FFV Tas protein produced early during FFV infection [169].

FFV and FIV in vitro co-infection titrations

FFV and FIV viral stocks were titrated on FeFAB and GFox cells, respectively. For FFV titration, light emission from FFV-infected FeFAB cells was determined using a luminometer. FeFAB cells were seeded at a density of 1 x 10^4 cells/well on black-walled and clear bottomed 96-well plates and incubated for 3-6 h in a humidified chamber at 37°C and 5% CO_2. 25 µl of FFV-containing cell-free supernatant was added to all initial wells and a 1:5 serial dilution in triplicates was conducted down the row of the plate. The plates were incubated for 3 days and visual assessment of CPE (syncytia formation, vacuolization, and cell death) was conducted daily [9-12]. The GalactoStar System (Applied Biosystems, Foster City, CA), a chemiluminescent reporter assay that causes light emission in the presence of β-gal protein (Fig. 1), was used to detect FFV-infected wells [207]. FeFAB cells were washed with 100 µl/well 1X PBS then incubated with Lysis Solution (10 µl/well) for 10 min to lyse cells and release β-gal.

Galacton-Star Substrate (100 µl/well, diluted 1:50 in Reaction Buffer Diluent and equilibrated to room temperature) was added and plates were covered in foil and incubated for 1 h. The Galacton-Star substrate is deglycosylated by β-gal, producing an unstable intermediate that emits light (Fig. 1) [207]. After the 1 h incubation, light emission was measured with an LD 400 luminometer (Beckman Coulter, Brea, CA) for 0.1-1 sec/well (1-2 min/plate). Uninfected FeFAB cells were used as negative controls and the average of their read-out x 2 was used as the cut-off for positivity. For a positive control, *E. coli*-derived β-gal (Sigma-Aldrich) was used to generate a standard curve by serial 1:10 dilutions in Galacto-Star Lysis Buffer containing 0.1% BSA. 10 µl of each dilution was added per well, in triplicate, from 1:10 to $1:10^8$ and incubated with Galacton-Star Substrate concurrently with samples as described above. The AD LD Analysis Software (Beckman Coulter) was used to calculate the relative light unit (RLU) emission readout. The number of positive wells was used to determine $TCID_{50}$/ml through the Spearman & Kärber algorithm as described [208].

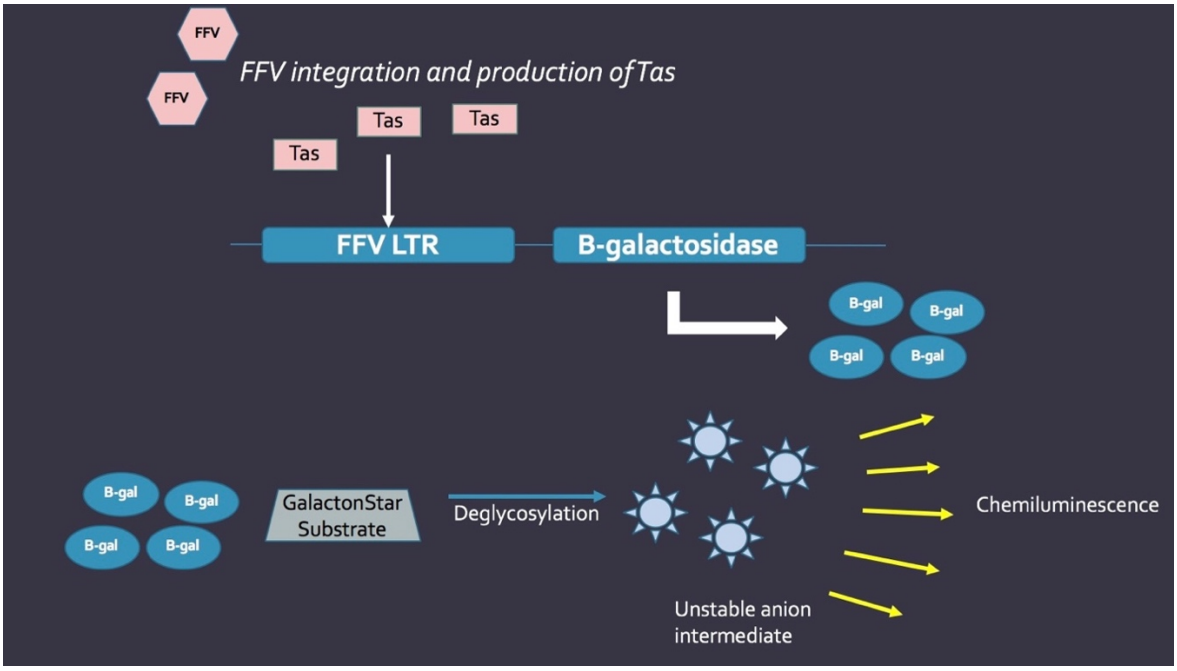

Figure 1. FeFAB cell β-gal production and diagram of GalactoStar chemiluminescence assay. β-gal is produced by FeFAB cells in the presence of FFV Tas. Tas binding to the FFV LTR leads to expression of the *β-gal* gene. β-gal deglycosylates the Galacton-Star substrate, leading to a detectable chemiluminescence.

FIV titer was determined on serial dilutions of supernatant using an FIV p26 capsid capture ELISA to detect presence of virus as described [209, 210]. GFox cells were seeded at 2 x 10^4 cells/well and allowed to attach for 3-6 h in a 37°C humidified incubator. 20 µl of FIV C36-containing supernatant was added to the first well dilution and 1:10 serial dilutions conducted down the row. Plates were incubated for 7 days after which supernatant was collected for titration by the p26 capture ELISA [209-211]. Briefly, 96-well plates were coated with 500 ng/well FIV p26 monoclonal antibody (donated by Dr. Greg Dean, Colorado State University, Fort Collins, CO) diluted in carbonate buffer overnight at 4°C. Plates were then blocked with TEN buffer and 2% BSA for 2 h. Afterwards, 100 µl of supernatant from the GFox viral dilution plates were added and incubated for 2 h. Anti-FIV antibody containing sera from chronically FIV-infected cat 2104 (100 µl/well, diluted 1:200 in ELISA diluent) was added and incubated for 1 h. Goat anti-cat IgG horseradish peroxidase (MP Biomedicals, Santa Ana, CA) was diluted 1:5000 in ELISA diluent and 5% mouse serum and incubated for 1 h. TMB (100 µl/well) was used for the substrate reaction with an incubation of 10 min, after which sulfuric acid was used to stop the reaction. Absorbance (OD_{450}) was measured and the average of negative supernatant controls subtracted from positive wells. Wells were scored as positive or negative based on a cutoff value of the average of the negative control wells x 2. $TCID_{50}$/ml was calculated as described above [208]. FIV C36-containing supernatant (100 µl/well, diluted 1:10 in ELISA diluent) was used as positive control.

FFV/FIV in vitro co-infections

FFV/FIV in vitro co-infection studies were carried out in 6-well plates. GFox cells were seeded at a density of 10^5 cells in 5 ml media per well and submitted to one of the following treatments per well after 6 h of incubation to allow attachment: 1) sham infection using GFox media, 2) single FFV infection, 3) single FIV infection, 4) FFV then FIV infection (FFV → FIV), 5) FIV then FFV infection (FIV → FFV), and 6) simultaneous co-infection (FFV + FIV). An MOI of

0.01 was used for all inoculations. All treatment conditions were conducted in triplicate. For the staggered co-infection assays, the second virus was added 24 h post-initial inoculation (day 1 for the second virus is thus technically day 0 for that second virus). Cells were observed daily, and CPE were recorded. Both FFV- and FIV-infected GFox cells display CPE of vacuolization, syncytia formation, and cytomegaly; FFV additionally causes lysis of GFox cells at a varying rate based on amount of infecting virus [9]. 1 ml supernatant was collected on days 1, 2, 3, 5, 7, and 10 p.i. and frozen in -20°C to conduct viral measurement experiments over time (see below). 1 ml of fresh media was added to each well following supernatant collection. At the end of the 10-day timeline, GFox cells were collected and frozen in -80°C by trypsinization and washing with 1X PBS through two rounds of centrifugation to pellet cells and remove supernatant. A second co-infection experiment with a 100-fold increase of FFV and same amount of FIV was conducted to evaluate the effect of increased FFV load. All conditions remained the same with the exception of a shorter 7-day timeline due to lytic effects from the increased FFV inoculum. Collections took place on days 1, 2, 3, 5, and 7 post initial inoculation and cells were similarly washed and pelleted at the conclusion of the study period. The timeline for the second virus added was adjusted as in the first round of co-infections.

Viral measurements over time

As noted previously, the second virus added on the staggered co-infections had an adjusted timeline. The second virus was added one day after the initial virus and this day was marked as “day 0” for the second virus. Upcoming days for the second virus were added to the nearest day of single infection and timeline adjusted to match the single infection for comparison of single versus co-infection viral titer measurements over time. FFV was measured over time by the GalactoStar assay (Fig. 1) by adding 25 µl of each infection treatment per well in a 96-well plate containing FeFAB cells as described above. The RLU readout from the luminometer was used to calculate the amount of β-gal produced (ng) as a proxy of viral load in the supernatant sample

based on a β-gal dilution standard curve. For FIV, the average of the triplicate well ODs was used as read-out for each treatment condition through the p26 ELISA described previously.

One hundred and forty microliters of supernatant per treatment well was submitted to viral RNA purification using the QIAamp Viral RNA Mini Kit following manufacturer protocol (QIAGEN, Hilden, Germany). cDNA was reverse transcribed from extracted RNA using Superscript II (Invitrogen, Carlsbad, CA), random hexamer primers (Invitrogen), and RNAse Out (Invitrogen). FIV-*gag* was detected through real-time PCR on a C1000 Touch Thermal Cycler (Bio-Rad, Hercules, CA) using 704F and 756R primers (10 μM each) and 727P probe (10 μM) [212] under conditions modified from previous reports [128, 213, 214]. Briefly, each 25 μl reaction consisted of TaqMan 2x Universal PCR master mix (Applied Biosystems, Foster City, CA) (12.5 μl), water (5.3 μl), forward and reverse primers (1 μl each), and probe (0.2 μl), and 5 μl of DNA template, with the following cycling conditions: 2 min at 55°C, 8:30 min at 95°C, and 45 cycles of 15 s at 95°C and 1 min at 60°C. Virus was quantified based on a cDNA dilution standard curve of a known FIV-C36 positive supernatant. For FFV, cDNA was quantified over time based on a FFV plasmid standard curve as described previously in Chapter 2.

Statistical analyses

Student's t tests were used to determine statistically significant ($P< 0.05$) differences in FIV plasma viral load and CD4+:CD8+ ratio between FIV-infected and co-infected animals. FIV-positive animals that did not have a detectable viral load (n=7) were omitted from analyses; one additional animal was omitted due to lack of FIV viral load data. A general linear model was used with each cat as a random effect to account for the individual heterogeneity in the viral loads, using the statistical program R, version 3.4.2 [177].

Chi-square tests were performed to assess the independence of three pairs of categorical variables: 1) sex and FFV infection, 2) sex and FIV infection, and 3) FFV/FIV co-infection. For each pair of variables, cats were stratified by location (Chicago or Memphis), sex (male or

female), FFV status (+ or -), and FIV status (+ or -). If a Chi-square test produced a P-value less than a significance level of 0.05, risk ratios and 95% confidence intervals (95% CI) were calculated as an additional post-hoc test. Risk ratios (RRs) describe the probability of a health outcome occurring in an exposed group to the probability of the event occurring in a comparison, non-exposed group. A RR > 1 suggests an increased risk of that outcome in the exposed group, and a RR < 1 suggests a reduced risk in the exposed group. Chi-square tests and RRs were calculated using the R program and the 'epitools' package [180]. One cat was omitted from sex-related analyses due to lack of sex data.

A two-way ANOVA was conducted on the co-infection experiments to determine statistically significant differences between treatment groups over time. All treatments groups were compared to each other on specified collection dates. For FIV, the p26 antigen absorbance (OD_{450}) was used as the read-out and for the FFV GalactoStar assay, β-gal (ng) was used as read-out. P-values were included graphically as asterisks in the following manner: (*) = P-value < 0.05, (**) = P-value < 0.01, (***) = P-value < 0.001, (****) = P-value < 0.0001. Prism 7 (GraphPad, La Jolla, CA) was used for analyses and graphical output.

Results

FFV and FIV natural infections are associated and co-infection is common

We tested FFV and FIV prevalence on serum from cats in singly (n=71, Group 1/Chicago) or group housed (n=70, Group 2/Memphis) settings. Overall FFV prevalence (76%) was higher than FIV prevalence (44%) in both groups of cats (Fig. 2). Overall rates of co-infection and single FFV infection were the same (38%) and more common than single FIV infection (6%). In the Group 1/Chicago cohort, co-infection (48%) was more common than either single FFV (38%) or FIV infection (7%). In the Group 2/Memphis cohort, single FFV infection (39%) was more common than co-infection (27%) and single FIV infection (6%). FIV plasma viral load, WBC count, lymphocyte count, and CD4+:CD8+ ratio were not significantly different between

co-infected and singly FIV infected groups (data not shown). In both the Chicago and Memphis groups, nearly all animals that died were co-infected (Fig. 3). Males had higher rates of FFV infection than females in all groups (FFV "Overall" bars, Fig. 4).

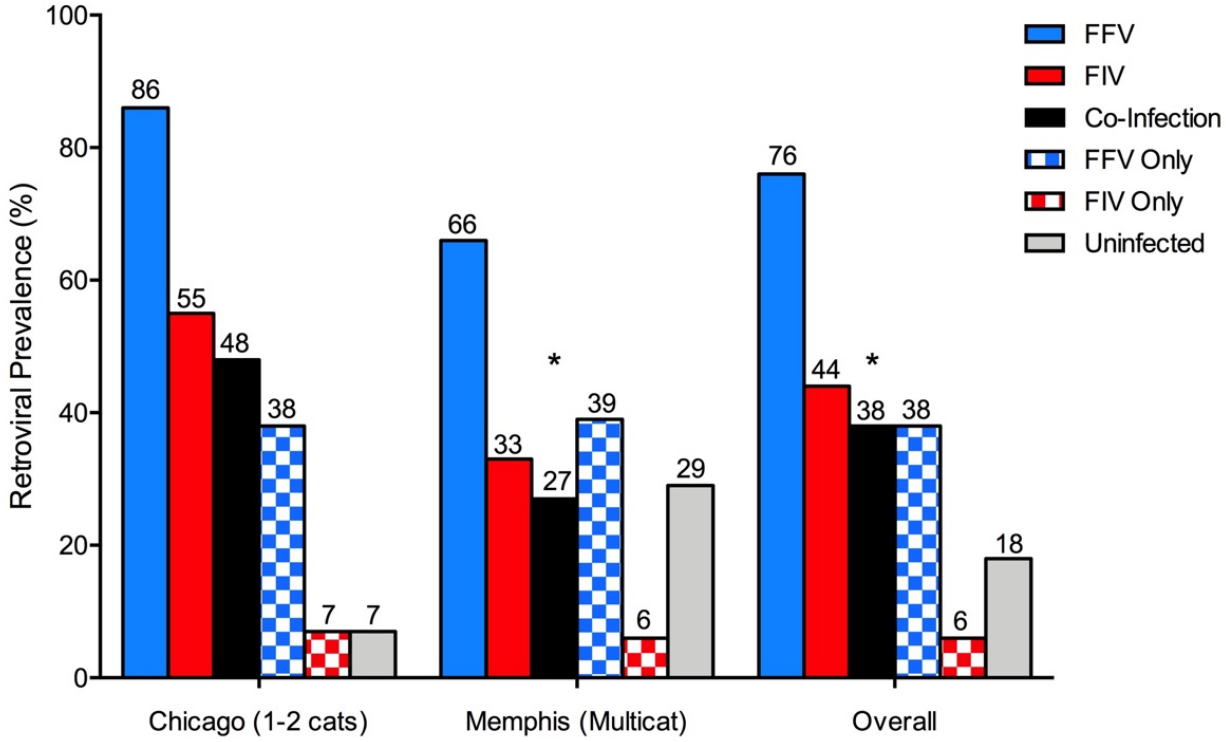

Figure 2. FFV is more prevalent than FIV, and co-infection is common. FFV overall prevalence (blue bar) was much higher than FIV overall prevalence (red bar) in both groups tested. Cats were more likely to be co-infected (black bars) in the Chicago group, whereas in the Memphis group, single FFV infection (blue checkered bar) was more common than single FIV (red checkered bar) and co-infection. Single FIV infection was the least common in both groups. There was a significant association (*) between FFV and FIV infection in the Memphis cohort (X^2=4.413 P-value=0.036) and Overall (X^2=5.573, P-value=0.018).

Five chi-squared tests had statistically significant associations. When the Chicago and Memphis cohorts were combined, a significant association was found between sex and FFV infection (X^2=7.331, P-value=0.007) (Fig. 4). FFV and FIV co-infection was also more common than single FIV infection (X^2=5.573, P-value=0.018) (Fig. 2). Male cats had a RR of 1.36 for FFV infection (95% CI: 1.07, 1.73); female cats had a RR of 0.74 (95% CI: 0.58, 0.94). FFV+ cats had a RR of 2.04 for FIV infection (95% CI: 1.09, 3.85), whereas FFV- cats had a RR of 0.49 (95% CI: 0.26, 0.92).

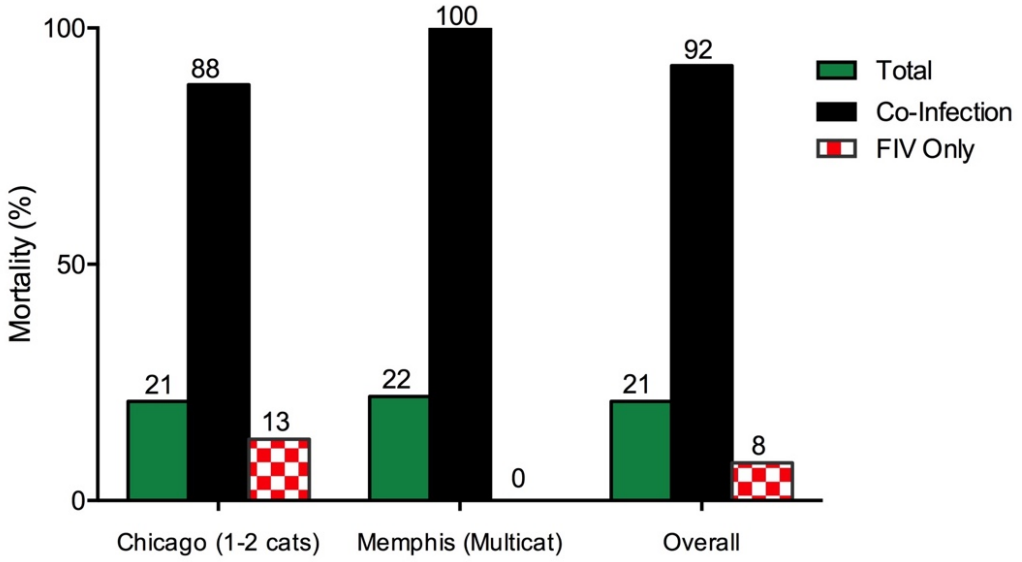

Figure 3. Most cats that died were co-infected. Overall mortality per group is shown by the green bar. Across both groups, most or all animals that died were co-infected (black bars) versus singly FIV infected (red checkered bars).

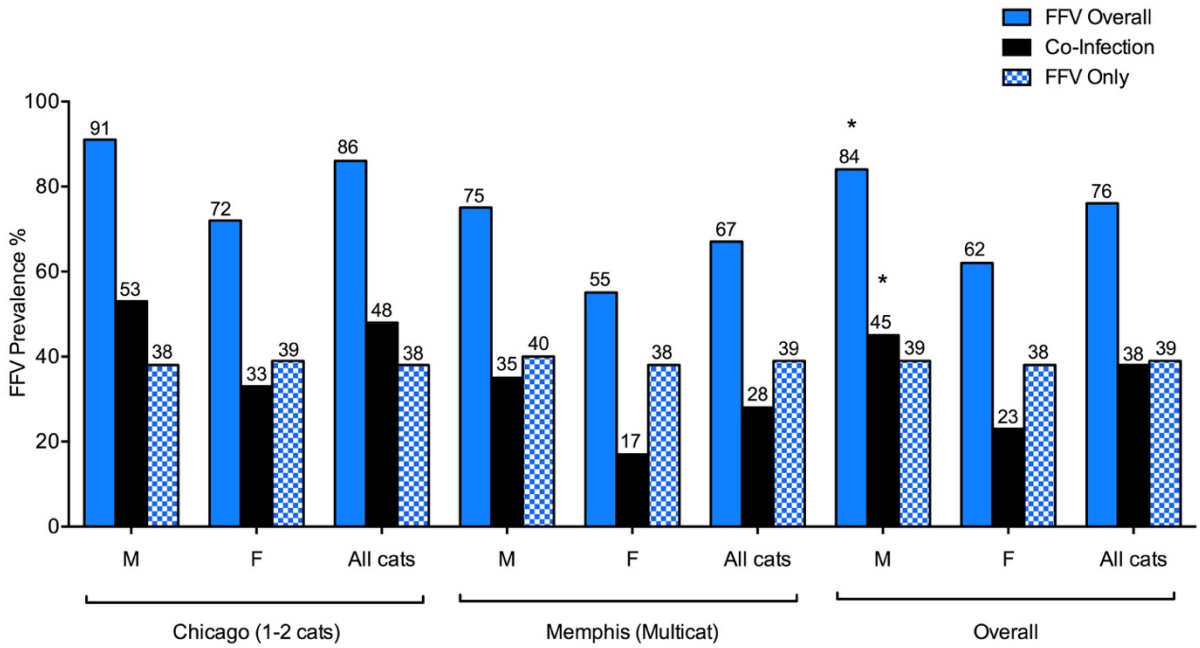

Figure 4. Males are at increased risk of FFV/FIV co-infection. FFV infection was much higher in males than females in all groups tested. A Chi square analysis showed that there is a significant association (*) between the male sex and FFV infection (X^2=7.331, P-value=0.007) and that in males, there is also an association between FFV and FIV infection (X^2=4.495 P-value=0.034). In FIV+ cats, males were also at an increased risk of FFV infection (X^2=4.289, P-value=0.038).

Amongst all male cats from Chicago and Memphis, there was a significant association between FFV infection and FIV infection (X^2=4.495 P-value=0.034) (Fig. 4); male FFV+ cats had a RR of 2.69 for FIV infection (95% CI: 0.96, 7.56), whereas male FFV- cats had a RR of 0.37 (95% CI: 0.13, 1.04). There was also a significant association between sex and FFV infection status amongst all FIV+ cats from Chicago and Memphis (X^2=4.289, P-value=0.038) (Fig. 4). Male FIV+ cats had a RR of 1.36 for FFV infection (95% CI: 0.97, 1.91), whereas female FIV+ cats had a RR of 0.74 (95% CI: 0.52, 1.03). Finally, there was a significant association between FFV and FIV infection in the Memphis cohort (X^2=4.413 P-value=0.036) (Fig. 2). Memphis FFV+ cats had an RR of 3.17 for FIV infection (95% CI: 1.04, 9.61), whereas Memphis FFV- cats had a RR of 0.32 (95% CI: 0.1, 0.96).

In vitro FFV and FIV infection is enhanced or suppressed relative to order of viral infection

$TCID_{50}$/ml for FFV stocks was calculated as 1.76×10^7; FIV stock $TCID_{50}$/ml was calculated to be 2.15×10^4. An MOI of 0.01 was used in initial infection studies. FIV-only inoculated cells began displaying CPE of multinucleation and syncytia development 2 days p.i. (Fig. 5A) while FFV-only infected cells began showing CPE at 8 days p.i. (Fig. 5B). The size and number of cells affected by CPE in the FIV-only wells progressed over time, but cell death was not remarkable. Cells co-infected with both FFV and FIV (both simultaneous and staggered) showed CPE similar in organization and timeline as singly FIV-infected cells (not pictured).

A second round of co-infections was conducted using FIV MOI of 0.01 and FFV MOI of 1. These cells (Fig. 6) experienced faster and more striking CPE development than the first round of co-infections (Fig. 5). All virus-inoculated wells began showing syncytial cells on day 2 p.i. (Fig. 6A), with increased number and size of syncytia in the simultaneously co-infected (FFV + FIV) wells (Fig. 6B). On day 3 p.i., FFV + FIV cells began developing larger syncytia than the FFV- and FIV-only infected cells.

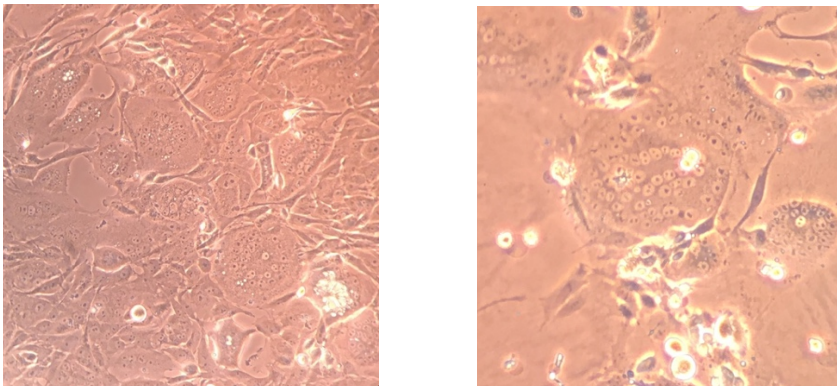

Figure 5. Both FIV and FFV infected cells developed CPE (MOI of 0.01 for both viruses). FIV-only infected cells started showing CPE 2 d p.i. (**A)** while FFV-only infected cells displayed CPE 8 d p.i. (**B).** FFV/FIV co-infected cells (both simultaneous and staggered) developed CPE at a similar rate and severity as FIV-only infected cells throughout the infection (not pictured).

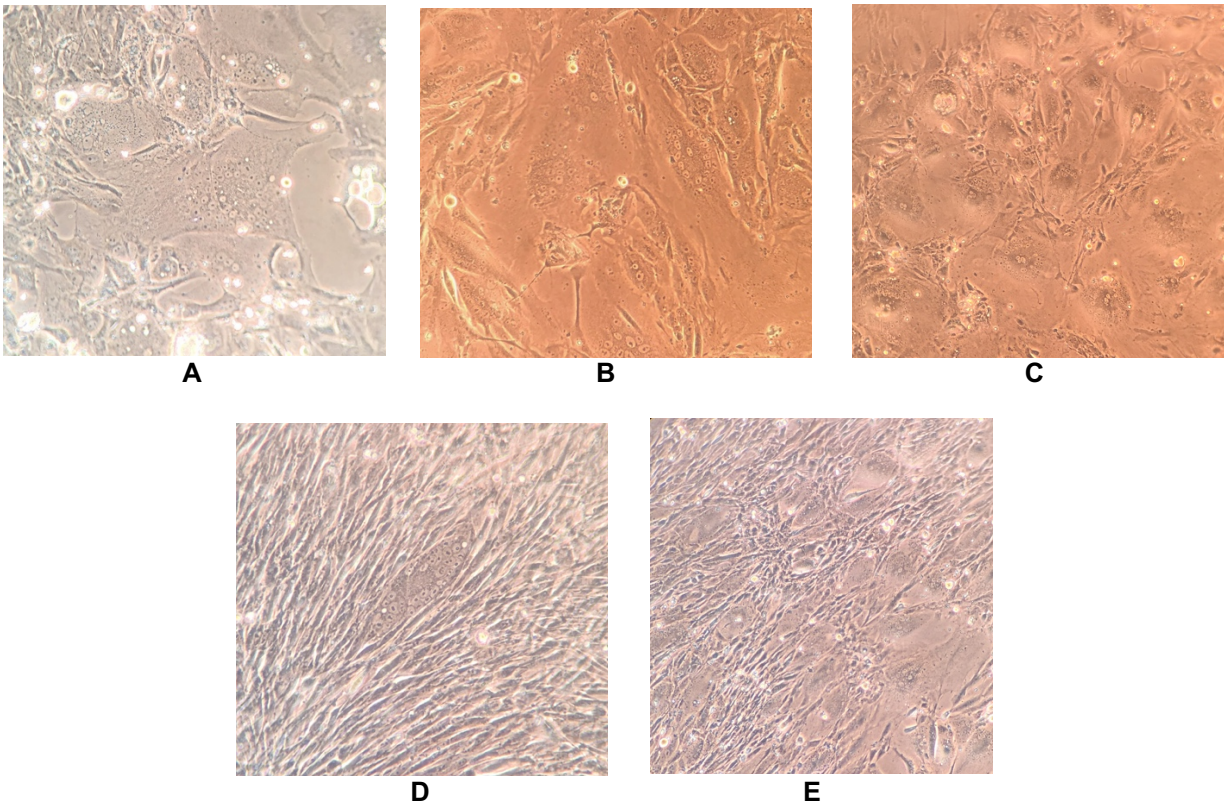

Figure 6. Expansive syncytia developed in all FFV-containing wells, particularly during simultaneous co-infection. All FFV-containing wells developed large syncytia by day 6 p.i. **A** FFV-only cells developed large syncytia by day 4 that grew in size by day 6, with more expansive syncytia present in simultaneous co-infection (FFV + FIV) (**B**). **C** Cells in FFV → FIV developed syncytia to a lesser degree than FFV + FIV. **D** FIV-only infected cells had scattered CPE that was not expansive as noted in FFV-infected wells. **E** CPE in FIV → FFV was more prevalent than FIV-only but less than other co-infected conditions.

FFV-only inoculated cells showed numerous syncytia grouped in clusters, compared to more scattered CPE noted in FIV-only wells. By day 5, syncytia in FFV + FIV co-infected cells were becoming large enough to occupy the whole microscopic field of view. On day 6, syncytia in FFV-only containing wells were similar in proportion to syncytia in the FFV + FIV co-infected wells, but fewer in number. By day 7, there was marked cell death in all FFV-infected cells. FFV + FIV co-infected wells were most severely affected, demonstrating large and numerous syncytia (Fig. 6C). In contrast, FIV-only wells demonstrated moderately sized syncytia scattered between normal looking cells (Fig. 6D). FFV-only and FFV + FIV co-infected cells had very large and expansive, almost ameboid shaped cells that were not present in FIV-only infected cells. The FFV → FIV inoculated syncytia (Fig. 6C) were similar to the other FFV-infected cells, while the FIV → FFV inoculated syncytia (Fig. 6E) were phenotypically similar to FIV-only infected cells.

FIV reactivity on the first round of co-infections (Fig 7A) was detected on day 1 p.i. for all FIV-containing wells and was highest on day 7 during simultaneous co-infection (FIV + FFV, red line, Fig. 7A). Full reactivity data and statistical analyses for both first and second rounds of co-infection are shown in Appendix File 9 and Appendix File 10, respectively. FIV-only reactivity (black line) was typically intermediate between FIV + FFV (highest) and FIV → FFV infection (lowest, green line). Interestingly, FFV → FIV (blue line) resulted in an increase in FIV reactivity on day 2 and an earlier peak in reactivity on day 3 compared to all other FIV conditions. On day 3, FFV → FIV reactivity was significantly higher than FIV-only, FIV + FFV, and FIV → FFV infections (blue ****, $p < 0.0001$ for the three conditions). After day 3, FIV-only reactivity was similar to other conditions until the end of the study. FIV growth during FIV + FFV infection was significantly higher than FIV → FFV infection on day 5 (red **, $p = 0.0023$) and day 7 (red ****, $p < 0.0001$), and significantly higher than FIV → FFV on day 7 (red ****, $p < 0.0001$). FIV-only infection had higher FIV reactivity than FIV → FFV infection on day 7 (black **, $p = 0.0041$). FIV

reactivity trended lowest in the FIV → FFV infection compared to all other conditions, but this finding was not always significant.

The second round of co-infections (FIV inoculated at an MOI of 0.01 and FFV at an MOI of 1, Fig 7B) demonstrated a similar trend as the first round of co-infections (Fig. 7A). FIV reactivity was higher at an earlier timepoint for the FFV → FIV condition (blue line, Fig. 7B). Day 2 FIV reactivity in this condition was significantly higher than FFV + FIV (blue *, p = 0.0167), FIV → FFV (blue **, p = 0.0032), and FIV-only (blue **, p = 0.0022). On day 3, FFV → FIV reactivity was again significantly higher than the three other conditions (blue ****, p < 0.0001).

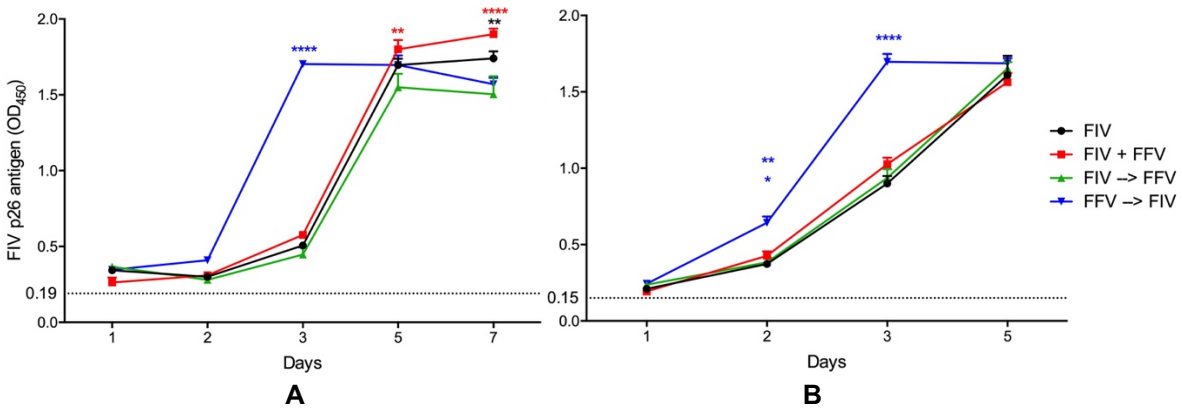

Figure 7. FIV infection is accelerated following initial FFV infection. **A** MOI of 0.01 for both viruses. FIV reactivity determined by p26 ELISA shows that a secondary FIV infection is significantly accelerated by an already established FFV infection (FFV → FIV, blue line) on day 3 when compared to FIV-only infection (black line) and other co-infection conditions (blue ****, p < 0.0001 in all comparisons). Conversely, initial FIV infection was inhibited by a secondary FFV infection (green line) compared to simultaneous co-infection on day 5 (red **, p = 0.0023) and day 7 (red ****, p < 0.0001), and to FIV-only infection on day 7 (black **, p = 0.0041). **B** FIV MOI 0.01 and FFV MOI 1. The FFV → FIV infection showed a similar trend as the initial round of co-infections. Day 2 FIV reactivity in this condition was significantly higher than FFV + FIV (blue *, p = 0.0167), FIV → FFV (blue **, p = 0.0032), and FIV only (blue **, p = 0.0022). On day 3, FFV → FIV reactivity was again significantly higher than the three other conditions (blue ****, p < 0.0001).

FFV β-gal (ng) results are summarized in Fig. 8. Full β-gal results and statistical analyses for first and second rounds of infection are shown in Appendix File 11 and Appendix File 12, respectively. Similarly to FIV, it appears that a secondary FFV infection is enhanced by an initial FIV infection (FIV→ FFV, green line) compared to other FFV infection conditions. For the first

round of co-infections (Fig. 8A) (MOI of 0.01 for both viruses), β -gal concentration was significantly higher on day 7 in the FIV → FFV condition compared to FFV-only infection (black line) (green *, p = 0.0139), FFV + FIV (red line) (green *, p = 0.0384), and FFV → FIV (blue line) (green **, p = 0.0018). Also similarly to FIV, initial FFV infection appears somewhat inhibited by a secondary FIV infection.

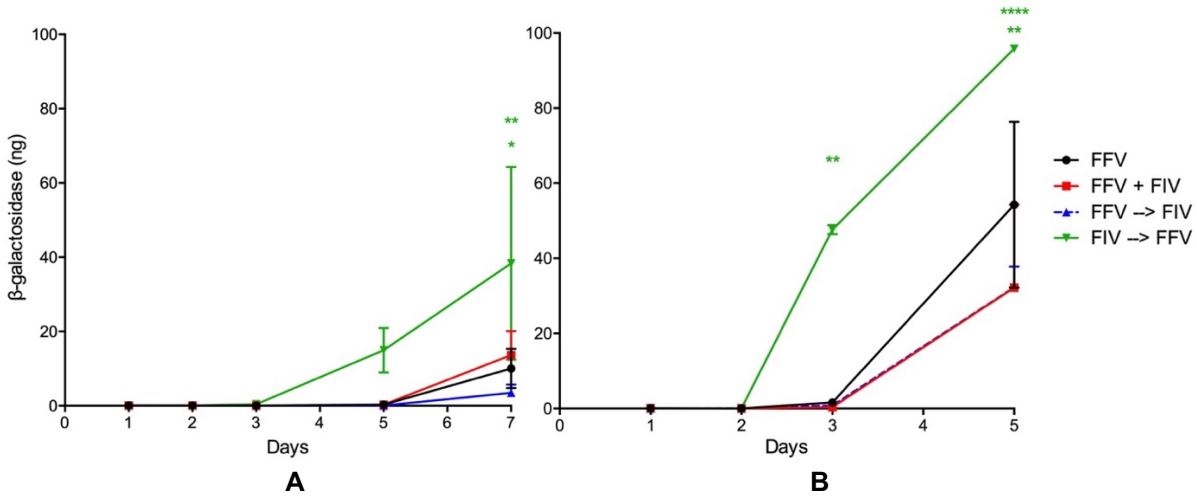

Figure 8. FFV infection is accelerated following initial FIV infection. A FFV and FIV MOI 0.01. FIV → FFV (green line) β-gal concentration was significantly higher than FFV-only infection (green *, p = 0.0139), FFV + FIV (red line) (green *, 0.0384), and FFV → FIV (blue line) (green **, p = 0.0018). Similarly to FIV, FFV was partially inhibited by a secondary FIV infection (FFV → FIV, blue line) when comparing to other conditions. **B** FIV MOI 0.01 and FFV MOI 1**.** On day 2, β-gal was significantly higher in the FIV → FFV than FIV-only (green **, p = 0.0015), FFV + FIV (green **, p = 0.0011), and FFV → FIV (green **, p = 0.0012). On day 5, the FIV → FFV β-gal amount was again significantly higher than FFV-only (green **, p = 0.0043), and FFV + FIV and FFV → FIV (both green ****, p < 0.0001).

In the second round of co-infections (Fig. 8B) a higher FFV MOI of 1 was applied (Fig. 8B). The same trend of increased β-gal concentration in FIV → FFV was noted. On day 2, β-gal was significantly higher in the FIV → FFV condition than FIV-only (green **, p = 0.0015), FFV + FIV (green **, p = 0.0011), and FFV → FIV (green **, p = 0.0012). The FIV → FFV β-gal amount was again significantly higher than FFV-only (green **, p = 0.0043), and FFV + FIV and FFV → FIV (both green ****, p < 0.0001).

Preliminary FFV qPCR results for days 1 and 2 post-infection show positivity starting at day 1 p.i. but do not show a specific trend or evidence of potentiation during co-infection versus single infection (data not shown).

Discussion

This work was conducted to determine associations between FFV and FIV infection. In our initial studies, we evaluated two groups of FIV-infected cats with different clinical outcomes to determine whether FFV infection impacted FIV clinical disease. FIV-infected cats living in multicat household (Group 2/Memphis) exhibited severe weight loss, stomatitis, dermatitis, neoplasia (lymphoma most commonly), and death, whereas FIV-infected cats in 1-2 cat households (Group 1/Chicago) remained healthy, with only one death reported [205].

We hypothesized that the cats in Group 2/Memphis that suffered increased mortality would have a higher prevalence of FFV, and that there would be evidence of worsened disease due to FFV/FIV co-infection. While we did not find statistically significant differences in FFV infection rates between the two populations, we found a significant association between FIV and FFV infection overall, as previously reported [62, 63, 71]. In one of these reports, FFV was highly prevalent in sick cats infected with either FIV, FeLV, both FIV and FeLV, and in cats negative for both FIV and FeLV. The authors of this study found that, especially in the case of FIV, it was more common than not to be co-infected with FFV, which suggested a role for FFV in potentiating effects on the initial FFV infection [71]. In our study, it was more common in the Group 1/Chicago cohort to have FFV/FIV co-infection versus single infection of either FFV or FIV, while in Group 2/Memphis, single FFV infection was more common than co-infection. Thus, the cohort with higher morbidity and mortality had lower overall FFV infection rates but equal co-infection rates compared to the cohort with mostly healthy animals. This suggests that the higher morbidity and mortality in the multicat household may not have been primarily due to concomitant FFV infection. FIV viral loads, CD4+:CD8+ ratios, and white blood cell populations

in the co-infected versus singly FIV-infected animals were similar, also suggesting that FFV may not lead to increased FIV viral burden and subsequent worsened clinical symptoms. The authors of this study suggested housing modality and management as reasons for increased morbidity and mortality [205].

Perhaps most significantly, cats most likely to die were co-infected with FFV and FIV, suggesting a comorbidity that was not detectable by comparison of blood and viral parameters measured. Mortality rates were higher in the multicat group and 100% of those animals were co-infected, compared to 88% in the 1-2 cat households. One of the limitations in our study is that we did not have access to all the samples used in previous studies, and thus may not have a larger sample size of clinically affected and euthanized animals that could have contributed to a significant difference in parameters influencing worsened disease. In a previous report of experimental FFV/FIV co-infection, FFV infection was not found to potentiate FIV disease [141].

Considering the highly-varied duration of acute, clinical, and terminal stages of FIV infection, it is not yet possible to make assumptions regarding the effect of FFV co-infection on progression to or severity of later stages of FIV infection. Perhaps FFV may play a role in the more clinically severe terminal stage of disease (the third and final stage of disease progression) when animals succumb to clinical symptoms related to FAIDS as the authors theorized [141]. High FFV prevalence rates of FIV-positive cats with terminal illness supports an added risk of co-infection. Additionally, the reports on worsened SIV-related disease and mortality, and the expanded SFV tissue tropism in areas of increased CD4+ depletion during co-infection in NHP support this assumption [67, 142]. Co-infection studies assessing chronic FIV infection, and studies that sequentially evaluate co-infection, viral loads, and hematologic parameters are needed to further assess the potential association between these two viruses during later stages of FIV disease.

Another possible reason for the association between these viruses is their shared salivary transmission [58, 62, 63, 149]. FIV transmission is thought to be via biting [62, 63] whereas both

biting and amicable grooming between cats have been suggested for FFV [58, 62, 63]. Thus, it is possible that based on the interactions between animals, both viruses could be transmitted concomitantly. Other reports have noted significant variation in the amount of salivary shedding of FFV, which could account for varied transmission rates between animals (Chapter 2 and [9, 66]). This has also been reported for NHP infected with SFV [68, 69, 183].

FFV and FIV infections were strongly correlated with male cats as reported by others [62, 63, 138]. Increased risk in FFV has been documented in both domestic and feral cat populations (Chapter 2 and [62, 81]). A previous study found that feral cats were at increased risk compared to desexed pet cats, and the authors suggested this may be due to behavior related to intact male behavior, implying feral males roam more and are at increased risk of exposure [62]. However, our sampled population consisted of desexed animals, thus in our population, behavioral changes due to being intact did not contribute to the association. We have also found domestic neutered male pet cats to have an increased risk of FFV infection (Chapter 2) . It is possible that their behavior and time of desexing before study enrollment have influenced viral exposure or susceptibility.

FFV/FIV in vitro co-infection assays were conducted to determine if viral kinetics and CPE development are altered during co-infection versus single infection with either virus. Increased permissiveness to HIV infection has been described in cells initially infected with SFV [204]. We thus theorized that part of the reason these viruses are associated is due to a co-factor effect during co-infection that potentiates one or both infections. Results from initial round co-infections (MOI of 0.01 for both viruses) indicated that the timing and order of infections have different effects on both viruses. Our data indicates that the presence of an initial infection with either FFV or FIV accelerates infection of the second virus, causing an accelerated increase in replication compared to the other conditions. In the case of FIV, all infection conditions reach similar levels of viral replication. Thus it appears that FIV replication is accelerated if FFV infection is initiated first, however FIV replication during co-infection does not surpass replication

in the other single and dual infection conditions. In the case of a secondary FFV infection however, replication is not only accelerated but it also significantly surpasses all other single and dual conditions. In other words, secondary FIV infection is accelerated following initial FFV infection, and a secondary FFV infection is accelerated and boosted following initial FIV infection (Fig. 7 and 8). Increasing FFV MOI did not appear to cause a dose dependent enhancement or decrease of FIV (Fig. 7 and 8). FFV replication did reach higher levels in the second round of co-infections which is most likely attributed to the increased MOI (Fig. 8). Interestingly, during both FFV and FIV infections, exposure to a second virus appears to have an inhibitory effect on the initial virus at some of the timepoints, though not always significantly.

This data shows that similarly to the findings in the PFV/HIV study, cells initially infected with one virus increased permissivity for the secondary virus. Reasons for this are numerous and could include: (1) change in cell surface receptors following initial viral infection, allowing enhanced binding and/or entry into the cell; (2) changes in cell metabolism/machinery changes following initial infection that enhance replication of a second viral infection. In the case of the PFV/HIV study, the authors found increased HIV permissivity in PFV-infected without enhanced HIV reverse transcription, nuclear import, or integration. They also found increased cell-to-cell HIV transmission from these co-infected cells. The authors determined this was mediated by a heparan-sulfate expression [204]. Heparan sulfate has also been found to be an attachment factor for PFV [23]. A similar mechanism could function in FIV/FFV co-infection perturbations.

Conversely, initial infection by either virus dampened replication of a second viral infection. It is possible that following initial viral insult, a second virus usurps some of the host cell's resources and machinery activated by the initial viral infection, resulting in enhanced, or 'jump-started' infection. This effect was not always present or significant, thus it may not have a critical effect on initial viral infection. Follow-up experiments should be conducted with varying amounts of virus, altering the dose of FIV, employing the use of more relevant cell lines to retroviral infection such as PBMCs, longer culture durations, and with different viruses to determine if this

enhanced permissivity extends to other viral infections. The potential role of heparan sulfate in viral binding during co-infection should also be explored.

Overall, our data support an association between FFV and FIV infection in the natural domestic host and in vitro models. Our in vitro studies show increased permissivity to a secondary infection of either retrovirus, and CPE findings demonstrate enhanced effects during co-infection, suggesting potentiated viral replication and pathologic effects. It is possible one of the reasons we did not see an association between increased FIV-related morbidity and FFV co-infection in naturally infected animals may be due to the timing and order of which virus infected the cats first (or simultaneously). Notably, almost all of the FIV-infected cats that died were co-infected with FIV and FFV, suggesting potentiation of FIV clinical effects—though associations with typical hematological indicators of pathology were not identified. Future studies should further interrogate whether the timing, order, and inoculum dose of infection impact on disease outcomes. Primary lymphoid cells should also be tested in co-infection experiments to validate preliminary experiments conducted in GFox cells. In vivo inoculation studies could be carried out in SPF cats to validate natural infections.

Conclusions

FFV and FIV infections are associated in the cat populations we sampled. Possible reasons for this may be related to sex, behavior, shared route of transmission, or synergistic interactions between the two viruses. In vitro studies showed increased permissivity to a secondary infection following either FIV or FFV infection, indicating approaches to study mechanisms for viral interaction that relate to potentiation of FIV disease by FFV infection. Future studies should be conducted to further understand in vitro dynamics and kinetics during co-infection, including in relevant cell lines, in addition to disease monitoring in chronically co-infected cats. Practitioners should be aware of the potential effects FFV can have on FIV-infected animals in relation to management and possible development of disease.

CONCLUSIONS

FFV is a sometimes highly prevalent retrovirus with a global distribution that has a unique molecular biology and causes an outwardly apathogenic infection during acute time periods. Due to this apathogenicity, researchers have used FVs to develop novel vaccine and gene therapy therapies with potential benefits to both animals and humans. Many questions still remain about infection in the host and about its molecular biology despite ancient origins and hundreds of thousands of years of co-evolution with their respective hosts. Therefore, investigating these viruses further could prove of much importance in filling these knowledge gaps in addition to clinical management of infected animals, and future therapies that could benefit both animals and humans.

I inoculated SPF cats with two FFV strains and collected biological samples over a 6 month time period. One was the wild-type pCF-7 FFV and the second a novel chimeric vaccine vector with FIV *vif* replacing a truncated FFV *bet*. In Chapter 1, I investigated whether this in vitro replicative FFV-Vif chimera could infect immunocompetent cats, and compared findings to wild-type infection. I found that the FFV-Vif chimera was able to induce a specific immune response against FFV Gag and Bet proteins at antibody titers comparable to wild-type infection following boosting, and also against the inserted Vif. While able to elicit an immune response, the chimeric virus displayed an attenuated infection in vivo, as we were unable to detect virus through PCR in chimera-only inoculated animals. I furthermore found that cats can be superinfected with different strains of FFV, which adds more plausibility to the use of this virus in a population of pet cats which may already be infected by FFV. This chimeric vaccine construct could be used as a vector against lentiviral infection. However, more work would need to be performed to examine animals already infected with wild-type virus before being challenged with the vaccine candidate for further support of this vector.

In Chapter 2, I further characterized infection in terms of specific PBMC response to infection, viral tropism, and evidence of pathology, especially due to the reports in the literature of FFV being isolated from animals suffering from various morbidities. We found subclinical alterations in hematological and biochemical parameters and micropathology that could potentially lead to pathology over time, such as the ultrastructural kidney changes and histopathological changes in the lungs and brain, in addition to evidence of a potential susceptibility in unique cases, such as the cat with decreased lymphocytes and increased viral loads and expanded tissue tropism to non-lymphoid sites.

Due to the renal changes we saw and the reports in the literature of renal pathology and FFV isolation from animals suffering from renal and urinary diseases, I further investigated the effect FFV could have on chronic kidney disease (CKD). After collecting samples from the USA and Australia, we did find an association of FFV and CKD in male cats, in addition to males in general also being at higher risk for FFV infection. More work should be conducted to determine the cause of this association, and more attention could be given to male cats suffering from CKD in relation to their FFV status.

In addition to an association with CKD, I sought to determine if FFV was associated and could cause potentiation of FIV, a sometimes clinically important viruses in feline health management. The literature documents these two viruses being frequently co-isolated, and the reports in nonhuman primates show SFV and SIV potentiate each other in co-infected animals, leading to expanded tissue tropism, increased morbidity and mortality. Chapter 3 had two aims, first to investigate whether FFV was a factor in increased morbidity in a group of cats reported in another study, and to conduct in vitro co-infection experiments to determine if the frequent co-isolation and association of these two viruses could be due to viral synergy during co-infection. I found that FFV and FIV are associated in these animals, and that again males were at increased risk of FFV infection in general. Others have suggested that the association between FFV and FIV could be due to a shared mode of transmission, or it could be due to desexing

status in males. In our laboratory we have seen increased risk in both feral and pets, and have also seen it in desexed animals, decreasing support for behavior related to increased aggressive encounters and spreading of virus.

I conducted in vitro co-infection assays and these showed that FFV and FIV enhance each other's replication. Regardless of which virus causes the initial infection, the secondary infecting virus' replication is accelerated compared to single infection. This suggests that the reason for these viruses being associated could be not only due to potentially similar routes of transmission but also due to viral synergy based on the order of infecting viruses.

Our data show that while FFV could make an attractive vector to develop vaccines and gene therapies, more studies should be conducted to understand the effect FFV has on other disease syndromes in cats, especially in certain population subsets such as males, and in chronic conditions such as chronic FIV infection.

REFERENCES

1. Aiewsakun P, Katzourakis A: **Marine origin of retroviruses in the early Palaeozoic Era**. *Nat Commun* 2017, **8**:13954.
2. Delelis O, Lehmann-Che J, Saib A: **Foamy viruses - a world apart**. *Curr Opin Microbiol* 2004, **7**(4):400-406.
3. Linial ML: **Foamy viruses are unconventional retroviruses**. *J Virol* 1999, **73**(3):1747-1755.
4. Switzer WM, Salemi M, Shanmugam V, Gao F, Cong ME, Kuiken C, Bhullar V, Beer BE, Vallet D, Gautier-Hion A *et al*: **Ancient co-speciation of simian foamy viruses and primates**. *Nature* 2005, **434**(7031):376-380.
5. Kehl T, Tan J, Materniak M: **Non-simian foamy viruses: Molecular virology, tropism and prevalence and zoonotic/interspecies transmission**. *Viruses* 2013, **5**(9):2169-2209.
6. Lindemann D, Steffen I, Pohlmann S: **Cellular entry of retroviruses**. *Adv Exp Med Biol* 2013, **790**:128-149.
7. Rethwilm A, Lindemann D: **Foamy Viruses**. In: *Field's Virology. Volume II*, 6th edn. Edited by Knipe D, Howley P. Philadelphia, PA: Lippincott Williams & Wilkins; 2013: 1613-1632.
8. Rethwilm A: **Molecular biology of foamy viruses**. *Medical Microbiology and Immunology* 2010, **199**(3):197-207.
9. Shroyer EL, Shalaby MR: **Isolation of feline syncytia-forming virus from oropharyngeal swab samples and buffy coat cells**. *American Journal of Veterinary Research* 1978, **39**(4):555-560.
10. Arzi B, Kol A, Murphy B, Walker NJ, Wood JA, Clark K, Verstraete FJM, Borjesson DL: **Feline Foamy Virus Adversely Affects Feline Mesenchymal Stem Cell Culture and Expansion: Implications for Animal Model Development**. *Stem Cells and Development* 2014.
11. Kasza L, Hayward AH, Betts AO: **Isolation of a virus from a cat sarcoma in an established canine melanoma cell line**. *Res Vet Sci* 1969, **10**(2):216-218.
12. Riggs JL, Oshiro LS, Taylor DO, Lennette EH: **Syncytium-forming agent isolated from domestic cats**. *Nature* 1969, **222**(5199):1190-1191.
13. Yu SF, Sullivan MD, Linial ML: **Evidence that the human foamy virus genome is DNA**. *J Virol* 1999, **73**(2):1565-1572.
14. Löchelt M, Romen F, Bastone P, Muckenfuss H, Kirchner N, Kim YB, Truyen U, Rosler U, Battenberg M, Saib A *et al*: **The antiretroviral activity of APOBEC3 is inhibited by the foamy virus accessory Bet protein**. *Proc Natl Acad Sci U S A* 2005, **102**(22):7982-7987.
15. Chareza S, Slavkovic Lukic D, Liu Y, Räthe A-M, Münk C, Zabogli E, Pistello M, Löchelt M: **Molecular and functional interactions of cat APOBEC3 and feline foamy and immunodeficiency virus proteins: different ways to counteract host-encoded restriction**. *Virology* 2012, **424**(2):138-146.
16. Perkovic M, Schmidt S, Marino D, Russell Ra, Stauch B, Hofmann H, Kopietz F, Kloke B-P, Zielonka J, Ströver H *et al*: **Species-specific inhibition of APOBEC3C by the prototype foamy virus protein bet**. *J Biol Chem* 2009, **284**(9):5819-5826.
17. Russell RA, Wiegand HL, Moore MD, Schafer A, McClure MO, Cullen BR: **Foamy virus Bet proteins function as novel inhibitors of the APOBEC3 family of innate antiretroviral defense factors**. *J Virol* 2005, **79**(14):8724-8731.

18. Jaguva Vasudevan AA, Perkovic M, Bulliard Y, Cichutek K, Trono D, Haussinger D, Münk C: **Prototype foamy virus Bet impairs the dimerization and cytosolic solubility of human APOBEC3G**. *J Virol* 2013, **87**(16):9030-9040.
19. Cullen BR: **Role and mechanism of action of the APOBEC3 family of antiretroviral resistance factors**. *J Virol* 2006, **80**(3):1067-1076.
20. Löchelt M: **Foamy virus transactivation and gene expression**. *Curr Top Microbiol* 2003, **277**:27-61.
21. Boyer PL, Stenbak CR, Hoberman D, Linial ML, Hughes SH: **In vitro fidelity of the prototype primate foamy virus (PFV) RT compared to HIV-1 RT**. *Virology* 2007, **367**(2):253-264.
22. Gartner K, Wiktorowicz T, Park J, Mergia A, Rethwilm A, Scheller C: **Accuracy estimation of foamy virus genome copying**. *Retrovirology* 2009, **6**:32.
23. Plochmann K, Horn A, Gschmack E, Armbruster N, Krieg J, Wiktorowicz T, Weber C, Stirnnagel K, Lindemann D, Rethwilm A *et al*: **Heparan sulfate is an attachment factor for foamy virus entry**. *J Virol* 2012, **86**(18):10028-10035.
24. Picard-Maureau M, Jarmy G, Berg A, Rethwilm A, Lindemann D: **Foamy virus envelope glycoprotein-mediated entry involves a pH-dependent fusion process**. *J Virol* 2003, **77**(8):4722-4730.
25. Saib A, Puvion-Dutilleul F, Schmid M, Peries J, de The H: **Nuclear targeting of incoming human foamy virus Gag proteins involves a centriolar step**. *J Virol* 1997, **71**(2):1155-1161.
26. Patton GS, Erlwein O, McClure MO: **Cell-cycle dependence of foamy virus vectors**. *J Gen Virol* 2004, **85**(Pt 10):2925-2930.
27. Bieniasz PD, Weiss RA, McClure MO: **Cell cycle dependence of foamy retrovirus infection**. *J Virol* 1995, **69**(11):7295-7299.
28. Trobridge G, Russell DW: **Cell cycle requirements for transduction by foamy virus vectors compared to those of oncovirus and lentivirus vectors**. *J Virol* 2004, **78**(5):2327-2335.
29. Trobridge GD, Miller DG, Jacobs MA, Allen JM, Kiem HP, Kaul R, Russell DW: **Foamy virus vector integration sites in normal human cells**. *Proc Natl Acad Sci U S A* 2006, **103**(5):1498-1503.
30. Modlich U, Navarro S, Zychlinski D, Maetzig T, Knoess S, Brugman MH, Schambach A, Charrier S, Galy A, Thrasher AJ *et al*: **Insertional transformation of hematopoietic cells by self-inactivating lentiviral and gammaretroviral vectors**. *Mol Ther* 2009, **17**(11):1919-1928.
31. Beard BC, Keyser KA, Trobridge GD, Peterson LJ, Miller DG, Jacobs M, Kaul R, Kiem HP: **Unique integration profiles in a canine model of long-term repopulating cells transduced with gammaretrovirus, lentivirus, or foamy virus**. *Hum Gene Ther* 2007, **18**(5):423-434.
32. Hendrie PC, Huo Y, Stolitenko RB, Russell DW: **A rapid and quantitative assay for measuring neighboring gene activation by vector proviruses**. *Mol Ther* 2008, **16**(3):534-540.
33. Pietschmann T, Heinkelein M, Heldmann M, Zentgraf H, Rethwilm A, Lindemann D: **Foamy virus capsids require the cognate envelope protein for particle export**. *J Virol* 1999, **73**(4):2613-2621.
34. Alke A, Schwantes A, Kido K, Flotenmeyer M, Flugel RM, Löchelt M: **The bet gene of feline foamy virus is required for virus replication**. *Virology* 2001, **287**(2):310-320.
35. Goepfert PA, Shaw KL, Ritter GD, Jr., Mulligan MJ: **A sorting motif localizes the foamy virus glycoprotein to the endoplasmic reticulum**. *J Virol* 1997, **71**(1):778-784.

36. Moebes A, Enssle J, Bieniasz PD, Heinkelein M, Lindemann D, Bock M, McClure MO, Rethwilm A: **Human foamy virus reverse transcription that occurs late in the viral replication cycle**. *J Virol* 1997, **71**(10):7305-7311.
37. Yap MW, Lindemann D, Stanke N, Reh J, Westphal D, Hanenberg H, Ohkura S, Stoye JP: **Restriction of foamy viruses by primate Trim5alpha**. *J Virol* 2008, **82**(11):5429-5439.
38. Delebecque F, Suspene R, Calattini S, Casartelli N, Saib A, Froment A, Wain-Hobson S, Gessain A, Vartanian JP, Schwartz O: **Restriction of foamy viruses by APOBEC cytidine deaminases**. *J Virol* 2006, **80**(2):605-614.
39. Xu F, Tan J, Liu R, Xu D, Li Y, Geng Y, Liang C, Qiao W: **Tetherin inhibits prototypic foamy virus release**. *Virol J* 2011, **8**:198.
40. Holtz CM, Sadler HA, Mansky LM: **APOBEC3G cytosine deamination hotspots are defined by both sequence context and single-stranded DNA secondary structure**. *Nucleic Acids Res* 2013, **41**(12):6139-6148.
41. Münk C, Hechler T, Chareza S, Löchelt M: **Restriction of feline retroviruses: lessons from cat APOBEC3 cytidine deaminases and TRIM5alpha proteins**. *Veterinary immunology and immunopathology* 2010, **134**(1-2):14-24.
42. Malim MH, Bieniasz PD: **HIV Restriction Factors and Mechanisms of Evasion**. *Cold Spring Harb Perspect Med* 2012, **2**(5):a006940.
43. Zielonka J, Marino D, Hofmann H, Yuhki N, Löchelt M, Münk C: **Vif of feline immunodeficiency virus from domestic cats protects against APOBEC3 restriction factors from many felids**. *J Virol* 2010, **84**(14):7312-7324.
44. Kehl T, Bleiholder A, Rossmann F, Rupp S, Lei J, Lee J, Boyce W, Vickers W, Crooks K, Vandewoude S *et al*: **Complete Genome Sequences of Two Novel Puma concolor Foamy Viruses from California**. *Genome Announc* 2013, **1**(2):e0020112.
45. Daniels MJ, Golder MC, Jarrett O, MacDonald DW: **Feline viruses in wildcats from Scotland**. *Journal of Wildlife Diseases* 1999, **35**(1):121-124.
46. Mochizuki M, Akuzawa M, Nagatomo H: **Serological survey of the Iriomote cat (Felis iriomotensis) in Japan**. *Journal of Wildlife Diseases* 1990, **26**(2):236-245.
47. Butera ST, Brown J, Callahan ME, Owen SM, Matthews AL, Weigner DD, Chapman LE, Sandstrom PA: **Survey of veterinary conference attendees for evidence of zoonotic infection by feline retroviruses**. *J Am Vet Med Assoc* 2000, **217**(10):1475-1479.
48. Switzer WM, Garcia AD, Yang C, Wright A, Kalish ML, Folks TM, Heneine W: **Coinfection with HIV-1 and simian foamy virus in West Central Africans**. *The Journal of infectious diseases* 2008, **197**(10):1389-1393.
49. Buseyne F, Betsem E, Montange T, Njouom R, Bilounga Ndongo C, Hermine O, Gessain A: **Clinical Signs and Blood Test Results Among Humans Infected With Zoonotic Simian Foamy Virus: A Case-Control Study**. *J Infect Dis* 2018, **218**(1):144-151.
50. Rua R, Betsem E, Montange T, Buseyne F, Gessain A: **In vivo cellular tropism of gorilla simian foamy virus in blood of infected humans**. *J Virol* 2014, **88**(22):13429-13435.
51. Switzer WM, Bhullar V, Shanmugam V, Cong ME, Parekh B, Lerche NW, Yee JL, Ely JJ, Boneva R, Chapman LE *et al*: **Frequent simian foamy virus infection in persons occupationally exposed to nonhuman primates**. *J Virol* 2004, **78**(6):2780-2789.
52. Rua R, Betsem E, Gessain A: **Viral latency in blood and saliva of simian foamy virus-infected humans**. *PLoS One* 2013, **8**(10):e77072.
53. Cummins JE, Jr., Boneva RS, Switzer WM, Christensen LL, Sandstrom P, Heneine W, Chapman LE, Dezzutti CS: **Mucosal and systemic antibody responses in humans infected with simian foamy virus**. *J Virol* 2005, **79**(20):13186-13189.

54. Boneva RS, Switzer WM, Spira TJ, Bhullar VB, Shanmugam V, Cong ME, Lam L, Heneine W, Folks TM, Chapman LE: **Clinical and virological characterization of persistent human infection with simian foamy viruses**. *AIDS Res Hum Retroviruses* 2007, **23**(11):1330-1337.
55. Weikel J, Löchelt M, Truyen U: **Demonstration of feline foamy virus in experimentally infected cats by immunohistochemistry**. *Journal of Veterinary Medicine A, Physiology, pathology, clinical medicine* 2003, **50**(8):415-417.
56. Alke A, Schwantes A, Zemba M, Flugel RM, Löchelt M: **Characterization of the humoral immune response and virus replication in cats experimentally infected with feline foamy virus**. *Virology* 2000, **275**(1):170-176.
57. Ledesma-Feliciano C, Hagen S, Troyer R, Zheng X, Musselman E, Slavkovic Lukic D, Franke AM, Maeda D, Zielonka J, Munk C *et al*: **Replacement of feline foamy virus bet by feline immunodeficiency virus vif yields replicative virus with novel vaccine candidate potential**. *Retrovirology* 2018, **15**(1):38.
58. Pedersen NC: **Feline syncytium-forming virus infection**. In: *Diseases of the Cat.* edn. Edited by Holyworth J. Philadelphia, PA: The W. B. Saunder Co.; 1986: 268-272.
59. German AC, Harbour DA, Helps CR, Gruffydd-Jones TJ: **Is feline foamy virus really apathogenic?** *Veterinary Immunology and Immunopathology* 2008, **123**(1-2):114-118.
60. Murray SM, Picker LJ, Axthelm MK, Hudkins K, Alpers CE, Linial ML: **Replication in a superficial epithelial cell niche explains the lack of pathogenicity of primate foamy virus infections**. *J Virol* 2008, **82**(12):5981-5985.
61. von Laer D, Neumann-Haefelin D, Heeney JL, Schweizer M: **Lymphocytes are the major reservoir for foamy viruses in peripheral blood**. *Virology* 1996, **221**(1):240-244.
62. Winkler IG, Löchelt M, Flower RLP: **Epidemiology of feline foamy virus and feline immunodeficiency virus infections in domestic and feral cats: a seroepidemiological study**. *Journal of Clinical Microbiology* 1999, **37**(9):2848-2851.
63. Yamamoto JK, Hansen H, Ho EW, Morishita TY, Okuda T, Sawa TR, Nakamura RM, Pedersen NC: **Epidemiologic and clinical aspects of feline immunodeficiency virus infection in cats from the continental United States and Canada and possible mode of transmission**. *J Am Vet Med Assoc* 1989, **194**(2):213-220.
64. Hood S, Mitchell JL, Sethi M, Almond NM, Cutler KL, Rose NJ: **Horizontal acquisition and a broad biodistribution typify simian foamy virus infection in a cohort of Macaca fascicularis**. *Virology journal* 2013, **10**(1):326-326.
65. Johnson RH, de la Rosa J, Abher I, Kertayadnya IG, Entwistle KW, Fordyce G, Holroyd RG: **Epidemiological studies of bovine spumavirus**. *Vet Microbiol* 1988, **16**(1):25-33.
66. Cavalcante LTF, Muniz CP, Jia H, Augusto AM, Troccoli F, Medeiros SO, Dias CGA, Switzer WM, Soares MA, Santos AF: **Clinical and Molecular Features of Feline Foamy Virus and Feline Leukemia Virus Co-Infection in Naturally-Infected Cats**. *Viruses* 2018, **10**(12).
67. Murray SM, Picker LJ, Axthelm MK, Linial ML: **Expanded tissue targets for foamy virus replication with simian immunodeficiency virus-induced immunosuppression**. *Journal of Virology* 2006, **80**(2):663-670.
68. Soliven K, Wang X, Small CT, Feeroz MM, Lee E-G, Craig KL, Hasan K, Engel Ga, Jones-Engel L, Matsen Fa *et al*: **Simian foamy virus infection of rhesus macaques in Bangladesh: relationship of latent proviruses and transcriptionally active viruses**. *Journal of virology* 2013, **87**(24):13628-13639.
69. Falcone V, Leupold J, Clotten J, Urbanyi E, Herchenroder O, Spatz W, Volk B, Bohm N, Toniolo A, Neumann-Haefelin D *et al*: **Sites of simian foamy virus persistence in naturally infected African green monkeys: latent provirus is ubiquitous, whereas viral replication is restricted to the oral mucosa**. *Virology* 1999, **257**(1):7-14.

70. Romen F, Backes P, Materniak M, Sting R, Vahlenkamp TW, Riebe R, Pawlita M, Kuzmak J, Löchelt M: **Serological detection systems for identification of cows shedding bovine foamy virus via milk**. *Virology* 2007, **364**(1):123-131.
71. Bandecchi P, Matteucci D, Baldinotti F, Guidi G, Abramo F, Tozzini F, Bendinelli M: **Prevalence of feline immunodeficiency virus and other retroviral infections in sick cats in Italy**. *Veterinary Immunology and Immunopathology* 1992, **31**(3-4):337-345.
72. Glaus T, Hofmann-Lehmann R, Greene C, Glaus B, Wolfensberger C, Lutz H: **Seroprevalence of Bartonella henselae infection and correlation with disease status in cats in Switzerland**. *J Clin Microbiol* 1997, **35**(11):2883-2885.
73. Winkler IG, Lochelt M, Levesque JP, Bodem J, Flugel RM, Flower RL: **A rapid streptavidin-capture ELISA specific for the detection of antibodies to feline foamy virus**. *J Immunol Methods* 1997, **207**(1):69-77.
74. Winkler IG, Flügel RM, Löchelt M, Flower RLP: **Detection and molecular characterisation of feline foamy virus serotypes in naturally infected cats**. *Virology* 1998, **247**(2):144-151.
75. Miyazawa T, Ikeda Y, Maeda K, Horimoto T, Tohya Y, Mochizuki M, Vu D, Vu GD, Cu DX, Ono K *et al*: **Seroepidemiological survey of feline retrovirus infections in domestic and leopard cats in northern Vietnam in 1997**. *The Journal of Veterinary Medical Science* 1998, **60**(11):1273-1275.
76. Nakamura K, Miyazawa T, Ikeda Y, Sato E, Nishimura Y, Nguyen NT, Takahashi E, Mochizuki M, Mikami T: **Contrastive prevalence of feline retrovirus infections between northern and southern Vietnam**. *The Journal of Veterinary Medical Science* 2000, **62**(8):921-923.
77. Bleiholder A, Mühle M, Hechler T, Bevins S, vandeWoude S, Denner J, Löchelt M: **Pattern of seroreactivity against feline foamy virus proteins in domestic cats from Germany**. *Veterinary Immunology and Immunopathology* 2011, **143**(3-4):292-300.
78. Mochizuki M, Konishi S: **Feline syncytial virus spontaneously detected in feline cell cultures**. *Nihon Juigaku Zasshi* 1979, **41**(4):351-362.
79. Flower RL, Wilcox GE, Cook RD, Ellis TM: **Detection and prevalence of serotypes of feline syncytial spumaviruses**. *Archives of Virology* 1985, **83**(1-2):53-63.
80. Romen F, Pawlita M, Sehr P, Bachmann S, Schroder J, Lutz H, Lochelt M: **Antibodies against Gag are diagnostic markers for feline foamy virus infections while Env and Bet reactivity is undetectable in a substantial fraction of infected cats**. *Virology* 2006, **345**(2):502-508.
81. Kechejian S, Dannemiller N, Kraberger S, Ledesma-Feliciano C, Löchelt M, Carver S, VandeWoude S: **Feline foamy virus prevalence and demographic risk factors in United States feral domestic cat populations**. *J Feline Med Surg* 2018, **(Manuscript under review)**.
82. Glick AD, Horn RG, Holscher M: **Characterization of feline glomerulonephritis associated with viral-induced hematopoietic neoplasms**. *The American Journal of Pathology* 1978, **92**(2):321-332.
83. Fabricant CG, King JM, Gaskin JM, Gillespie JH: **Isolation of a virus from a female cat with urolithiasis**. *J Am Vet Med Assoc* 1971, **158**(2):200-201.
84. Martens JG, McConnell S, Swanson CL: **The role of infectious agents in naturally occurring feline urologic syndrome**. *Vet Clin North Am Small Anim Pract* 1984, **14**(3):503-511.
85. Pedersen NC, Pool RR, O'Brien T: **Feline chronic progressive polyarthritis**. *Am J Vet Res* 1980, **41**(4):522-535.
86. Inkpen H: **Chronic progressive polyarthritis in a domestic shorthair cat**. *Can Vet J* 2015, **56**(6):621-623.

87. McKissick GE, Lamont PH: **Characteristics of a virus isolated from a feline fibrosarcoma**. *J Virol* 1970, **5**(2):247-257.
88. Powers JA, Chiu ES, Kraberger SJ, Roelke-Parker M, Lowery I, Erbeck K, Troyer R, Carver S, VandeWoude S: **Feline leukemia virus disease outcomes in a domestic cat breeding colony: Relationship to endogenous FeLV and other chronic viral infections**. *J Virol* 2018.
89. Whitman JE, Jr., Cockrell KO, Hall WT, Gilmore CE: **An unusual case of feline leukemia and an associated syncytium-forming virus**. *Am J Vet Res* 1975, **36**(7):873-880.
90. Ward BC, Pederson N: **Infectious peritonitis in cats**. *J Am Vet Med Assoc* 1969, **154**(1):26-35.
91. Schwantes A, Ortlepp I, Löchelt M: **Construction and functional characterization of feline foamy virus-based retroviral vectors**. *Virology* 2002, **301**(1):53-63.
92. Pandya S, Klimatcheva E, Planelles V: **Lentivirus and foamy virus vectors: novel gene therapy tools**. *Expert Opin Biol Ther* 2001, **1**(1):17-40.
93. Cavazzana M, Six E, Lagresle-Peyrou C, Andre-Schmutz I, Hacein-Bey-Abina S: **Gene Therapy for X-Linked Severe Combined Immunodeficiency: Where Do We Stand?** *Hum Gene Ther* 2016, **27**(2):108-116.
94. Hacein-Bey-Abina S, Garrigue A, Wang GP, Soulier J, Lim A, Morillon E, Clappier E, Caccavelli L, Delabesse E, Beldjord K *et al*: **Insertional oncogenesis in 4 patients after retrovirus-mediated gene therapy of SCID-X1**. *J Clin Invest* 2008, **118**(9):3132-3142.
95. Erlwein O, McClure MO: **Progress and prospects: foamy virus vectors enter a new age**. *Gene Ther* 2010, **17**(12):1423-1429.
96. Trobridge GD, Allen J, Peterson L, Ironside C, Russell DW, Kiem HP: **Foamy and lentiviral vectors transduce canine long-term repopulating cells at similar efficiency**. *Hum Gene Ther* 2009, **20**(5):519-523.
97. Kiem HP, Wu RA, G. S, von Laer D, Rossi JJ, Trobridge GD: **Foamy combinatorial anti-HIV vectors with MGMTP140K potently inhibit HIV-1 and SHIV replication and mediate selection in vivo**. *Gene Therapy* 2010, **17**(1):37-49.
98. Trobridge GD: **Foamy virus vectors for gene transfer**. *Expert Opin Biol Ther* 2009, **9**(11):1427-1436.
99. Trobridge G, Josephson N, Vassilopoulos G, Mac J, Russell DW: **Improved foamy virus vectors with minimal viral sequences**. *Mol Ther* 2002, **6**(3):321-328.
100. Bastone P, Löchelt M: **Kinetics and characteristics of replication-competent revertants derived from self-inactivating foamy virus vectors**. *Gene Ther* 2004, **11**(5):465-473.
101. Bastone P, Romen F, Liu W, Wirtz R, Koch U, Josephson N, Langbein S, Löchelt M: **Construction and characterization of efficient, stable and safe replication-deficient foamy virus vectors**. *Gene Ther* 2007, **14**(7):613-620.
102. Liu W, Lei J, Liu Y, Lukic DS, Rathe AM, Bao Q, Kehl T, Bleiholder A, Hechler T, Löchelt M: **Feline foamy virus-based vectors: advantages of an authentic animal model**. *Viruses* 2013, **5**(7):1702-1718.
103. Taylor JA, Vojtech L, Bahner I, Kohn DB, Laer DV, Russell DW, Richard RE: **Foamy virus vectors expressing anti-HIV transgenes efficiently block HIV-1 replication**. *Mol Ther* 2008, **16**(1):46-51.
104. Bauer TR, Jr., Allen JM, Hai M, Tuschong LM, Khan IF, Olson EM, Adler RL, Burkholder TH, Gu YC, Russell DW *et al*: **Successful treatment of canine leukocyte adhesion deficiency by foamy virus vectors**. *Nat Med* 2008, **14**(1):93-97.

105. Burtner CR, Beard BC, Kennedy DR, Wohlfahrt ME, Adair JE, Trobridge GD, Scharenberg AM, Torgerson TR, Rawlings DJ, Felsburg PJ *et al*: **Intravenous injection of a foamy virus vector to correct canine SCID-X1**. *Blood* 2014, **123**(23):3578-3584.
106. Schwantes A, Truyen U, Weikel J, Weiss C, Lochelt M: **Application of chimeric feline foamy virus-based retroviral vectors for the induction of antiviral immunity in cats**. *J Virol* 2003, **77**(14):7830-7842.
107. Vassilopoulos G, Trobridge G, Josephson NC, Russell DW: **Gene transfer into murine hematopoietic stem cells with helper-free foamy virus vectors**. *Blood* 2001, **98**(3):604-609.
108. Marino CL, Lascelles BD, Vaden SL, Gruen ME, Marks SL: **Prevalence and classification of chronic kidney disease in cats randomly selected from four age groups and in cats recruited for degenerative joint disease studies**. *J Feline Med Surg* 2014, **16**(6):465-472.
109. Hamilton JB, Hamilton RS, Mestler GE: **Duration of life and causes of death in domestic cats: influence of sex, gonadectomy, and inbreeding**. *J Gerontol* 1969, **24**(4):427-437.
110. O'Neill DG, Church DB, McGreevy PD, Thomson PC, Brodbelt DC: **Longevity and mortality of cats attending primary care veterinary practices in England**. *J Feline Med Surg* 2015, **17**(2):125-133.
111. Jepson RE: **Current Understanding of the Pathogenesis of Progressive Chronic Kidney Disease in Cats**. *Vet Clin North Am Small Anim Pract* 2016, **46**(6):1015-1048.
112. Reynolds BS, Lefebvre HP: **Feline CKD: Pathophysiology and risk factors -- what do we know?** *Journal of Feline Medicine and Surgery* 2013, **15**(Supplement 1):3-14.
113. Bartges JW: **Chronic Kidney Disease in Dogs and Cats**. *Vet Clin N Am-Small* 2012, **42**(4):669-+.
114. Brown CA, Elliott J, Schmiedt CW, Brown SA: **Chronic Kidney Disease in Aged Cats: Clinical Features, Morphology, and Proposed Pathogeneses**. *Vet Pathol* 2016, **53**(2):309-326.
115. McLeland SM, Cianciolo RE, Duncan CG, Quimby JM: **A comparison of biochemical and histopathologic staging in cats with chronic kidney disease**. *Vet Pathol* 2015, **52**(3):524-534.
116. Polzin DJ: **Chronic kidney disease in small animals**. *Vet Clin North Am Small Anim Pract* 2011, **41**(1):15-30.
117. Chakrabarti S, Syme HM, Brown CA, Elliott J: **Histomorphometry of feline chronic kidney disease and correlation with markers of renal dysfunction**. *Vet Pathol* 2013, **50**(1):147-155.
118. DiBartola SP, Rutgers HC, Zack PM, Tarr MJ: **Clinicopathologic findings associated with chronic renal disease in cats: 74 cases (1973-1984)**. *J Am Vet Med Assoc* 1987, **190**(9):1196-1202.
119. **IRIS Staging of CKD** [http://www.iris-kidney.com/guidelines/staging.html]
120. Quimby JM: **Update on Medical Management of Clinical Manifestations of Chronic Kidney Disease**. *Vet Clin North Am Small Anim Pract* 2016, **46**(6):1163-1181.
121. Poli A, Abramo F, Taccini E, Guidi G, Barsotti P, Bendinelli M, Malvaldi G: **Renal involvement in feline immunodeficiency virus infection: a clinicopathological study**. *Nephron* 1993, **64**(2):282-288.
122. Baxter KJ, Levy JK, Edinboro CH, Vaden SL, Tompkins MB: **Renal disease in cats infected with feline immunodeficiency virus**. *Journal of Veterinary Internal Medicine* 2012, **26**(2):238-243.
123. Poli A, Tozon N, Guidi G, Pistello M: **Renal alterations in feline immunodeficiency virus (FIV)-infected cats: Anatural model of lentivirus-induced renal disease changes**. *Viruses* 2012, **4**(9):1372-1389.

124. Fabricant CG, Rich LJ, Gillespie JH: **Feline viruses. XI. Isolation of a virus similar to a myxovirus from cats in which urolithiasis was experimentally induced**. *Cornell Vet* 1969, **59**(4):667-672.
125. Gaskell RM, Gaskell CJ, Page W, Dennis P, Voyle CA: **Studies on a possible viral aetiology for the feline urological syndrome**. *Vet Rec* 1979, **105**(11):243-247.
126. Kruger JM, Osborne CA: **The role of viruses in feline lower urinary tract disease**. *Journal of Veterinary Internal Medicine* 1990, **4**(2):71-78.
127. Hartmann K: **Feline immunodeficiency virus infection: an overview**. *Vet J* 1998, **155**(2):123-137.
128. de Rozìeres S, Thompson J, Sundstrom M, Gruber J, Stump DS, de Parseval AP, VandeWoude S, Elder JH: **Replication properties of clade A/C chimeric feline immunodeficiency viruses and evaluation of infection kinetics in the domestic cat**. *Journal of Virology* 2008, **82**(16):7953-7963.
129. Tomonaga K, Mikami T: **Molecular biology of the feline immunodeficiency virus auxiliary genes**. *J Gen Virol* 1996, **77 (Pt 8)**:1611-1621.
130. Orandle M, Baldwin C: **Clinical and Pathological Features Associated with Feline Immunodeficiency Virus Infection in Cats**. *Iowa State University Veterinarian* 1995, **57**(2):61-65.
131. Murphy B, Vapniarsky N, Hillman C, Castillo D, McDonnel S, Moore P, Luciw PA, Sparger EE: **FIV establishes a latent infection in feline peripheral blood CD4+ T lymphocytes in vivo during the asymptomatic phase of infection**. *Retrovirology* 2012, **9**:12.
132. TerWee JA, Carlson JK, Sprague WS, Sondgeroth KS, Shropshire SB, Troyer JL, VandeWoude S: **Prevention of immunodeficiency virus induced CD4+ T-cell depletion by prior infection with a non-pathogenic virus**. *Virology* 2008, **377**(1):63-70.
133. de Parseval A, Chatterji U, Sun P, Elder JH: **Feline immunodeficiency virus targets activated CD4+ T cells by using CD134 as a binding receptor**. *Proceedings of the National Academy of Sciences of the United States of America* 2004, **101**(35):13044-13049.
134. Elder JH, Lin YC, Fink E, Grant CK: **Feline immunodeficiency virus (FIV) as a model for study of lentivirus infections: parallels with HIV**. *Curr HIV Res* 2010, **8**(1):73-80.
135. Murphy BG, Eckstrand C, Castillo D, Poon A, Liepnieks M, Harmon K, Moore P: **Multiple, Independent T Cell Lymphomas Arising in an Experimentally FIV-Infected Cat during the Terminal Stage of Infection**. *Viruses* 2018, **10**(6).
136. Hartmann K: **Clinical aspects of feline retroviruses: a review**. *Viruses* 2012, **4**(11):2684-2710.
137. Magden E, Miller C, MacMillan M, Bielefeldt-Ohmann H, Avery A, Quackenbush SL, Vandewoude S: **Acute virulent infection with feline immunodeficiency virus (FIV) results in lymphomagenesis via an indirect mechanism**. *Virology* 2013, **436**(2):284-294.
138. Liem BP, Dhand NK, Pepper AE, Barrs VR, Beatty JA: **Clinical Findings and Survival in Cats Naturally Infected with Feline Immunodeficiency Virus**. *Journal of Veterinary Internal Medicine* 2013, **27**(4):798-805.
139. Yamamoto JK, Sparger E, Ho EW, Andersen PR, O'Connor TP, Mandell CP, Lowenstine L, Munn R, Pedersen NC: **Pathogenesis of experimentally induced feline immunodeficiency virus infection in cats**. *Am J Vet Res* 1988, **49**(8):1246-1258.
140. Gleich S, Hartmann K: **Hematology and serum biochemistry of feline immunodeficiency virus-infected and feline leukemia virus-infected cats**. *Journal of Veterinary Internal Medicine* 2009, **23**(3):552-558.

141. Zenger E, Brown WC, Song W, Wolf AM, Pedersen NC, Longnecker M, Li J, Collisson EW: **Evaluation of cofactor effect of feline syncytium-forming virus on feline immunodeficiency virus infection**. *Am J Vet Res* 1993, **54**(5):713-718.
142. Choudhary A, Galvin TA, Williams DK, Beren J, Bryant MA, Khan AS: **Influence of naturally occurring simian foamy viruses (SFVs) on SIV disease progression in the rhesus macaque (Macaca mulatta) model**. *Viruses* 2013, **5**(6):1414-1430.
143. Rethwilm A, Bodem J: **Evolution of foamy viruses: the most ancient of all retroviruses**. *Viruses* 2013, **5**(10):2349-2374.
144. Mouinga-Ondeme A, Kazanji M: **Simian foamy virus in non-human primates and cross-species transmission to humans in Gabon: an emerging zoonotic disease in central Africa?** *Viruses* 2013, **5**(6):1536-1552.
145. Schwantes A, Truyen U, Weikel J, Weiss C, Löchelt M: **Application of chimeric feline foamy virus-based retroviral vectors for the induction of antiviral immunity in cats**. *Journal of Virology* 2003, **77**(14):7830-7842.
146. Lei J, Osen W, Gardyan A, Hotz-Wagenblatt A, Wei G, Gissmann L, Eichmuller S, Löchelt M: **Replication-Competent Foamy Virus Vaccine Vectors as Novel Epitope Scaffolds for Immunotherapy**. *PLoS One* 2015, **10**(9):e0138458.
147. Gupta S, Leutenegger CM, Dean GA, Steckbeck JD, Cole KS, Sparger EE: **Vaccination of cats with attenuated feline immunodeficiency virus proviral DNA vaccine expressing gamma interferon**. *J Virol* 2007, **81**(2):465-473.
148. Maksaereekul S, Dubie RA, Shen X, Kieu H, Dean GA, Sparger EE: **Vaccination with vif-deleted feline immunodeficiency virus provirus, GM-CSF, and TNF-alpha plasmids preserves global CD4 T lymphocyte function after challenge with FIV**. *Vaccine* 2009, **27**(28):3754-3765.
149. Pedersen NC, Yamamoto JK, Ishida T, Hansen H: **Feline immunodeficiency virus infection**. *Vet Immunol Immunopathol* 1989, **21**(1):111-129.
150. Moris A, Murray S, Cardinaud S: **AID and APOBECs span the gap between innate and adaptive immunity**. *Front Microbiol* 2014, **5**:534.
151. Yan N, Chen ZJ: **Intrinsic antiviral immunity**. *Nat Immunol* 2012, **13**(3):214-222.
152. Iwasaki A, Medzhitov R: **Regulation of adaptive immunity by the innate immune system**. *Science* 2010, **327**(5963):291-295.
153. Lukic DS, Hotz-Wagenblatt A, Lei J, Rathe AM, Muhle M, Denner J, Münk C, Löchelt M: **Identification of the feline foamy virus Bet domain essential for APOBEC3 counteraction**. *Retrovirology* 2013, **10**:76.
154. Wang JW, Zhang WY, Lv MY, Zuo T, Kong W, Yu XH: **Identification of a Cullin5-ElonginB-ElonginC E3 Complex in Degradation of Feline Immunodeficiency Virus Vif-Mediated Feline APOBEC3 Proteins**. *Journal of Virology* 2011, **85**(23):12482-12491.
155. Zhang ZL, Gu QY, Vasudevan AAJ, Hain A, Kloke BP, Hasheminasab S, Mulnaes D, Sato K, Cichutek K, Haussinger D *et al*: **Determinants of FIV and HIV Vif sensitivity of feline APOBEC3 restriction factors**. *Retrovirology* 2016, **13**.
156. Stern MA, Hu CL, Saenz DT, Fadel HJ, Sims O, Peretz M, Poeschla EM: **Productive Replication of vif-Chimeric HIV-1 in Feline Cells**. *Journal of Virology* 2010, **84**(14):7378-7395.
157. Sato K, Izumi T, Misawa N, Kobayashi T, Yamashita Y, Ohmichi M, Ito M, Takaori-Kondo A, Koyanagi Y: **Remarkable Lethal G-to-A Mutations in vif-Proficient HIV-1 Provirus by Individual APOBEC3 Proteins in Humanized Mice**. *Journal of Virology* 2010, **84**(18):9546-9556.
158. Lockridge KM, Himathongkham S, Sawai ET, Chienand M, Sparger EE: **The feline immunodeficiency virus vif gene is required for productive infection of feline**

peripheral blood mononuclear cells and monocyte-derived macrophages. *Virology* 1999, **261**(1):25-30.
159. Münk C, Beck T, Zielonka J, Hotz-Wagenblatt A, Chareza S, Battenberg M, Thielebein J, Cichutek K, Bravo IG, O'Brien SJ *et al*: **Functions, structure, and read-through alternative splicing of feline APOBEC3 genes**. *Genome Biology* 2008, **9**(3):R48.
160. Kozak M: **An analysis of 5'-noncoding sequences from 699 vertebrate messenger RNAs**. *Nucleic Acids Res* 1987, **15**(20):8125-8148.
161. O'Neil C, Lee D, Clewley G, Johnson MA, Emery VC: **Prevalence of anti-vif antibodies in HIV-1 infected individuals assessed using recombinant baculovirus expressed vif protein**. *J Med Virol* 1997, **51**(3):139-144.
162. Wieland U, Kuhn JE, Jassoy C, Rubsamen-Waigmann H, Wolber V, Braun RW: **Antibodies to recombinant HIV-1 vif, tat, and nef proteins in human sera**. *Med Microbiol Immunol* 1990, **179**(1):1-11.
163. Ayyavoo V, Nagashunmugam T, Boyer J, Mahalingam S, Fernandes LS, Le P, Lin J, Nguyen C, Chattargoon M, Goedert JJ *et al*: **Development of genetic vaccines for pathogenic genes: construction of attenuated vif DNA immunization cassettes**. *AIDS* 1997, **11**(12):1433-1444.
164. Wieland U, Kratschmann H, Kehm R, Kuhn JE, Naher H, Kramer MD, Braun RW: **Antigenic domains of the HIV-1 vif protein as recognized by human sera and murine monoclonal antibodies**. *AIDS Res Hum Retroviruses* 1991, **7**(11):861-867.
165. Schwander S, Braun RW, Kuhn JE, Hufert FT, Kern P, Dietrich M, Wieland U: **Prevalence of antibodies to recombinant virion infectivity factor in the sera of prospectively studied patients with HIV-1 infection**. *J Med Virol* 1992, **36**(2):142-146.
166. Pistello M: **Should accessory proteins be structural components of lentiviral vaccines? Lessons learned from the accessory ORF-A protein of FIV**. *Vet Immunol Immunopathol* 2008, **123**(1-2):144-149.
167. Inoshima Y, Miyazawa T, Mikami T: **In vivo functions of the auxiliary genes and regulatory elements of feline immunodeficiency virus**. *Vet Microbiol* 1998, **60**(2-4):141-153.
168. Lee JS, Mackie RS, Harrison T, Shariat B, Kind T, Kehl T, Löchelt M, Boucher C, VandeWoude S: **Targeted Enrichment for Pathogen Detection and Characterization in Three Felid Species**. *J Clin Microbiol* 2017, **55**(6):1658-1670.
169. Zemba M, Alke A, Bodem J, Winkler IG, Flower RL, Pfrepper K, Delius H, Flügel RM, Löchelt M: **Construction of infectious feline foamy virus genomes: cat antisera do not cross-neutralize feline foamy virus chimera with serotype-specific Env sequences**. *Virology* 2000, **266**(1):150-156.
170. Reed L, Muench H: **A simple method of estimating fifty per cent endpoints**. *The American Journal of Hygiene* 1938, **27**:493-497.
171. Winkler I, Bodem J, Haas L, Zemba M, Delius H, Flower R, Flügel RM, Löchelt M: **Characterization of the genome of feline foamy virus and its proteins shows distinct features different from those of primate spumaviruses**. *Journal of Virology* 1997, **71**(9):6727-6741.
172. Sehr P, Zumbach K, Pawlita M: **A generic capture ELISA for recombinant proteins fused to glutathione S-transferase: validation for HPV serology**. *J Immunol Methods* 2001, **253**(1-2):153-162.
173. Ellis TM, MacKenzie JS, Wilcox GE, Cook RD: **Isolation of feline syncytia-forming virus from oropharyngeal swabs of cats**. *Australian Veterinary Journal* 1979, **55**(4):202-203.
174. Switzer WM, Bhullar V, Shanmugam V, Cong Me, Parekh B, Lerche NW, Yee JL, Ely JJ, Boneva R, Chapman LE *et al*: **Frequent Simian Foamy Virus Infection in Persons**

Occupationally Exposed to Nonhuman Primates. *Journal of Virology* 2004, **78**(6):2780-2789.
175. Betsem E, Rua R, Tortevoye P, Froment A, Gessain A: **Frequent and recent human acquisition of simian foamy viruses through apes' bites in central Africa**. *PLoS Pathog* 2011, **7**(10):e1002306.
176. Cianciolo RE, Brown CA, Mohr FC, Spangler WL, Aresu L, van der Lugt JJ, Jansen JH, James C, Clubb FJ, Lees GE: **Pathologic evaluation of canine renal biopsies: methods for identifying features that differentiate immune-mediated glomerulonephritides from other categories of glomerular diseases**. *J Vet Intern Med* 2013, **27 Suppl 1**:S10-18.
177. Team RC: **R: A language and environment for statistical computing.** In., vol. 3.4.2. Vienna, Austria: R Foundation for Statistical Computing; 2017.
178. Delignette-Muller ML, Dutang C: **fitdistrplus: An R Package for Fitting Distributions**. *2015* 2015, **64**(4):34.
179. Brooks M, Kristensen K, van Benthem K, Magnusson A, Berg C, Nielsen A, Skaug H, Mächler M, Bolker B: **glmmTMB Balances Speed and Flexibility Among Packages for Zero-inflated Generalized Linear Mixed Modeling**. *The R Journal* 2017, **9**(2):378-400.
180. Aragon T, Fay M, Wollschlaeger D, Omidpanah A: **epitools: Epidemiology Tools**. In., vol. R package 0.5-10; 2017.
181. Cowgill LD, Polzin DJ, Elliott J, Nabity MB, Segev G, Grauer GF, Brown S, Langston C, van Dongen AM: **Is Progressive Chronic Kidney Disease a Slow Acute Kidney Injury?** *Vet Clin North Am Small Anim Pract* 2016, **46**(6):995-1013.
182. Brooks JI, Merks HW, Fournier J, Boneva RS, Sandstrom PA: **Characterization of blood-borne transmission of simian foamy virus**. *Transfusion* 2007, **47**(1):162-170.
183. Murray SM, Linial ML: **Foamy virus infection in primates**. *J Med Primatol* 2006, **35**(4-5):225-235.
184. Gray F, Lescs MC, Keohane C, Paraire F, Marc B, Durigon M, Gherardi R: **Early brain changes in HIV infection: neuropathological study of 11 HIV seropositive, non-AIDS cases**. *J Neuropathol Exp Neurol* 1992, **51**(2):177-185.
185. Bell JE: **The neuropathology of adult HIV infection**. *Rev Neurol (Paris)* 1998, **154**(12):816-829.
186. Torres L, Noel RJ, Jr.: **Astrocytic expression of HIV-1 viral protein R in the hippocampus causes chromatolysis, synaptic loss and memory impairment**. *J Neuroinflammation* 2014, **11**:53.
187. Wilcox GE, Flower RL, Cook RD: **Recovery of viral agents from the central nervous system of cats**. *Vet Microbiol* 1984, **9**(4):355-366.
188. Grauer GF: **Proteinuria: measurement and interpretation**. *Top Companion Anim Med* 2011, **26**(3):121-127.
189. Syme HM: **Proteinuria in cats. Prognostic marker or mediator?** *J Feline Med Surg* 2009, **11**(3):211-218.
190. Harley L, Langston C: **Proteinuria in dogs and cats**. *Can Vet J* 2012, **53**(6):631-638.
191. Wharram BL, Goyal M, Wiggins JE, Sanden SK, Hussain S, Filipiak WE, Saunders TL, Dysko RC, Kohno K, Holzman LB *et al*: **Podocyte depletion causes glomerulosclerosis: diphtheria toxin-induced podocyte depletion in rats expressing human diphtheria toxin receptor transgene**. *J Am Soc Nephrol* 2005, **16**(10):2941-2952.
192. Chiswell DJ, Pringle CR: **Feline syncytium-forming virus: identification of a virion associated reverse transcriptase and electron microscopical observations of infected cells**. *J Gen Virol* 1979, **43**(2):429-434.

193. Cook RD: **Observations on focal demyelinating lesions in cat optic nerves**. *Neuropathol Appl Neurobiol* 1979, **5**(5):395-404.
194. Toribio JA, Norris JM, White JD, Dhand NK, Hamilton SA, Malik R: **Demographics and husbandry of pet cats living in Sydney, Australia: results of cross-sectional survey of pet ownership**. *J Feline Med Surg* 2009, **11**(6):449-461.
195. Johnston L, Szczepanski J, McDonagh P: **Demographics, lifestyle and veterinary care of cats in Australia and New Zealand**. *J Feline Med Surg* 2017, **19**(12):1199-1205.
196. White JD, Norris JM, Baral RM, Malik R: **Naturally-occurring chronic renal disease in Australian cats: a prospective study of 184 cases**. *Aust Vet J* 2006, **84**(6):188-194.
197. Hellard E, Fouchet D, Rey B, Mouchet A, Poulet H, Pontier D: **Differential association between circulating testosterone and infection risk by several viruses in natural cat populations: a behavioural-mediated effect?** *Parasitology* 2013, **140**(4):521-529.
198. Tejerizo G, Domenech A, Illera JC, Silvan G, Gomez-Lucia E: **Altered plasma concentrations of sex hormones in cats infected by feline immunodeficiency virus or feline leukemia virus**. *Domest Anim Endocrinol* 2012, **42**(2):113-120.
199. Hofmann-Lehmann R, Holznagel E, Lutz H: **Female cats have lower rates of apoptosis in peripheral blood lymphocytes than male cats: correlation with estradiol-17beta, but not with progesterone blood levels**. *Vet Immunol Immunopathol* 1998, **65**(2-4):151-160.
200. Klein SL, Flanagan KL: **Sex differences in immune responses**. *Nat Rev Immunol* 2016, **16**(10):626-638.
201. Ruggieri A, Anticoli S, D'Ambrosio A, Giordani L, Viora M: **The influence of sex and gender on immunity, infection and vaccination**. *Ann Ist Super Sanita* 2016, **52**(2):198-204.
202. Obert LA, Hoover EA: **Relationship of lymphoid lesions to disease course in mucosal feline immunodeficiency virus type C infection**. *Vet Pathol* 2000, **37**(5):386-401.
203. Litster A, Lin JM, Nichols J, Weng HY: **Diagnostic utility of CD4%:CD8 low% T-lymphocyte ratio to differentiate feline immunodeficiency virus (FIV)-infected from FIV-vaccinated cats**. *Vet Microbiol* 2014, **170**(3-4):197-205.
204. Schiffer C, Lecellier CH, Mannioui A, Felix N, Nelson E, Lehmann-Che J, Giron ML, Gluckman JC, Saib A, Canque B: **Persistent infection with primate foamy virus type 1 increases human immunodeficiency virus type 1 cell binding via a Bet-independent mechanism**. *J Virol* 2004, **78**(20):11405-11410.
205. Beczkowski PM, Litster A, Lin TL, Mellor DJ, Willett BJ, Hosie MJ: **Contrasting clinical outcomes in two cohorts of cats naturally infected with feline immunodeficiency virus (FIV)**. *Vet Microbiol* 2015, **176**(1-2):50-60.
206. de Rozieres S, Mathiason CK, Rolston MR, Chatterji U, Hoover EA, Elder JH: **Characterization of a highly pathogenic molecular clone of feline immunodeficiency virus clade C**. *J Virol* 2004, **78**(17):8971-8982.
207. Olesen CE, Yan YX, Liu B, Martin D, D'Eon B, Judware R, Martin C, Voyta JC, Bronstein I: **Novel methods for chemiluminescent detection of reporter enzymes**. *Methods Enzymol* 2000, **326**:175-202.
208. Hierholzer J, Killington R: **Virus Isolation and Quantitation**. In: *Virology Methods Manual.* edn. Edited by Kangro H, Mahy B. San Diego, CA: Academic Press; 1996: 24–32.
209. Miller C, Boegler K, Carver S, MacMillan M, Bielefeldt-Ohmann H, VandeWoude S: **Pathogenesis of oral FIV infection**. *PLoS One* 2017, **12**(9):e0185138.

210. Dreitz MJ, Dow SW, Fiscus SA, Hoover EA: **Development of monoclonal antibodies and capture immunoassays for feline immunodeficiency virus**. *Am J Vet Res* 1995, **56**(6):764-768.
211. Miller C, Emanuelli M, Fink E, Musselman E, Mackie R, Troyer R, Elder J, VandeWoude S: **FIV vaccine with receptor epitopes results in neutralizing antibodies but does not confer resistance to challenge**. *NPJ Vaccines* 2018, **3**:16.
212. Pedersen NC, Leutenegger CM, Woo J, Higgins J: **Virulence differences between two field isolates of feline immunodeficiency virus (FIV-APetaluma and FIV-CPGammar) in young adult specific pathogen free cats**. *Vet Immunol Immunopathol* 2001, **79**(1-2):53-67.
213. Miller C, Bielefeldt-Ohmann H, MacMillan M, Huitron-Resendiz S, Henriksen S, Elder J, VandeWoude S: **Strain-specific viral distribution and neuropathology of feline immunodeficiency virus**. *Veterinary Immunology and Immunopathology* 2011, **143**(3-4):282-291.
214. Thompson J, MacMillan M, Boegler K, Wood C, Elder JH, VandeWoude S: **Pathogenicity and rapid growth kinetics of feline immunodeficiency virus are linked to 3' elements**. *PloS One* 2011, **6**(8):e24020.

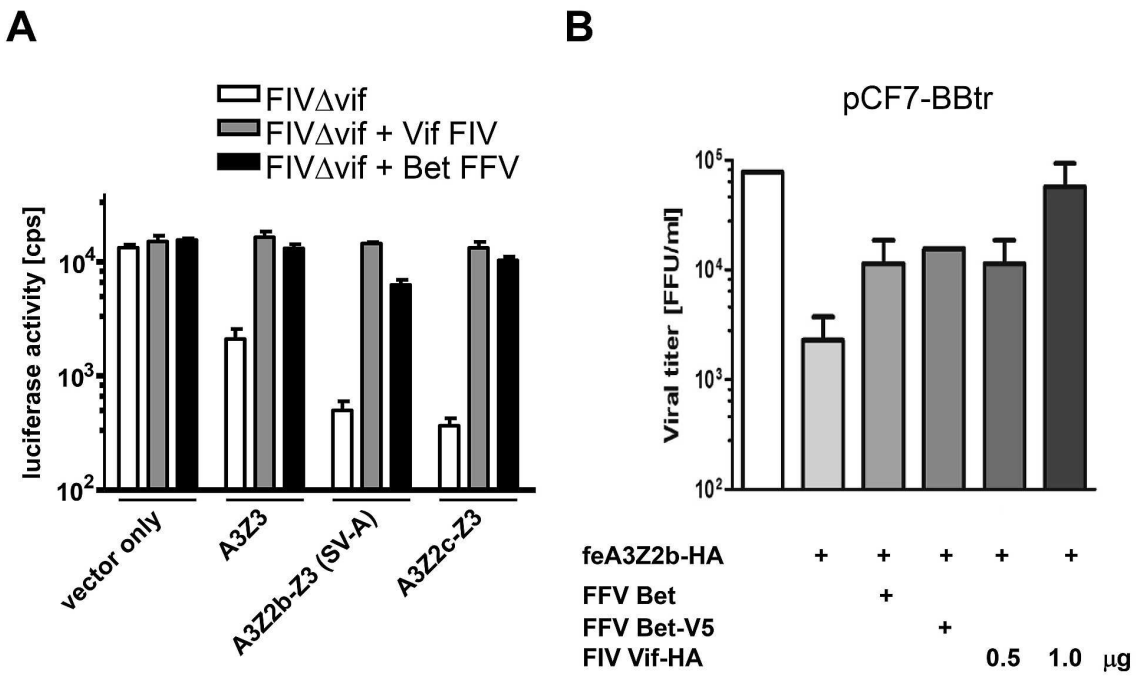

Appendix File 1. Rescue of Vif-deficient FIV and Bet-deficient FFV by FIV Vif and FFV Bet. A Vif-deficient FIV plasmid DNA was co-transfected with plasmids expressing FIV Vif or FFV Bet together with different feA3 restriction factors as given in the legend (left panel). Empty vector pcDNA3.1 served as control. Two days after transfection, cell-free supernatants were used to infect FIV reporter cells and luc activity induced by FIV infection was measured two days p.i. Titers are expressed as luc values of a representative experiment. **B** The Bet-deficient FFV genome pCF7-BBtr was co-transfected with plasmids expressing untagged and V5-tagged FFV Bet or two different amounts of FIV Vif expression plasmid together with the major FFV-restricting feA3Z2b-HA as shown below the bar diagram (right panel). Empty vector pcDNA3.1 served as control. Two days after transfection, cell-free supernatants were titrated in triplicate using FFV reporter cells as described in the “Methods” section and are expressed as focus-forming units (FFU) per ml inoculum of a representative experiment. Error bars represent the standard deviation.

Appendix File 2. Partial genome sequences from pCF7-Vif-4 and the stop mutations of the in vitro-selected FFV-Vif variants. The Trp codon and the downstream G residue (TGGG) ~ 130 bp upstream of the *vif* coding sequence are in bold face letters and underlined. In pCF7-Vif W/*1 (in blue), the mutation is from TGG to TGA and for mutant W/*2 (in green) the mutation is from TGGG to TAGA, with both mutations resulting in a Trp (W) to Stop (*) mutation (W/*) as indicated. The *bet* nucleotide sequence is in black, the linker sequence in pink with recognition sites for *Nhe*I (in brown) and *Sac*II (in light violet). The *vif* gene is marked in blue with the authentic Met start codon in bold. The Bet^{tr}Vif fusion protein is highlighted in yellow with the amino acids color-coded as described above for the genes. The Met residue 14 amino acids upstream of the authentic *vif* start codon is highlighted in bold and underlining. The C-terminal amino acid sequence of *tas* is highlighted in red.

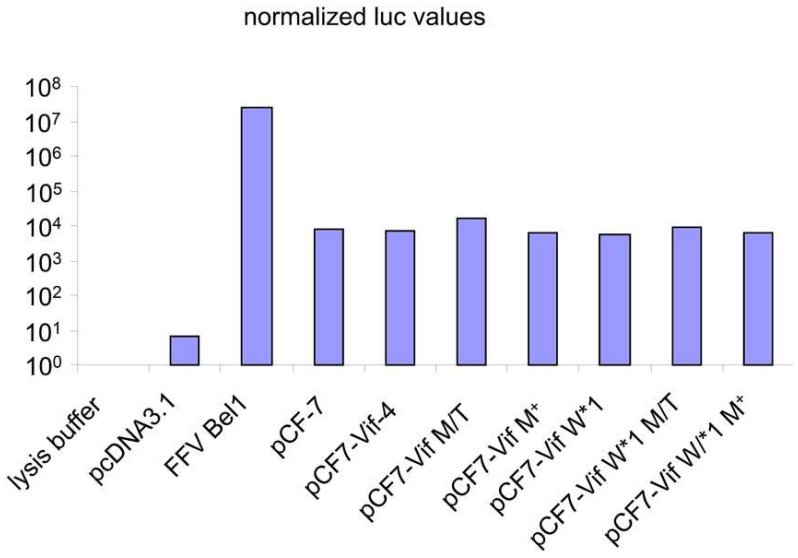

Appendix File 3. Mutations in *Tas* generated during the analysis of the upstream ATG do not affect Tas-mediated LTR transactivation. The LTR promoter-based luc reporter construct pFeFV-LTR-luc [73] was cotransfected into HEK 293T cells together with a CMV-IE-driven FFV Tas expression construct, the empty control pcDNA3.1 and proviral genomes pCF-7, pCF7-Vif-4, pCF7-Vif W/*1, and pCF7-Vif W/*2, and their engineered M/T and M$^+$ variants. Two days post transfection, luc activity induced by FFV Tas expression was measured in duplicates. Data from a representative experiment normalized to co-expressed β-gal are expressed in a logarithmic bar diagram.

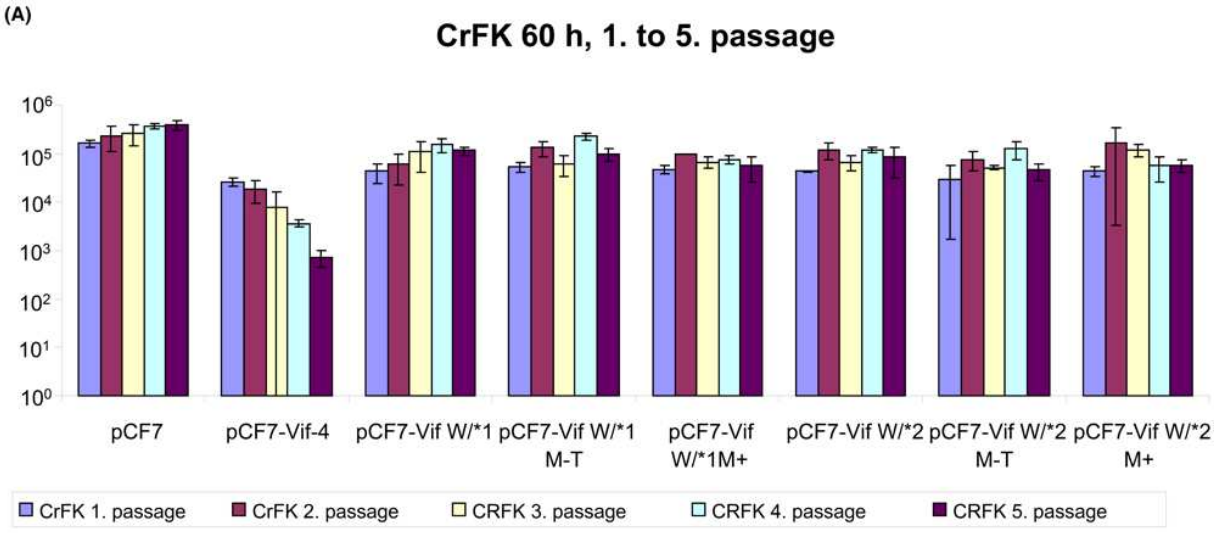

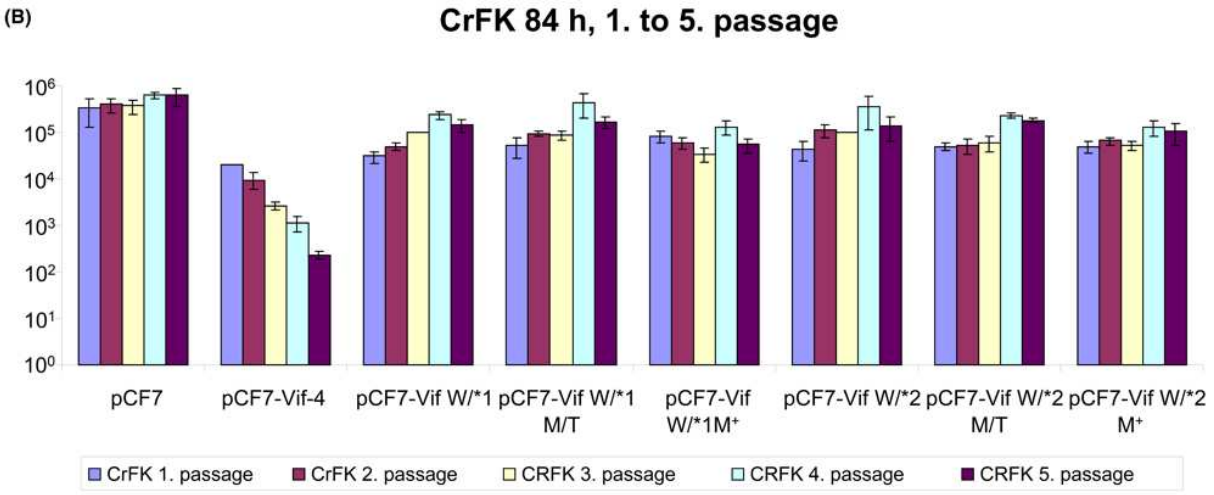

Appendix File 4. Titers of pCF-7, pCF7-Vif-4 and engineered pCF7-Vif W/*1 and pCF7-Vif W/*2 variants. Plasmid pCF-7, pCF7-Vif-4, pCF7-Vif W/*1, and pCF7-Vif W/*2 and their engineered M/T and M^+ variants were transfected into HEK 293T cells and 2 days post-transfection, cell-free supernatants were inoculated on CrFK cells and serially passaged every (**A)** 60 and (**B)** 84 h p.i. FFV titers were determined in duplicate using FeFAB reporter cells and are shown as bar diagrams for the different passages. Error bars represent the standard deviation.

Cat	qPCR		nPCR	ELISA		
	Indeterminate	Positive		Gag	Bet	Vif
WT1	15	21	21	21	42	-
WT2	3	21	21	21	28	-
WT3	15	70	42	21	42	-
WT4	15	21	21	28	42	-
CH1WT	98	-	-	15	98	15
CH2WT	3	63	77	21	86	15
CH3CH	21	-	-	28	-	15
CH4CH	21	-	-	21	-	63
Naïve	-	-	-	-	-	-

Appendix File 5. Date FFV was first detected by PCR and ELISA in experimentally infected cats. Day of first detection of FFV genomic DNA by qPCR with indeterminate and clear positive results (two left columns) and nested PCR (nPCR, middle column) after experimental infection with either wild-type FFV (WT), FFV-Vif W/*1 chimera (CH), chimera then wild-type FFV (CH1WT and CH2WT), twice with FFV-Vif W/*1 chimera (CH3CH and CH4CH), or sham inoculation in naïve cats. In addition, first detection of FFV Gag and Bet, and FIV Vif antibodies by ELISA is displayed correspondingly (right columns). Hyphens (-) mark negative results due to absence of reactivity.

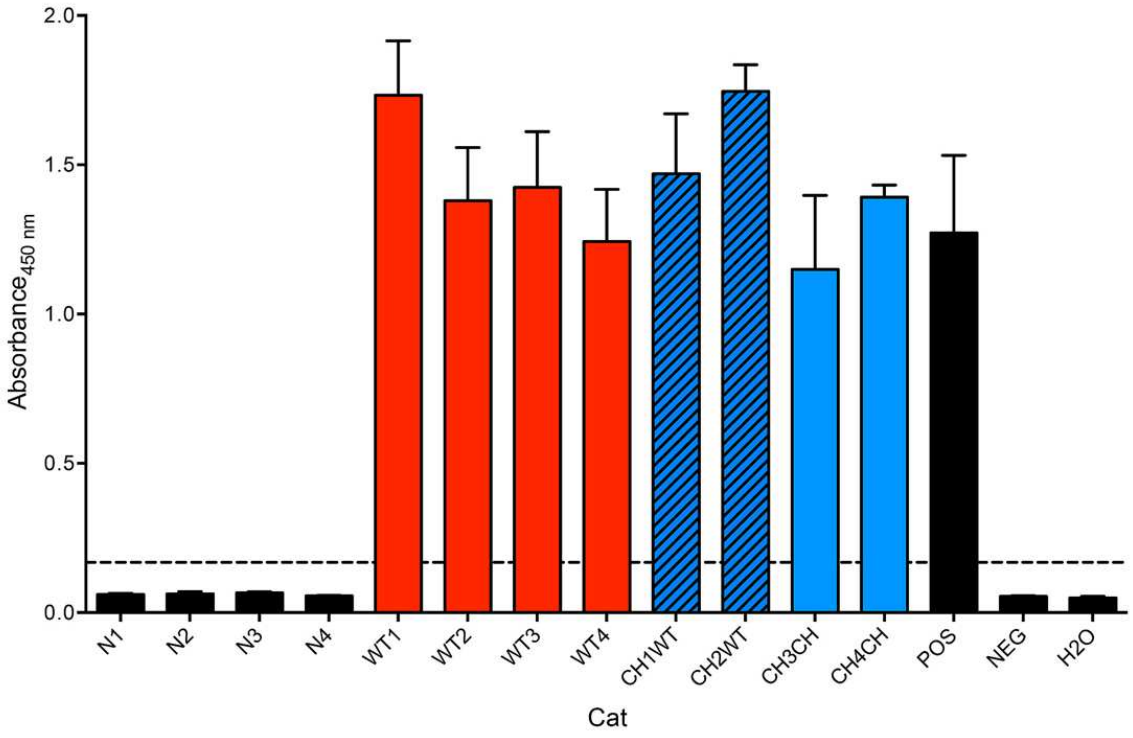

Appendix File 6. All cats infected with wild-type FFV and FFV-Vif W/*1 developed FFV Gag-specific immunoreactivity. A GST-capture ELISA was performed to evaluate antibody response to FFV infection. Anti-Gag reactivity (1:50 dilution) at the final time point for each animal is shown. All animals exposed to wild-type FFV (red bars) or FFV-Vif W/*1 (blue bars) seroconverted against Gag antigen and for many of these samples, reactivity is out of the linear range. Naïve animals (black bars) remained below the cutoff for detection (black dotted line). Black and blue striped bars denote chimeric animals re-inoculated with wild-type virus (CHxWT). Error bars represent standard deviation. POS = positive control, NEG = negative control, H2O = absolute negative (water) control.

Appendix File 7. Antibody marker combinations used for PBMC phenotype analysis by flow cytometry.

Antibody-Marker Combination	Panel	Dilution	Species specificity	Source
CD4-FITC	A	1:200	Cat	SouthernBiotech
CD8-PE	A	1:200	Cat	SouthernBiotech
CD25-PE/Cy7[a]	A	1:20	Cat	Dr. Gregg Dean[c]
CD134-647	A	1:20	Cat	AbD Serotec
Fas-APC/Cy7[b]	A, B	1:200	Cat	R&D Systems
CD56-APC	B	1:20	Human	BioLegend
CD14-PE	B	1:40	Human	Caltag Medsystems
CD21-PE/Cy7	B	1:20	Human	BD Pharmingen
MHCII-FITC	B	1:20	Human	BD Pharmingen

[a] antibody conjugated to fluorophore with an Abcam conjugation kit (ab102903), [b] antibody conjugated to fluorophore with an Abcam conjugation kit (ab102859), [c] Colorado State University.

Appendix File 8. FFV prevalence and chi-squared analysis data for CKD studies. Seven cats were ommited from sex-specific analyses due to lack of sex data.

Group	Collected Data							Prevalence Rates		Chi-Squared Analyses		
			FFV+		FFV-		Total	Subgroup	Prevalence	Variables	X^2 Statistic	P-Value
USA	All	CKD+	24	24%	29	30%	53	**All**	**44%**	**Sex vs. FFV**	5.188	0.023
		CKD-	19	19%	26	27%	45	CKD+FFV+	45%	(Sex | CKD+) vs. FFV	6.594	0.010
		Total	43	44%	55	56%	98	CKD-FFV+	42%	(Sex | CKD-) vs. FFV	0.021	0.886
	Male		FFV+		FFV-		Total	Subgroup	Prevalence	Variables	X^2 Statistic	P-Value
		CKD+	16	41%	8	21%	24	**M FFV+**	**59%**	**Sex vs. CKD**	0.677	0.411
		CKD-	7	18%	8	21%	15	CKD+FFV+	67%	(Sex | FFV+) vs. CKD	2.181	0.140
		Total	23	59%	16	41%	39	CKD-FFV+	47%	(Sex | FFV-) vs. CKD	0.003	0.956
	Female		FFV+		FFV-		Total	Subgroup	Prevalence	Variables	X^2 Statistic	P-Value
		CKD+	8	14%	21	37%	29	**F FFV+**	**33%**	**FFV vs. CKD**	0.017	0.897
		CKD-	11	19%	17	30%	28	CKD+FFV+	28%	(FFV | M) vs CKD	0.811	0.368
		Total	19	33%	38	67%	57	CKD-FFV+	39%	(FFV | F) vs. CKD	0.430	0.512
AU	All		FFV+		FFV-		Total	Subgroup	Prevalence	Variables	X^2 Statistic	P-Value
		CKD+	59	47%	28	22%	87	**All**	**67%**	**Sex vs. FFV**	0.000	1.000
		CKD-	25	20%	13	10%	38	CKD+FFV+	68%	(Sex | CKD+) vs. FFV	0.142	0.707
		Total	84	67%	41	33%	125	CKD-FFV+	66%	(Sex | CKD-) vs. FFV	0.468	0.494
	Male		FFV+		FFV-		Total	Subgroup	Prevalence	Variables	X^2 Statistic	P-Value
		CKD+	27	48%	10	18%	37	**M FFV+**	**68%**	**Sex vs. CKD**	0.091	0.763
		CKD-	11	20%	8	14%	19	M CKD+FFV+	73%	(Sex | FFV+) vs. CKD	0.002	0.967
		Total	38	68%	18	32%	56	M CKD-FFV+	58%	(Sex | FFV-) vs. CKD	0.845	0.358
	Female		FFV+		FFV-		Total	Subgroup	Prevalence	Variables	X^2 Statistic	P-Value
		CKD+	30	47%	15	23%	45	**F FFV+**	**69%**	**FFV vs. CKD**	0.039	0.844
		CKD-	14	22%	5	8%	19	F CKD+FFV+	67%	(FFV | M) vs CKD	0.709	0.400
		Total	44	69%	20	31%	64	F CKD-FFV+	74%	(FFV | F) vs. CKD	0.067	0.796
OVERALL	All		FFV+		FFV-		Total	Subgroup	Prevalence	Variables	X^2 Statistic	P-Value
		CKD+	83	37%	57	26%	140	**All**	**57%**	**Sex vs. FFV**	2.733	0.098
		CKD-	44	20%	39	17%	83	CKD+FFV+	59%	(Sex | CKD+) vs. FFV	4.338	0.037
		Total	127	57%	96	43%	223	CKD-FFV+	53%	(Sex | CKD-) vs. FFV	0.000	1.000
	Male		FFV+		FFV-		Total	Subgroup	Prevalence	Variables	X^2 Statistic	P-Value
		CKD+	43	45%	18	19%	61	**M FFV+**	**64%**	**Sex vs. CKD**	0.101	0.750
		CKD-	18	19%	16	17%	34	M CKD+FFV+	70%	(Sex | FFV+) vs. CKD	1.003	0.317
		Total	61	64%	34	36%	95	M CKD-FFV+	53%	(Sex | FFV-) vs. CKD	0.408	0.523
	Female		FFV+		FFV-		Total	Subgroup	Prevalence	Variables	X^2 Statistic	P-Value
		CKD+	38	31%	36	30%	74	**F FFV+**	**52%**	**FFV vs. CKD**	0.727	0.394
		CKD-	25	21%	22	18%	47	F CKD+FFV+	51%	(FFV | M) vs CKD	2.212	0.137
		Total	63	52%	58	48%	121	F CKD-FFV+	53%	(FFV | F) vs. CKD	0.000	0.991

Appendix File 9. FIV Absorbance (OD_{450}) values for first (1-X) and second (2-X) round of FIV and FFV co-infections. Absorbance values were obtained through p26 ELISA. Cutoff values for positivity are shown on the right column.

Day	FIV			FIV + FFV			FIV → FFV			FFV → FIV			Cutoff
1-1	0.36	0.33	0.34	0.28	0.31	0.20	0.39	0.36	0.35	0.35	0.35	0.34	0.19
1-2	0.29	0.30	0.31	0.30	0.32	0.31	0.25	0.32	0.27	0.38	0.40	0.45	
1-3	0.47	0.53	0.52	0.55	0.56	0.62	0.37	0.53	0.44	1.72	1.71	1.68	
1-5	1.65	1.66	1.78	1.88	1.84	1.68	1.38	1.59	1.68	1.82	1.61	1.66	
1-7	1.66	1.74	1.82	1.95	1.83	1.92	1.28	1.54	1.69	1.65	1.51	1.55	
Day	**FIV**			**FIV + FFV**			**FIV → FFV**			**FFV → FIV**			**Cutoff**
2-1	0.20	0.22	0.21	0.20	0.18	0.20	0.21	0.23	0.27	0.27	0.22	0.23	0.15
2-2	0.35	0.38	0.39	0.48	0.37	0.42	0.35	0.45	0.35	0.63	0.72	0.58	
2-3	0.82	0.99	0.89	1.10	0.95	1.03	0.83	1.03	0.95	1.80	1.65	1.64	
2-5	1.36	1.70	1.77	1.56	1.67	1.46	1.59	1.73	1.64	1.75	1.68	1.63	

Appendix File 10. Significant differences in FIV absorbance (OD_{450}) values for first (1-X) and second (2-X) round of FIV and FFV co-infections. Values and symbols attributed to significant differences in the co-infection studies (Fig. 7). Conditions in the left column are significantly higher than the second column.

Day	Condition significantly higher than		Symbol	P-value
1-3	FFV → FIV	FIV	****	< 0.0001
		FIV + FFV	****	< 0.0001
		FIV → FFV	****	< 0.0001
1-5	FIV + FFV	FIV → FFV	**	0.0023
1-7	FIV + FFV	FIV → FFV	****	< 0.0001
		FFV → FIV	****	< 0.0001
	FIV	FIV → FFV	**	0.0041
Day	**Condition significantly higher than**		**Symbol**	**P-value**
2-2	FFV → FIV	FIV	**	0.0022
		FIV + FFV	*	0.0167
		FIV → FFV	**	0.0032
2-3	FFV → FIV	FIV	****	< 0.0001
		FIV + FFV	****	< 0.0001
		FIV → FFV	****	< 0.0001

Appendix File 11. β-gal (ng) values for first (1-X) and second (2-X) FFV and FIV co-infections. β-gal amounts were obtained through a FFV Galacton-Star Luminescence assay standard curve. Cutoff values for positivity are shown on the far right column. Cutoff values for the adjusted timeline of staggered FIV → FFV infections that were different from the original date's cutoff are the second reported.

Day	FFV			FFV + FIV			FFV → FIV			FIV → FFV			Cutoff
1-1	0.05	0.05	0.05	0.06	0.05	0.05	0.05	0.06	0.05	0.04	0.05	0.08	0.09
1-2	0.05	0.06	0.14	0.05	0.06	0.16	0.05	0.05	0.14	0.00	0.00	0.00	0.09, 0.15
1-3	0.00	0.00	0.00	0.00	0.00	0.00	0.00	0.00	0.00	0.79	0.42	0.00	0.15
1-5	0.34	0.08	0.56	0.19	0.01	0.67	0.07	0.00	0.12	26.73	7.14	11.07	0.15
1-7	20.33	2.94	6.87	22.69	1.12	17.07	2.77	0.00	7.67	88.68	24.30	2.10	0.15, 0.06
Day	**FFV**			**FFV + FIV**			**FFV → FIV**			**FIV → FFV**			**Cutoff**
2-1	0.09	0.03	0.05	0.11	0.03	0.06	0.03	0.01	0.04	0.00	0.00	0.00	0.06
2-2	0.05	0.01	0.01	0.01	0.01	0.12	0.11	0.04	0.00	0.04	0.02	0.00	0.06
2-3	2.57	1.34	0.97	0.51	0.28	0.29	0.57	0.83	0.99	47.08	45.90	49.98	0.06, 0.19
2-5	80.90	71.47	10.42	11.89	8.28	76.42	32.60	22.59	41.73	94.46	97.38	95.57	0.19, 0.26

Appendix File 12. Significant differences in β-gal (ng) values for first (1-X) and second (2-X) FFV and FIV co-infections. Values and symbols attributed to significant differences in the co-infection studies (Fig. 8). Conditions in the left column are significantly higher than the second column.

Day	Condition significantly higher than		Symbol	P-value
1-7	FIV → FFV	FFV	*	0.0139
		FFV + FIV	*	0.0384
		FFV → FIV	**	0.0018
Day	**Condition significantly higher than**		**Symbol**	**P-value**
2-3	FIV → FFV	FFV	**	0.0015
		FFV + FIV	**	0.0011
		FFV → FIV	**	0.0012
2-5	FIV → FFV	FFV	**	0.0043
		FFV + FIV	****	< 0.0001
		FFV → FIV	****	< 0.0001